Discovering the Potential of Photoluminescent Ruthenium(II) Complexes as Photodynamic Therapy Agents

Roberto Padilla

Dissertation submitted to the faculty of the Virginia Polytechnic Institute

and State University in partial fulfillment of the requirements for the degree of

Doctor of Philosophy
In
Chemistry

Brenda S. J. Winkel (Chair)

Karen J. Brewer

Paul A. Deck

Tijana Z. Grove

John R. Morris

10/31/2015

Blacksburg, VA

KeyWords:
Anthracene, photodynamic therapy, supramolecular complexes, subcellular localization, cytotoxicity, phototoxicity, DNA, protein, malignant glioma, ruthenium, MLCT, gel shift assay, confocal microscopy.

Probing the Subcellular Localization of Luminescent Supermolecular Complexes in F98 Malignant Glioma Cells

Roberto Padilla

Abstract

Anthracene was attached to light activated, ruthenium-based DNA disruptors to probe their distribution in cancer cells. The objective of this research is to understand the photophysical properties (Chapter 2), photoreactivity toward DNA and proteins (Chapter 3), and localization within cancer cells (Chapter 4) of ruthenium complexes that demonstrate promise as photodynamic therapy (PDT) agents.

$[(AnthbpyMe)(bpy)Ru(dpp)]^{2+}$ **(1)** and $[(AnthbpyMe)_2Ru(dpp)]^{2+}$ **(2)** absorb visible light with metal-to-ligand charge transfer (MLCT) transitions at 459 nm (16,000 $M^{-1}cm^{-1}$) and 461 nm (21,000 $M^{-1}cm^{-1}$), respectively. These species exhibit ^{3}MLCT emissions at λ_{em} = 661 nm and λ_{em} = 663 nm for **1** and **2**, respectively, while the anthracene show emissions at 450 – 560 nm. The anthracene unit(s) quench the ^{3}MLCT to give quantum yields (lifetime) of Φ_{em} = 0.0059 [398(1) ns] and Φ_{em} = 0.0011 [414(1) ns] for **1** and **2**, respectively. Voltammetry shows an irreversible anthracene oxidation at 1.23 – 1.28 V, $Ru^{III/II}$ oxidation at 1.53 – 1.55 V, and quasi-reversible reduction couples attributed to $dpp^{0/-1}$ at 0.98 V.

DNA gel shift assays demonstrate that complexes **1** and **2** modify DNA in the presence and absence of $^3O_2$ upon light activation to convert supercoiled DNA to a mixture of open circular (OC) DNA and a species that exhibit sa distinctly different migration rate than either OC and linear DNA. Binding constants, K_b, for complexes **1** and **2**, toward DNA are 3.50×10^5(3.50×10^4) and 4.50×10^3(4.50×10^2) respectively. SDS-PAGE assays show that the complexes **1** and **2** modify bovine serum albumin (BSA) through an $^3O_2$-dependent mechanism upon light

activation.

The localization and PDT potency of the anthracene-Ru-dpp complexes are tested against F98 cells, which are rat glioma cells that simulate the infiltrative patterns of growth in cancer. Confocal microscopy demonstrates that complexes **1** and **2** internalize and localize primarily along the cell membrane and associate with dot-like vesicles within the cytoplasm. Complexes **1** and **2** show IC_{50} values of 107 μM and 85 μM, respectively, after 15 min of drug exposure and 1 h of PDT-treatment (λ_{PDT} = 455 nm).

List of Abbreviations

AnthbpyMe = 4-[*N*-(2-anthryl)carbamoyl]-4′-methyl-2,2′- bipyridine)
BAS = bioactive sites
BL = bridging ligand
BSA = bovine serum albumin
bpy = 2,2'-bipyridine
CV = cyclic voltammetry
CT-DNA = calf thymus DNA
dpp = 2,3-bis(2-pyridyl)pyrazine
en = excited state energy transfer
et = excited state electron transfer
$E_{1/2}$ = half-wave potential in voltammetry
ES = excited state
ESI-MS = electrospray ionization-mass spectrometry
GBM = glioblastomas
GS = ground state
HOMO = highest occupied molecular orbital
HpD = hematoporphyrin
ic = internal conversion
IL = intra-ligand
ipa = anodic peak current
ipc = cathodic peak current
ivr = intramolecular vibrational relaxation
isc = intersystem crossing
k_x = rate constant of process "x"
LUMO = lowest unoccupied molecular orbital
MC:BP = metal complex to base pairs ratio
MLCT = metal-to-ligand charge transfer
m/z = mass-to-charge ratio
nr = non-radiative decay
$^1O_2$ = singlet oxygen
$^3O_2$ = ground state oxygen
PDT= photodynamic therapy
phen = 1,10-phenanthroline
Ph_2phen = 4,7-diphenyl-1,10-phenanthroline
rxn = photochemical reaction
ROS = reactive oxygen species
rt = room temperature
TBAH = tetrabutylammonium hexafluorophosphate
TL = terminal ligand
τ = electronic excited state lifetime
ϕ = quantum yield
λ_{maxabs} = absorption maximum
λ_{maxem} = emission maximum

Chapter 1 Introduction

1.1 **Cancer**

Cancer is a term describing diseases characterized by uncontrollable growth of abnormal cells.[1-3] Cancer is a consequence of the accumulation of mutations that influence the growth, control, diffusion, and survival of cells.[4-7] Traditionally, cancer is viewed as a multistage disease that is initiated by the alteration of DNA by genotoxic radiation, viruses, and carcinogenic materials.[2,7,8] In 2014, it was expected that over 500,000 individuals would die from a cancer-related disease in the United States.[3] Currently, cancers are treated by surgery, chemotherapy, and radiation therapy, which are frequently used in combination.

Although cancer originates from changes in gene expression, disruption of signaling pathways that regulate cell homeostasis can also trigger multicellular events that transform healthy cells to cancerous cells. The diagram in Figure 1.1 depicts the interdependent and extremely complex-signaling pathways that have numerous genes known to be functionally altered (highlighted in red) resulting in changes in gene expression.[2] The consequence of altering genetic material enables cancerous cells to proliferate rapidly and indefinitely and to accumulate at anatomical sites generating solid masses of cancerous cells known as primary tumors.[2] Secondary tumors form when cells from the primary tumor spread and metasticize into different organs of the body.

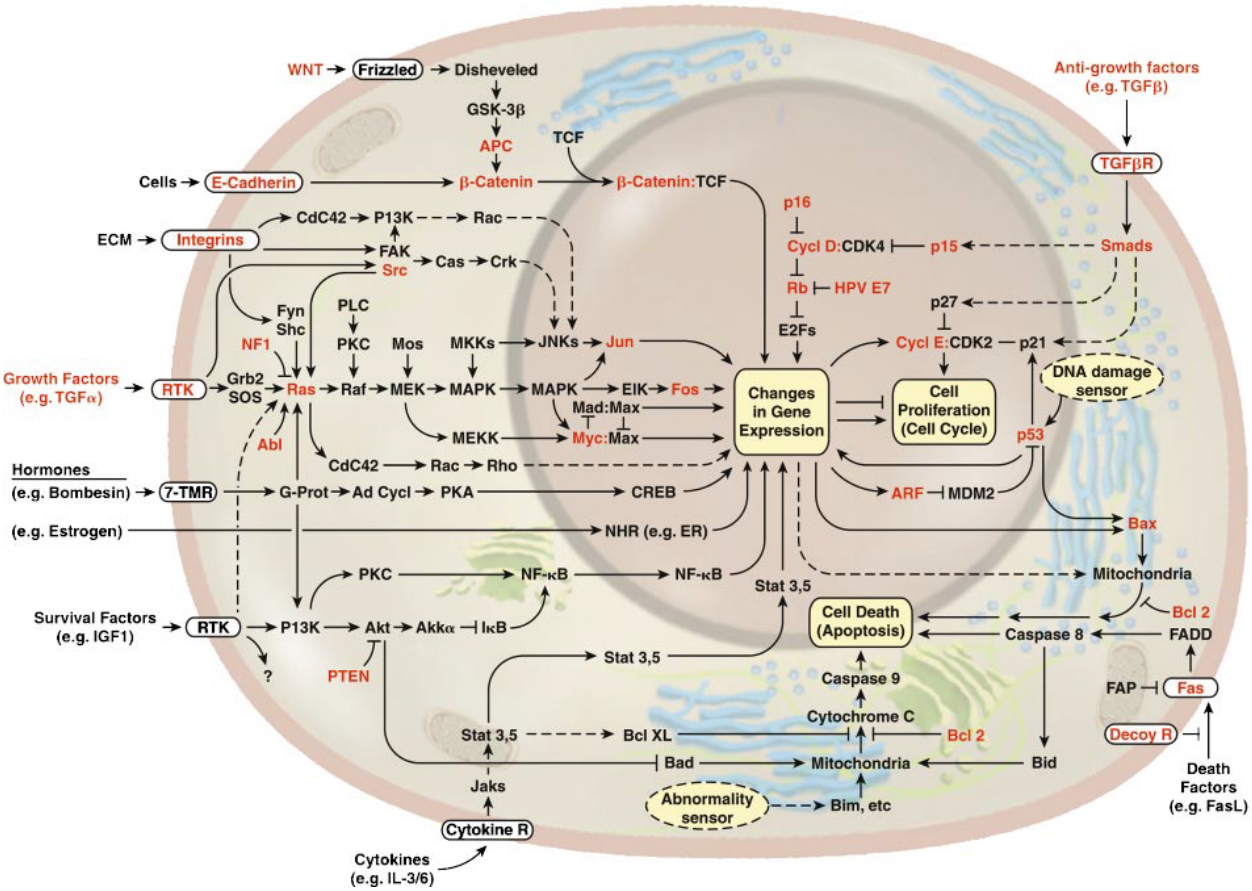

Figure 1.1. Integrated cell signaling pathways of the mammalian cell. Genes that are known to mutate are highlighted in red when there is a disruption of signal transaction (figure taken with permission from reference 2).

1.2 **Malignant glioma**

Although all types of cancer have their own characteristic challenges, malignant brain tumors are among the most biologically complex, aggressive, highly invasive, and neurologically destructive cancers. Malignant glioma (MG) brain tumors make up about 1.35% of total cancers.[9,10] Brain cancer cases have a low survival rate (about 29.6%).[1,9,11] Patients typically lose control of vital processes such as breathing, memory, movement, and cognitive response, and the often suffer excruciating pain. The inter- and intratumoral heterogeneity and location of MG tumors deep in the brain present challenges for many of the current treatment regimens, which warrants the investigation of novel drugs and therapies capable of treating MG tumors.

Glioblastomas (GBM) are classified into primary and secondary categories based on clinical and genetic features established by the World Health Organization, which are then further subdivided into classes (I-IV) used to establish the degree of malignancy.[1,12] Grade I tumors are solid masses that can be surgically removed, while Grade II are low-grade malignant tumors that follow infiltrative paths and are considered incurable to date. Grade III–IV are high-grade malignancies that result in death within a year of diagnosis.[1,12-14]

Malignant glioma (MG) cells, in particular exhibit significant integrated cellular signaling pathways abnormalities that disrupt proliferation, apoptosis, and infiltrative processes The abnormalities of cellular signaling pathways exhibited by MG can cause dysregulation of key cellular processes within the tumor colony, which results in the constant mutation of genetic material.[9,15]. Furthermore, these types of cells exhibit inter- and intratumoral heterogeneity, which is actually a result of normal, evolved defense mechanisms. The complexity of tumor heterogeneity exhibited by MG poses significant challenges for targeted lock and key therapeutic interventions to deliver efficient therapeutic potency due to their infiltrative growth and tumor regression properties as well as their eccentric signaling pathways.[1,9]. Thus, there is an urgent need for new therapeutic interventions that can deliver a burst of reactive cytotoxic agents through a variety of dynamic mechanisms to circumvent the drug resistance feature commonly associated with MGs. The desired therapy represents a sort of chemical and biological "shock and awe" approach.

1.3 **Current treatments for malignant glioma**

Current regimens to treat MG cases range from small molecule drug development, locoregional therapy, and targeted therapies.[9,13] Temozolomide (TMZ) is an attractive therapeutic molecule for brain cancers due to the ability of the drug to traverse the blood brain

barrier (BBB) with nearly 100% bioavailability after oral uptake.[16,17] TMZ was approved in the US in 1999 to treat MG.[16,17] Locoregional therapy is a value-added approach to treat MG cancers by administering therapeutic drugs during surgery.[9,18] This therapy circumvents the BBB, while increasing the intratumoral concentration of the drug lowering its systemic toxicity and minimizing recurrence, which typically occurs at the primary tumor site.[18]

1.4 **Photodynamic anti-cancer therapy**

Photodynamic therapy PDT is a combinatorial therapy that provides an alternative approach to treat MG cancers by using anticancer agents that can be light activated. An advantage of PDT is that guided light delivery can be used to activate PDT agents to treat diseased cells in a confined region and thereby minimize the harm to health tissue. PDT can be used in concert with locolregional therapy (surgery) to deliver the drug to the vicinity of tumor site and followed by activation using non-destructive light irradiation. For the treatment of MG tumors a laser can be employed to insure the needed pinpoint spatial resolution of the treatment.

PDT relies on uses light-sensitive agents known as photosensitizers (PS).[19-24] Most PDT agents are also designed to target and modify vital specific biological substrates, often DNA.[25,26] The emphasis on DNA goes back to the old assumption that cancer is primary a disease of the cell nucleus but we now know that this is not true, especially for complex cancers such as MG. An ideal PDT agent must adhere to the following criteria to optimize preferential accumulation and cytotoxicity toward diseased tissues:[19]

- Known molecular composition
- Photochemically stabilized
- No cytotoxicity in the absence of light
- High diseased tissue recognition capabilities

- Rapid expulsion from the body
- Efficient photoproduction of reactive toxic agents

Promising PDT agents should also achieve photoactivation within the therapeutic window, which is defined as light between 620 – 850 nm that efficiently penetrates the skin, propagates through tissue, and has sufficient energy to produce cytotoxic species.[27,28] PDT agents for cancer treatment have not been reported that meet all these criteria.

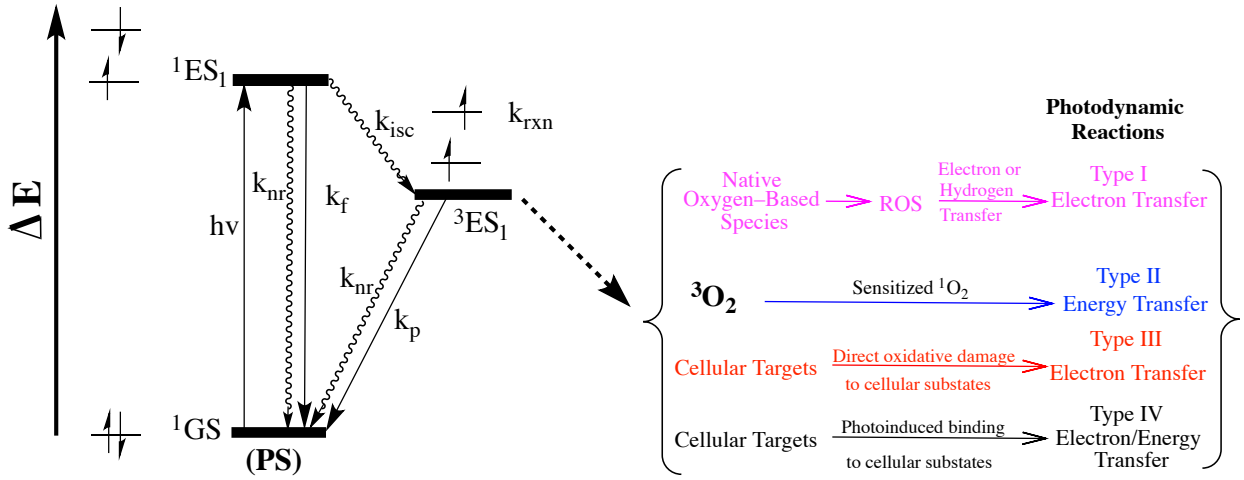

Figure 1.2. State diagram for the photosensitization (PS) of $^3O_2$ by photosensitizer (ES(excited state), k's (rate constants) for r (radiative decay), nr (non-radiative decay), isc (intersystem crossing), en (energy transfer), rxn (reaction), f (fluorescence) and p (phosphorescence), (figure reconstructed from literature reference [28]).

The principles of the phototoxic process are outlined in Figure 1.2. Starting at the ground state (GS), photoexcitation promotes an electron and forms an initial singlet excited state (^{1}ES). The triplet-excited state (^{3}ES) is then populated through intersystem crossing. The key ^{3}ES state can undergo electron/energy transfer processes to generate reactive toxic species according to four main mechanisms. These processes depend strongly on the photosensitizer having a long-lived ^{3}ES.[19,20,27,29] A Type I mechanism involves proton abstraction and/or electron transfer between the ^{3}ES and native substrates, especially biomolecules (proteins, RNA, DNA), resulting in the formation of reactive oxygen species (ROS). The Type II mechanism involves the transfer

of energy from ^{3}ES into a molecular oxygen, which generates cytotoxic singlet oxygen ($^1O_2$).[19,30,31] A Type III involves direct oxidative damage through electron transfer from native cellular substrates (enzymes, membranes, proteins, and DNA) to the PS.[27] Type III differs from Type I in that reactive oxygen species are not involved. Type IV is photobinding of the photosensitizer with biomacromolecules (proteins, RNA, DNA, ect.).[32-34] PS that exhibit an oxygen independent mechanism are of interest due to their potential to treat aggressive, highly-invasive, and neurologically-destructive brain cancers (i.e. malignant gliomas) due to the hypoxic environments commonly associated with these types of tumors. A desirable feature of next-generation PDT agents is the ability to operate simultaneously in more than one distinct pathway and thereby deliver a 'therapeutic burst' that will overcome the adaptability of MG.

1.5 **Polyazine-bridged Ru(II)-Pt(II) systems as PDT agents**

The quest to treat cancer by PDT has led to the development of photoactive metal complexes that can modify biological substrates to treat diseased tissue with low energy light. One approach to design a new PDT agent that disrupts biological substrates (DNA, RNA, and proteins) through multiple pathways is to incorporate PSs that efficiently sensitize $^3O_2$ and a metal-based DNA binding agent within a single molecule. Metal-based PDT agents offer stability toward ligand substitution, tunable redox properties, and orbital energetics based on ligand modification. These features are not offered by traditional non-metal-based PDT agents, such as Photofrin.[35-38] A variety of metal-based PDT agents have been shown to interact with biomacromolecules through intercalation, electrostatic association, and covalent binding, leading to significant structural modification that results in inhibition of transcription/translation and/or replication.[38-40]

Ruthenium polyazine complexes show promise as PDT agents due to their ability to

absorb visible light, utilize their ability to sensitize $^3O_2$, and reactivity toward DNA.[25,41-43] PS tris(2,2'-bipyridine) ruthenium(II), $[Ru(bpy)_3]^{2+}$ (bpy = 2,2'-bipyridine), and its analogs are proven PDT agents that promote $^1O_2$-mediated scission of DNA via quenching of the Ru(II) triplet metal-to-ligand charge transfer, ^{3}MLCT, excited state that are typically long-lived and efficiently generate $^1O_2$ upon light activation upon light activation.[42,44,45,42,46-48]

Although Ru(II) polyazines exhibit the right properties as photosensitizer toward oxygen, the lack of selectivity and the absolute dependence on oxygen limits the utility of Ru(II) complexes as PDT agents.[49-51] One approach to alleviate these limitations is to couple known metal-based DNA binding agents such as Pt(II) through a polyazine bridging ligand (BL) to generate Ru(II)-Pt(II) bimetallic systems that can target and photomodify DNA through multiple processes.[52,53] Ru(II)-Pt(II) systems are believed to function by concentrating the PS at the DNA target through initial binding of the Pt center with DNA.[45,54-60] The idea is to create a hybrid of the proven cancer drug cisplatin with an attached photosensitizer.

Several PDT candidates/models are shown in Figure 1.3. The heterobimetallic complex **1** binds to DNA through the Pt(II) unit, while the M(II) cation affords extra electrostatic attration.[61] Complex **2** intercalates into DNA and coordinates to the DNA duplex at the Pt(II) motif, while the Ru(II) unit facilitates additional electrostatic binding toward DNA.[62] Complex **3** and closely related species thermally bind to DNA and are the first Ru(II)-Pt(II) system(s) to inhibit bacterial growth.[60,63] Complex **4** binds and cleaves DNA upon irradiation at 455 nm.[64-66] Complex **5** was the first Ru(II)-Pt(II) compound to exhibit DNA binding and photocleavage with the use of visible light. In fact, close association of Pt(II) and Ru(II) through a conjugated bridging ligand such dpp tends to decrease ^{3}ES lifetime. However, complex **5** works because of electronic decoupling of the two distal Ru(II) chromophores from the reactive Pt(II) site.[67-72] Complex **6**

also decouples the Ru(II) PS from the Pt(II) site and was shown to target and photocleave DNA as well (λ_{ex} = 470 nm).[73] In summary heterobimetallic complexes that incorporate a Ru(II) PS to sensitize $^3O_2$ and a Pt(II) motif to bind DNA can modify biological substrates through multiple pathways, which can enhance their PDT potential.[74,75]

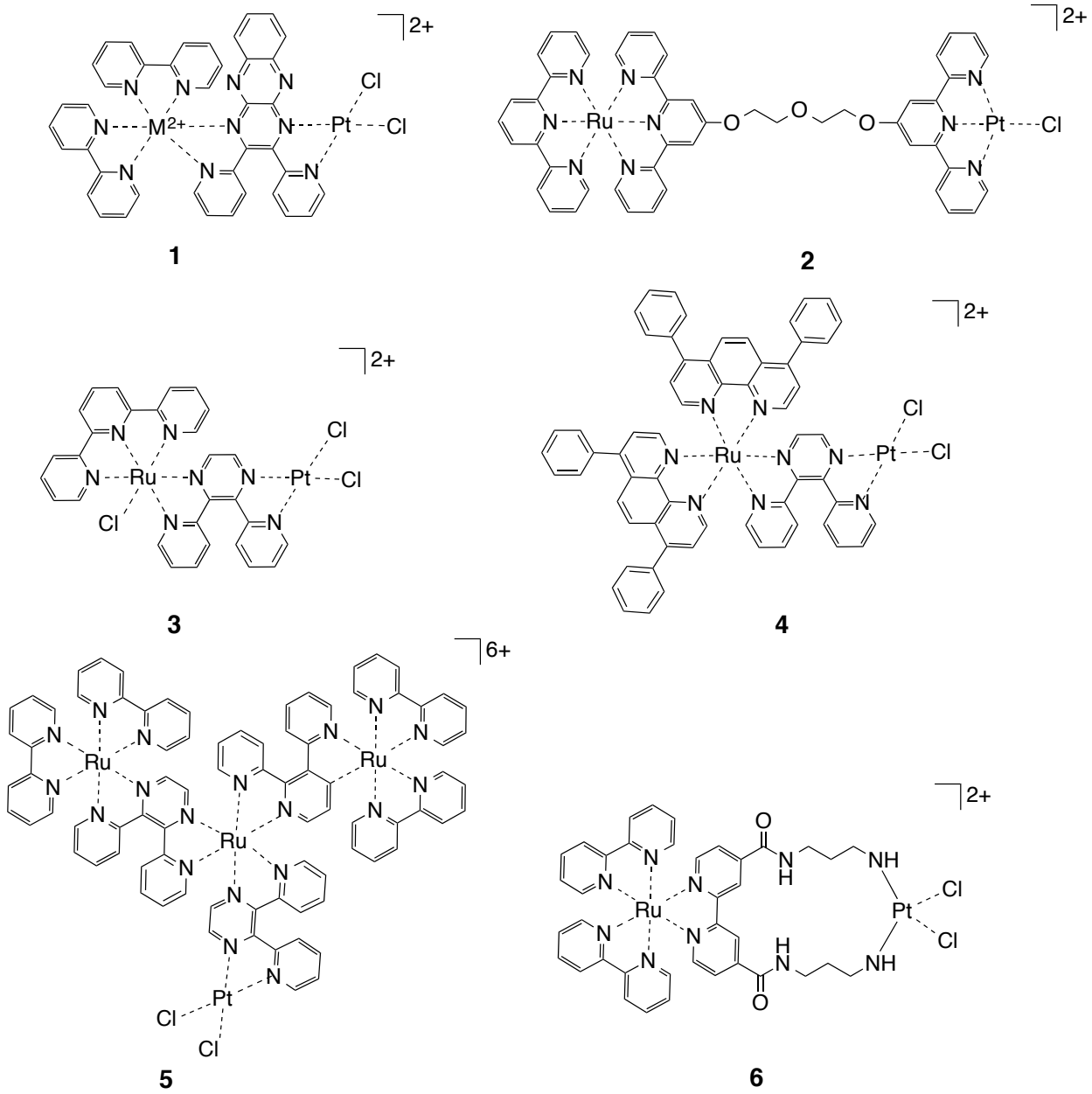

Figure 1.3. Chemical structures of Ru(II)-Pt(II) candidates for PDT agents $[(bpy)_2M(dpb)PtCl_2]^{2+}$ (**1**) (M = Ru(II) or Os(II)), $[(tpy)Ru(dtdeg\text{-}PtCl]^{3+}$ (**2**), $[(tpy)RuCl(dpp)PtCl_2]^{2+}$ (**3**), $[(Ph_2phen)_2Ru(dpp)PtCl_2]^{2+}$ (**4**), $[(bpy)_2Ru(dpp)PtCl_2]^{6+}$ (**5**), and $[Ru(bpy)_2\{m\text{-}bpy\text{-}(CONH\text{-}(CH_2)_3\text{-}NH_2)_2\}PtCl_2]^{2+}$ (**6**).

Despite the enormous potential that Ru(II)-Pt(II) complexes display for multifunctional PDT agents, there is limited information about the distribution, localization, and biological target within a cells. A potential reason for the absence of *in vitro* studies for Ru(II)-Pt(II) systems, specifically for $[(bpy)_2Ru(dpp)PtCl_2]^{2+}$ and its analogs, can be ascribed to the inherently short lived excited state lifetimes ($\tau \approx 45$ ns) relative to $[Ru(bpy)]^{2+}$, low quantum yield ($\phi \approx 10^{-4}$) of luminescence from the covalently coupled Ru(II) chromophores and shifted emission bands ($\lambda_{max} \approx 750$ nm) that are beyond the detection limits of current optical imaging techniques.[76] Although the ^{3}MLCT excited state of $[(bpy)_2Ru(dpp)PtCl_2]^{2+}$ can generate singlet oxygen and react with DNA, essential for PDT applications, the excited state properties are not suitable for optical imaging techniques. Thus, the localization, distribution, and biological targets of Ru(II)-Pt(II) complexes of the form $[(TL)_2Ru(dpp)PtCl_2]^{2+}$ (TL = bpy, phen, and Ph_2phen) within cells remains an unexplored area of research. One approach to the observation of complexes of the form $[(TL)_2Ru(dpp)PtCl_2]^{2+}$ within cells is to append a polycyclic aromatic hydrocarbon (PAH) unit that independently fluoresces onto the molecular structure, Figure 1.4. Tethering a fluorescent tag (FT) to the Ru(II)-Pt(II) molecular system can provide a non-destructive and highly sensitive approach to track the complex within cells to gain insight into the localization and biological targets of Ru(II)-Pt(II) systems, which could present a major contribution to the future development of Ru(II)-Pt(II) agents for cancer.

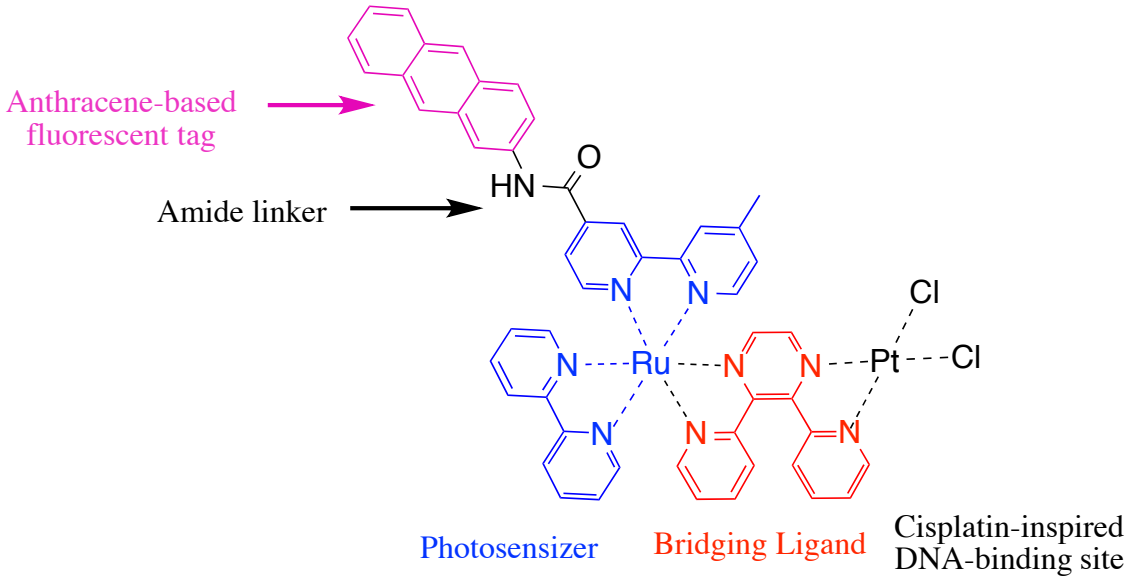

Figure 1.4. Illustration that describes fluorescent Ru(II)-Pt(II) complexes of the form $[(FT)(TL)Ru(BL)PtCl_2]^{2+}$.

Appending rigid, highly conjugated, and fluorescent organic chromophores to the Ru(II) PS unit within the Ru(II)-Pt(II) structure through insulating organic linkers (OL) serves as one approach to create fluorescent Ru(II)-Pt(II) complexes of the form $[(FT)(TL)Ru(BL)PtCl_2]^{2+}$. A systematic approach demands that the molecular building blocks are studied so that the effect of each on the PDT activity and cellular localization can be understood. Moreover it may turn out that the molecules without Pt(II) may have useful properties in their own right.

This dissertation concerns the design of fluorescent tagged Ru(II) photosensitizer to serve as molecular intermediates for fluorescent Ru(II)-Pt(II) complexes, while studying their photophysical properties, interactions with biomolecules (DNA and proteins), and localization within mammalian cells.

1.6 Exploring fluorescent metal-organic Ru(II) complexes as molecular precursors for fluorescent Ru(II)-Pt(II) systems

Metal-organic Ru(II) polyazine complexes that append PAH unit(s) through an insulating

organic linker offer three points of modulation (organic linker, PAH, and Ru(II) polyazine framework) that can be used to control the luminescence, DNA photobinding, and photocleavage within a single molecule, Figure 1.5.[44,77-80] In general, the properties of these Ru(II) hybrid complexes have been found depend on the nature of the covalent linker and the type of chromophore appended to the Ru(II) unit.[81-86] However, if designed correctly these metal-organic Ru(II) systems can append active chromophores that remotely retain their individual properties and can serve as molecular precursors for fluorescent Ru(II)-Pt(II) systems.[84,87-93] Thus, our aim was to create a modular molecular system of the form FT-OL-Ru(II) that can be used for Ru(II)-Pt(II) assemblies. The next few paragraphs describe the key features of our design.

Ru(II) polyazine complexes offers kinetic and thermodynamic stability for ligand substitution, ^{3}ES properties appropriate to singlet oxygen generation, accessible redox properties, tunable energetics, and immense flexibility of structure and properties by virtue of their octahedral geometry and bidentate ligand coordination. The one in Figure 1.5 is the simplest thing that we could choose as a starting point. The syntheses of these multifunctional systems are challenging due to the coupling of several units into a single molecule and can suffer from low-yield isolation and difficult purification processes. These complexes are therefore difficult and expensive to prepare in large quantities using current synthetic methods.

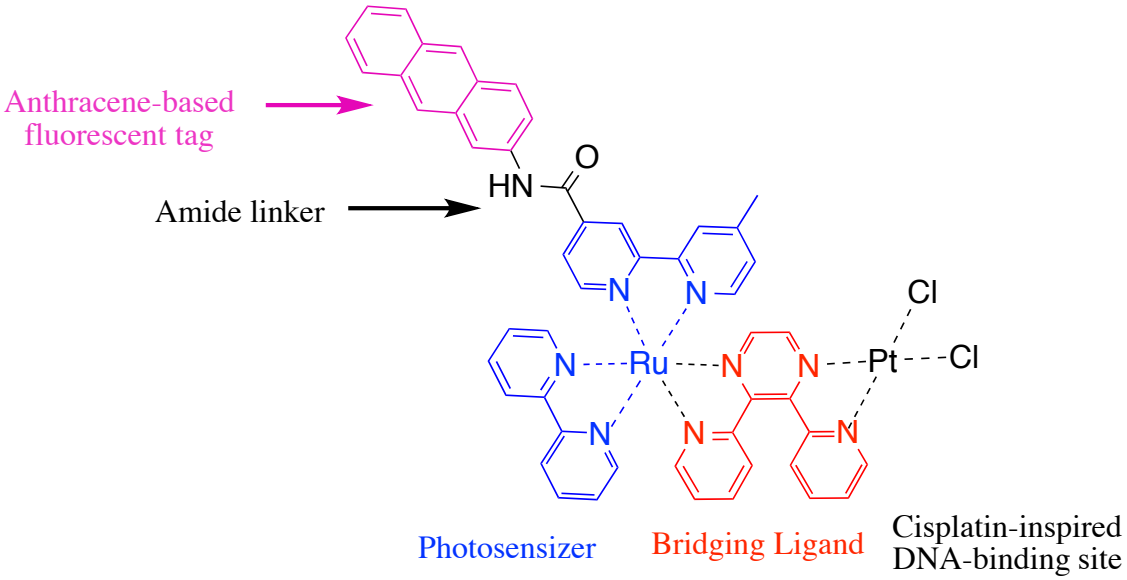

Figure 1.5. Illustration that describes the three-points of modulation for metal-organic Ru(II) polyazine complexes that covalently append PAH unit(s) through an insulating organic linkers.

The amide bond was used for the OL on the basis that these bonds have been shown to electronically decouple fluorescent subunits from Ru(II) PS and are unlikely to hydrolyze under cellular conditions, Figure 1.5.[84,94,95] Additionally, the amide bond is a synthetically versatile functional group to append different fluorescent units and can also alleviate potential twisted intramolecular charge transfer (TICT) processes commonly associated with metal-organic Ru(II) systems, which can introduce undesirable non-radiative decay pathways upon photoactivation.[96,97] The linkage amide minimizes the deactivation from TICT processes by insulating the two active chomophores and keeping them remote from each other such that they retain their individual properties.[84,94,96]

Anthracene was chosen as the fluorescent tag because it is the simplest unsubstituted PAH possessing the appropriate excited state lifetime (≈ 5 ns) appropriate for optical imaging techniques.[94,95,98-100] Furthermore, the anthracene motif has been shown to have the appropriate excited state orbital energetics, in comparison to naphthalene and pyrene, to minimize undesirable intramolecular interactions between the ^{3}MCLT and ^{3}arene states.[84,87,101-104] While

the photophysical behavior of these systems is complex, proof of the forgoing concepts has been demonstrated empirically as described in the next paragraph. The ruthenium complex $[Ru(bpy)_2(Mebpy\text{-}anthracene)]^{2+}$ combines $[Ru(bpy)_3]^{2+}$ with anthracene via an amide bond (Figure 1.6). The [Ru]-anthracene system exhibits bichromatic behavior, which allows the compound to fluoresce and phosphoresce from the anthracene and Ru(II) units, respectively.[105] Although, a cursory examination of the state diagram for this [Ru]-anthracene system may reveal various pathways for deactivation upon excitation, singlet-singlet, triplet-triplet, and/or singlet-triplet, this system is proof that fluorescent Ru(II) PS that append anthracene units through amide linkers is a reasonable design for molecular precursors to Ru(II)-Pt(II) assemblies that fluoresce from the PAH unit. It is hypothesized that the appended anthracene can be used to monitor the cellular distribution and localization using optical microscopy.. Additionally, these [Ru]-anthracene hybrid compound are hypothesized to deliver a burst of reactive cytotoxic agents through multiple photodynamic mechanisms, facilitated by the anthracene and Ru(II) unit(s) upon activation, to modify a variety of biological substrates, which can potentially circumvent the drug resistance feature commonly associated with MGs.

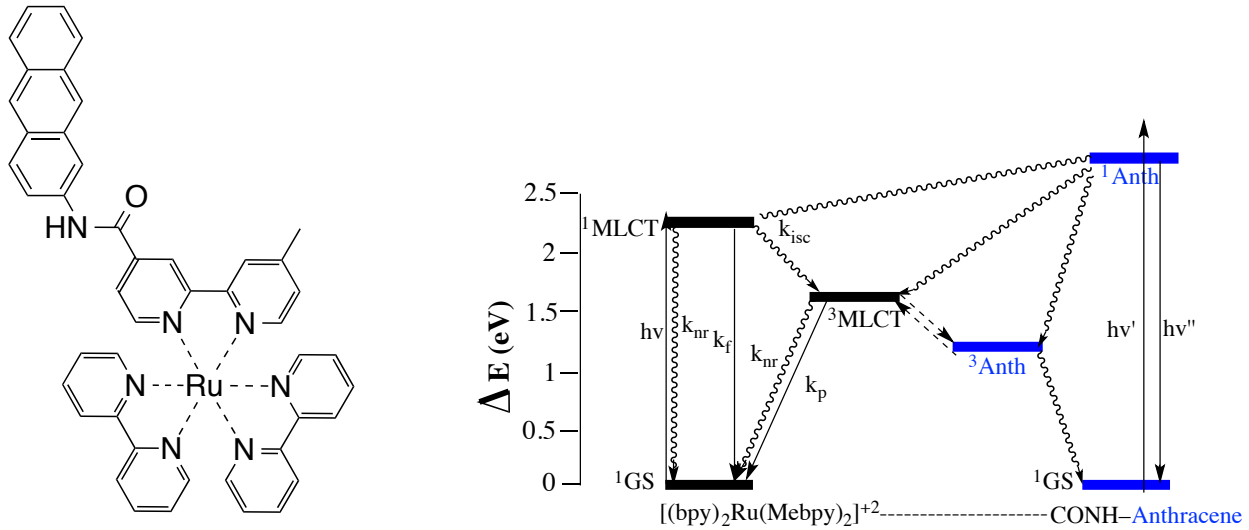

Figure 1.6. Structural representation of $[Ru(bpy)_2(Mebpy\text{-}anthracene)]^{2+}$ and relative energy diagrams.

Because cancer involves uncontrolled cell reproduction, DNA is a obvious intracellular target for drug therapy. DNA exists in a variety of topological configurations.[106-108] Ru(II) polyazine that append PAH units such as pyrene and anthracene units are capable of interacting with DNA by covalent and non-covalent interactions to cause significant structural modification to DNA.[25,68,106,109-111] The light-induced reactivity of the metal-organic Ru(II) complexes with DNA can be examined by DNA gel shift assays to determine the potential covalent and non-covalent modification process toward DNA.[68,110-112] These assays can monitor the binding propensity and oxidation of DNA, which is reflected by a change in size and charge as well as unwinding and/or cleavage of DNA.[48,112-115] Monitoring the change in electrophoretic migration and/or conversion of the native SC (Form I) to the open circular (Form II) through gel shift assays gives insight into the behavior of the metal complex-DNA adduct in the ground and excited state.[68,110,112] The oxidation of a single strand of DNA results in the unwinding of the SC form of DNA (Form I) to the relaxed OC form (Form II) significantly changing the size and migration of the DNA (Figure 1.7).

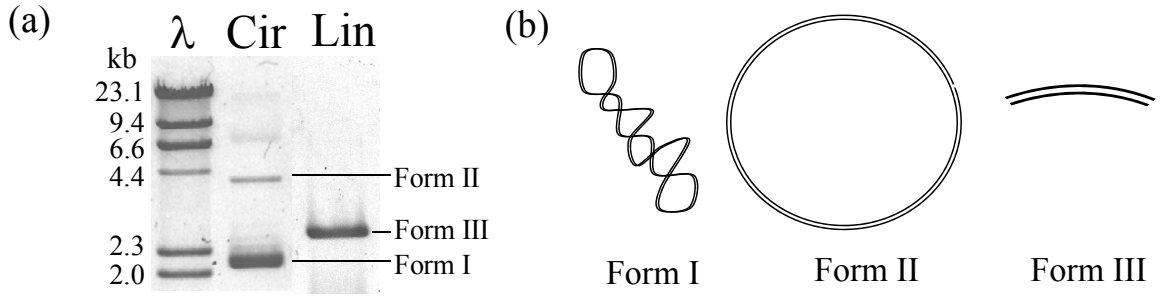

Figure 1.7. (a) DNA gel assay for supercoiled DAN illustrating supercoiled (Form I), open circular (Form II) and linear (Form III) DNA. Band assignments are based on Vinograd and Lebowitz. Reproduced from Zigler, D. F.; Brewer, K. J. "Toward Photodynamic Therapy of Cancer with Platinum Group Metal Polyazine Complexes" in Metal-Complexes-DNA Interactions, Wiley-Blackwell. λ is a Lambda DNA/HindIII molecular weight marker, Cir is circular plasmid DNA containing native supercoiled (Form I) and opencircular (Form II) plasmid DNA, and Lin is linear plasmid DNA (Form III) and (b) is a general illustration of the forms of DNA.

Cleavage of two DNA strands result in the linearization (Form III) of DNA displaying a different electrophoretic migration from the Form I and II.[106,107] Linearization of DNA by metal complexes can result in random and/or nonrandom double strand cleavage to yield DNA fragments of different sizes produced by multiple oxidation process.[107,116-122]

Metal-organic Ru(II) complexes can interact with DNA through electrostatic interactions, intercalation, minor and major grove binding, and covalent binding.[68,106] Photosensitizer $[Ru(phen)_2(pyip)]$ and $[Ru(phen)_2(aip)]^{2+}$ append pyrene and anthracene unit, respectively, to a Ru(II) photosensitizer with application in PDT (Figure 1.8).[123] The ruthenium complexes $[Ru(phen)_2(pyip)]^{2+}$ and $[Ru(phen)_2(aip)]^{2+}$ were shown to exhibit binding constant of $K_b = 1.57 \times 10^6\ M^{-1}$ and $K_b = 1.01 \times 10^6\ M^{-1}$, respectively, which suggest that these metal-organic Ru(II) complexes have enhanced intercalative attributed to the increase in surface area provided by the PAH units.[123] DNA photoclevage studies reveal that both $[Ru(phen)_2(pyip)]^{2+}$ and $[Ru(phen)_2(aip)]^{2+}$ cleave DNA through $^1O_2$ and •OH radicals mechanisms upon photoactivation with $\lambda = 450$ nm.

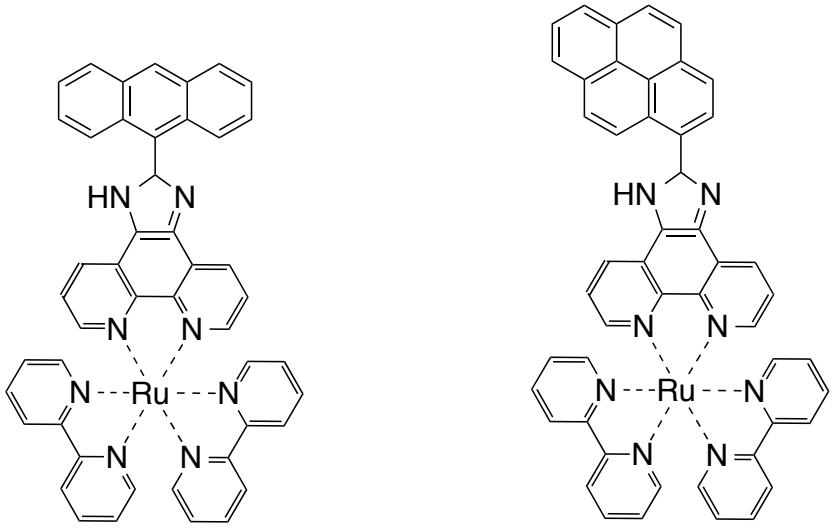

Figure 1.8. Molecular structure of metal-organic Ru(II) complexes.

Thus, in an effort to create a FT-OL-Ru(II) complex that can be used for Ru(II)-Pt(II) assemblies, anthracene fluorescent units will by appended to ruthenium systems of the form $[(bpy)_2Ru(dpp)]^{2+}$, (bpy = 2,2'-bipyridine and dpp = 2,3-bis(2-pyridyl)pyrazine), via amide linkers. This anthracene-Ru(II)-dpp PS arrangement will serve as a molecular precursor for novel Ru(II)-Pt(II) systems as well as structurally diverse Ru(II) photosensitizers for PDT.

1.7 **Exploring the anthracene-Ru(II)-dpp molecular architecture for fluorescent Ru(II)-Pt(II) systems**

The research in this dissertation describes the photophysical properties, interactions with biomolecules (DNA and proteins), and intracellular localization within mammalian cell of anthracene-Ru(II)-dpp complexes, Figure1.9.

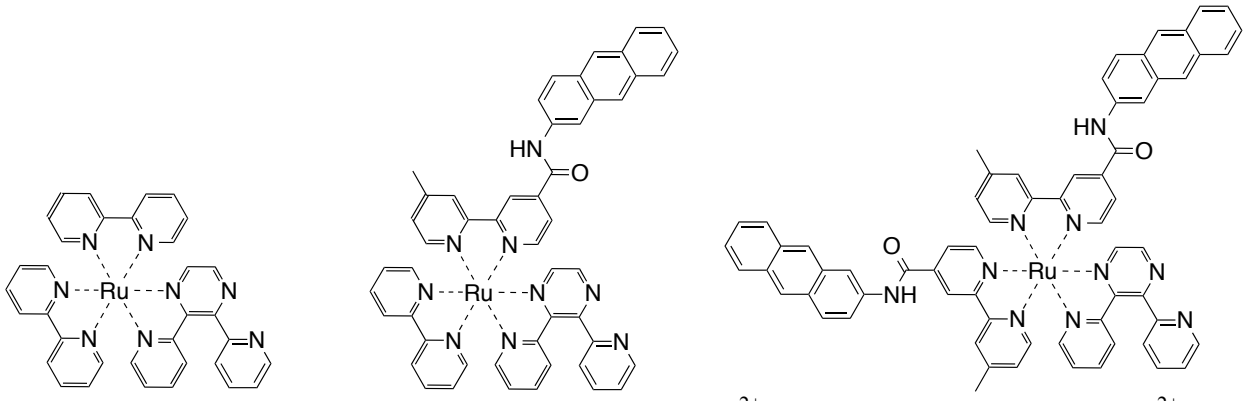

Figure 1.9. Structural representation of $[(bpy)_2Ru(dpp)]^{2+}$, $[(AnthbpyMe)(bpy)Ru(dpp)]^{2+}$, and $[(AnthbpyMe)_2Ru(dpp)]^{2+}$.

To the best of our knowledge this is the first attempt to synthesize fluorescent Ru(II) PSs for Ru(II)-Pt(II) assemblies of the form $[(bpy)_2Ru(dpp)PtCl_2]^{2+}$ by covalently appending anthracene motif(s) to the $[(bpy)_2Ru(dpp)]^{2+}$ framework through an amide linker. The photophysical properties (Chapter 2), the reactivity toward DNA and proteins structures (Chapter 3) and the *in vitro* behavior toward cells (Chapter 4) of these Ru(II)-anthracene hybrid systems are studied herein.

1.8 **References**

1. Maher, E. A.; Furnari, F. B.; Bachoo, R. M.; Rowitch, D. H.; Louis, D. N.; Cavenee, W. K.; DePinho, R. A., Malignant glioma: genetics and biology of a grave matter *Genes & Development.* **2001**, *15,* 1311-1333.
2. Hanahan, D.; Weinberg, R. A., The hallmarks of cancer *Cell.* **2000**, *100,* 57-70.
3. Society, A. C., Cancer facts and figures 2014 *American Cancer Society.* **2014**.
4. Farber, E., The multistep nature of cancer development *Cancer Research.* **1984**, *44,* 4217-4223.
5. Vogelstein, B.; Kinzler, K. W., The multistep nature of cancer *Trends in Genetics.* **1993**, *9,* 138-141.
6. Horne, S. D.; Pollick, S. A.; Heng, H. H. Q., Evolutionary mechanism unifies the hallmarks of cancer *International Journal of Cancer.* **2015**, *136,* 2012-2021.
7. Macheret, M.; Halazonetis, T. D., DNA replication stress as a hallmark of cancer *Annual review of pathology: mechanisms of disease.* **2015**, *10,* 425-448.
8. Wallach, D. F., Cellular membranes and tumor behavior: A new hypothesis *Proceedings of the National Academy of Sciences of the United States of America.* **1968**, *61,* 868-874.
9. Reardon, D. A.; Rich, J. N.; Friedman, H. S.; Bigner, D. D., Recent advances in the treatment of malignant astrocytoma *Journal of Clinical Oncology.* **2006**, *24,* 1253-1265.
10. Pobereskin, L.; Chadduck, J., Incidence of brain tumours in two English counties: a population based study *Journal of Neurology, Neurosurgery, and Psychiatry.* **2000**, *69,* 464-471.
11. Gudinaviciene, I.; Pranys, D.; Juozaityte, E., Impact of morphology and biology on the prognosis of patients with gliomas *Medicina.* **2004**, *40,* 112-120.
12. Goodenberger, M. L.; Jenkins, R. B., Genetics of adult glioma *Cancer Genetics.* **2012**, *205,* 613-621.
13. Castro, M. G.; Cowen, R.; Williamson, I. K.; David, A.; Jimenez-Dalmaroni, M. J.; Yuan, X.; Bigliari, A.; Williams, J. C.; Hu, J.; Lowenstein, P. R., Current and future strategies for the treatment of malignant brain tumors *Pharmacology & Therapeutics.* **2003**, *98,* 71-108.
14. Quick, A.; Patel, D.; Hadziahmetovic, M.; Chakravarti, A.; Mehta, M., Current therapeutic paradigms in glioblastoma *Reviews on Recent Clinical Trials.* **2010**, *5,* 14-27.
15. Burger, P. C.; Vogel, F. S.; Green, S. B.; Strike, T. A., Glioblastoma multiforme and anaplastic astrocytoma pathologic criteria and prognostic implications *Cancer.* **1985**, *56,* 1106-1111.
16. Yung, W. K. A.; Albright, R. E.; Olson, J.; Fredericks, R.; Fink, K.; Prados, M. D.; Brada, M.; Spence, A.; Hohl, R. J.; Shapiro, W.; Glantz, M.; Greenberg, H.; Selker, R. G.; Vick, N. A.; Rampling, R.; Friedman, H.; Phillips, P.; Bruner, J.; Yue, N.; Osoba, D.; Zaknoen, S.; Levin, V. A., A phase II study of temozolomide vs. procarbazine in patients with glioblastoma multiforme at first relapse *British Journal of Cancer.* **2000**, *83,* 588-593.
17. Friedman, H. S.; Kerby, T.; Calvert, H., Temozolomide and treatment of malignant glioma *Clinical Cancer Research.* **2000**, *6,* 2585-2597.

18. Westphal, M.; Hilt, D. C.; Bortey, E.; Delavault, P.; Olivares, R.; Warnke, P. C.; Whittle, I. R.; Jääskeläinen, J.; Ram, Z., A phase III trial of local chemotherapy with biodegradable carmustine wafers in patients with primary malignant glioma *Neuro-Oncology.* **2003**, *5,* 79-88.
19. Sharman, W. M.; Allen, C. M.; van Lier, J. E., Photodynamic therapeutics: basic principles and clinical applications *Drug Discovery Today.* **1999**, *4,* 507-517.
20. Muller, P. J.; Wilson, B. C., Photodynamic therapy of brain tumors-A work in progress *Lasers in Surgery and Medicine.* **2006**, *38,* 384-389.
21. Schmidt, M.; Meyer, G.; Reichert, K.; Cheng, J.; Krouwer, H.; Ozker, K.; Whelan, H., Evaluation of photodynamic therapy near functional brain tissue in patients with recurrent brain tumors *Journal of Neuro-Oncology.* **2004**, *67,* 201-207.
22. Allison, R. R.; Bagnato, V. S.; Cuenca, R.; Downie, G. H.; Sibata, C. H., The future of photodynamic therapy in oncology *Future Oncology.* **2006**, *2,* 53-71.
23. Castano, A. P.; Demidova, T. N.; Hamblin, M. R., Mechanisms in photodynamic therapy: part one—photosensitizers, photochemistry and cellular localization *Photodiagnosis and Photodynamic Therapy.* **2004**, *1,* 279-293.
24. Castano, A. P.; Demidova, T. N.; Hamblin, M. R., Mechanisms in photodynamic therapy: part two—cellular signaling, cell metabolism and modes of cell death *Photodiagnosis and Photodynamic Therapy.* **2005**, *2,* 1-23.
25. Fleisher, M. B.; Waterman, K. C.; Turro, N. J.; Barton, J. K., Light-induced cleavage of DNA by metal complexes *Inorganic Chemistry.* **1986**, *25,* 3549-3551.
26. Fiers, W.; Beyaert, R.; Declercq, W.; Vandenabeele, P., More than one way to die: apoptosis, necrosis and reactive oxygen damage *Oncogene.* **1999**, *18,* 7719.
27. Szaciłowski, K.; Macyk, W.; Drzewiecka-Matuszek, A.; Brindell, M.; Stochel, G., Bioinorganic photochemistry: Frontiers and mechanisms *Chemical Reviews.* **2005**, *105,* 2647-2694.
28. Wang, J.; Higgins, S. L. H.; Winkel, B. S. J.; Brewer, K. J., A new Os,Rh bimetallic with O_2 independent DNA cleavage and DNA photobinding with red therapeutic light excitation *Chemical Communications.* **2011**, *47,* 9786-9788.
29. Gomer, C. J., Preclinical examination of first and second generation photosensitizers used in photodynamic therapy *Photochemistry and Photobiology.* **1991**, *54,* 1093-1107.
30. Josefsen, L. B.; Boyle, R. W., Photodynamic therapy: novel third-generation photosensitizers one step closer? *British Journal of Pharmacology.* **2008**, *154,* 1-3.
31. Moan, J., Properties for optimal PDT sensitizers *Journal of Photochemistry and Photobiology B.* **1990**, *5,* 521-524.
32. Heidary, D. K.; Howerton, B. S.; Glazer, E. C., Coordination of hydroxyquinolines to a ruthenium bis-dimethyl-phenanthroline scaffold radically improves potency for potential as antineoplastic agents *Journal of Medicinal Chemistry.* **2014**, *57,* 8936-8946.
33. Heidary, D. K.; Glazer, E. C., A light-activated metal complex targets both DNA and RNA in a fluorescent in vitro transcription and translation assay *ChemBioChem.* **2014**, *15,* 507-511.
34. Shi, G.; Monro, S.; Hennigar, R.; Colpitts, J.; Fong, J.; Kasimova, K.; Yin, H.; DeCoste, R.; Spencer, C.; Chamberlain, L.; Mandel, A.; Lilge, L.; McFarland, S. A., Ru(II) dyads derived from α-oligothiophenes: A new class of potent and versatile photosensitizers for PDT *Coordination Chemistry Reviews.* **2015**, *282–283,* 127-138.

35. Hartinger, C. G.; Dyson, P. J., Bioorganometallic chemistry-from teaching paradigms to medicinal applications *Chemical Society Reviews.* **2009**, *38*.
36. Van Rijt, S. H.; Sadler, P. J., Current applications and future potential for bioinorganic chemistry in the development of anticancer drugs *Drug Discovery Today.* **2009**, *14,* 1089-1097.
37. Gasser, G.; Ott, I.; Metzler, N. N., Organometallic anticancer compounds *Journal of Medicinal Chemistry.* **2011**, *54,* 3-25.
38. Boerner, L. J. K.; Zaleski, J. M., Metal complex-DNA interactions: from transcription inhibition to photoactivated cleavage *Current Opinion in Chemical Biology.* **2005**, *9,* 135-144.
39. Milkevitch, M.; Brauns, E.; Brewer, K. J., Spectroscopic and electrochemical properties of a series of mixed-metal d6,d8 bimetallic complexes of the form $[(bpy)_2M(BL)PtCl_2]^{2+}$ (bpy=2,2'-bipyridine; BL=dpq (2,3-bis(2-pyridyl)quinoxaline) or dpb (2,3-bis(2-pyridyl)benzoquinoxaline); M=Os-II or Ru-II) *Inorganic Chemistry.* **1996**, *35,* 1737-&.
40. Erkkila, K. E.; Odom, D. T.; Barton, J. K., Recognition and reaction of metallointercalators with DNA *Chemical Reviews.* **1999**, *99,* 2777-2795.
41. Abdel-Shafi, A. A.; Worrall, D. R.; Ershov, A. Y., Photosensitized generation of singlet oxygen from ruthenium(II) and osmium(II) bipyridyl complexes *Dalton Transactions.* **2004**, 30-36.
42. Hergueta Bravo, A.; Jiménez Hernández, M. E.; Montero, F.; Oliveros, E.; Orellana, G., Singlet oxygen-mediated DNA photocleavage with Ru(II) polypyridyl complexes *Journal of Physical Chemistry B.* **2002**, *106,* 4010-4017.
43. Clarke, M. J., Ruthenium metallopharmaceuticals *Coordination Chemistry Reviews.* **2003**, *236,* 209-233.
44. Juris, A.; Balzani, V.; Barigelletti, F.; Campagna, S.; Belser, P.; Von Zelewsky, A., Ru(II) polypyridine complexes: photophysics, photochemistry, eletrochemistry, and chemiluminescence *Coordination Chemistry Reviews.* **1988**, *84,* 85-277.
45. Balzani, V.; Bergamini, G.; Marchioni, F.; Ceroni, P., Ru(II)-bipyridine complexes in supramolecular systems, devices and machines *Coordination Chemistry Reviews.* **2006**, *250,* 1254-1266.
46. Fleisher, M. B.; Waterman, K. C.; Turro, N. J.; Barton, J. K., Light-induced cleavage of DNA by metal-complexes *Inorganic Chemistry.* **1986**, *25,* 3349-3351.
47. Demas, J. N.; Diemente, D.; Harris, E. W., Oxygen quenching of charge-transfer excited states of ruthenium(II) complexes. Evidence for singlet oxygen production *Journal of the American Chemical Society.* **1973**, *95,* 6864-6865.
48. Mongelli, M. T.; Heinecke, J.; Mayfield, S.; Okyere, B.; Winkel, B. S. J.; Brewer, K. J., Variation of DNA photocleavage efficiency for $[(TL)_2Ru(dpp)]Cl_2$ complexes where TL=2,2'-bipyridine, 1,10-phenanthroline, or 4,7-diphenyl-1,10-phenanthroline *Journal of Inorganic Biochemistry.* **2006**, *100,* 1983-1987.
49. Jamieson, E. R.; Lippard, S. J., Structure, recognition, and processing of cisplatin-DNA adducts *Chemical Reviews.* **1999**, *99,* 2467-2498.
50. Weiss, R.; Christian, M., New cisplatin analogues in development *Drugs.* **1993**, *46,* 360-377.
51. Wang, X.; Guo, Z., Targeting and delivery of platinum-based anticancer drugs *Chemical Society Reviews.* **2013**, *42,* 202-224.

52. Lippard, S. J.; Bond, P. J.; Wu, K. C.; Bauer, W. R., Sterochmemical requirments for intercalation of platinum complexes into double-stranded DNAS *Science.* **1976**, *194,* 726-728.
53. Howegrant, M.; Wu, K. C.; Bauer, W. R.; Lippard, S. J., Binding of platinum and palladium metallointercalation reagents and antitumor drugs to closed and open DNA *Biochemistry.* **1976**, *15,* 4339-4346.
54. Balzani, V.; Juris, A.; Venturi, M.; Campagna, S.; Serroni, S., Luminescent and redox-active polynuclear transition metal complexes *Chemical Reviews.* **1996**, *96,* 759-834.
55. White, T. A.; Whitaker, B. N.; Brewer, K. J., Discovering the balance of steric and electronic factors needed to provide a new structural motif for photocatalytic hydrogen production from water *Journal of the American Chemical Society.* **2011**, *133,* 15332-15334.
56. Balzani, V.; Moggi, L.; Scandola, F., Towards a supramolecular photochemistry: assembly of molecular components to obtain photochemical molecular devices. In *Supramolecular Photochemistry*, Balzani, V., Ed. Springer Netherlands: 1987; Vol. 214, pp 1-28.
57. Manbeck, G. F.; Brewer, K. J., Photoinitiated electron collection in polyazine chromophores coupled to water reduction catalysts for solar H2 production *Coordination Chemistry Reviews.* **2013**, *257,* 1660-1675.
58. Fang, Z.; Swavey, S.; Holder, A.; Winkel, B.; Brewer, K. J., DNA binding of mixed-metal supramolecular Ru, Pt complexes *Inorganic Chemistry Communications.* **2002**, *5,* 1078-1081.
59. Williams, R. L.; Toft, H. N.; Winkel, B.; Brewer, K. J., Synthesis, characterization, and DNA binding properties of a series of Ru, Pt mixed-metal complexes *Inorganic Chemistry.* **2003**, *42,* 4394-4400.
60. Jain, A.; Wang, J.; Mashack, E. R.; Winkel, B. S. J.; Brewer, K. J., Multifunctional DNA interactions of Ru-Pt mixed metal supramolecular complexes with substituted terpyridine ligands *Inorganic Chemistry.* **2009**, *48,* 9077-9084.
61. Milkevitch, M.; Shirley, B. W.; Brewer, K. J., Mixed-metal polymetallic platinum complexes designed to interact with DNA *Inorganica Chimica Acta.* **1997**, *264,* 249-256.
62. van der Schilden, K.; Garcìa, F.; Kooijman, H.; Spek, A. L.; Haasnoot, J. G.; Reedijk, J., A highly flexible dinuclear ruthenium(III)–p[latinum(II) complex: Crystal structure and binding to 9-ethylguanine *Angewandte Chemie International Edition.* **2004**, *43,* 5668-5670.
63. Williams, R. L.; Toft, H. N.; Winkel, B.; Brewer, K. J., Synthesis, characterization, and DNA dinding properties of a series of Ru, Pt mixed-metal complexes *Inorganic Chemistry.* **2003**, *42,* 4394-4400.
64. Higgins, S. L. H.; White, T. A.; Winkel, B. S. J.; Brewer, K. J., Redox, spectroscopic, and photophysical properties of Ru-Pt mixed-metal complexes incorporating 4,7-diphenyl-1,10-phenanthroline as efficient DNA binding and photocleaving agents *Inorganic Chemistry.* **2011**, *50,* 463-470.
65. Higgins, S. L. H.; Tucker, A. J.; Winkel, B. S. J.; Brewer, K. J., Metal to ligand charge transfer induced DNA photobinding in a Ru(II)-Pt(II) supramolecule using red light in the therapeutic window: a new mechanism for DNA modification *Chemical Communications.* **2012**, *48,* 67-69.

66. Higgins, S. L. H.; Brewer, K. J., Designing red-light-activated multifunctional agents for the photodynamic therapy *Angewandte Chemie International Edition.* **2012**, *51,* 11420-11422.
67. Miao, R.; Mongelli, M. T.; Zigler, D. F.; Winkel, B. S. J.; Brewer, K. J., A multifunctional tetrametallic Ru-Pt supramolecular complex exhibiting both DNA binding and photocleavage *Inorganic Chemistry.* **2006**, *45,* 10413-10415.
68. Knoll, J. D.; Brewer, K. J., A new paradigm for photodynamic therapy drug design: multifunctional, supramolecular DNA photomodification agents featuring Ru(II)/Os(II) light absorbers coupled to Pt(II) or Rh(III) bioactive sites. In *Progress in Inorganic Chemistry: Volume 59*, John Wiley & Sons, Inc.: 2014; pp 189-244.
69. Knoll, J. D.; Arachchige, S. M.; Wang, G.; Rangan, K.; Miao, R.; Higgins, S. L. H.; Okyere, B.; Zhao, M.; Croasdale, P.; Magruder, K.; Sinclair, B.; Wall, C.; Brewer, K. J., Electrochemical, spectroscopic, and photophysical properties of structurally diverse polyazine-bridged Ru(II),Pt(II) and Os(II),Ru(II), Pt(II) supramolecular motifs *Inorganic Chemistry.* **2011**, *50,* 8850-8860.
70. Knoll, J. D.; Arachchige, S. M.; Brewer, K. J., A structurally diverse RuII,PtII tetrametallic motif for photoinitiated electron collection and photocatalytic hydrogen production *ChemSusChem.* **2011**, *4,* 252-261.
71. Knoll, J. D.; Arachchige, S. M.; Wang, G.; Rangan, K.; Miao, R.; Higgins, S. L. H.; Okyere, B.; Zhao, M.; Croasdale, P.; Magruder, K.; Sinclair, B.; Wall, C.; Brewer, K. J., Electrochemical, Spectroscopic, and Photophysical Properties of Structurally Diverse Polyazine-Bridged Ru(II),Pt(II) and Os(II),Ru(II),Pt(II) Supramolecular Motifs *Inorganic Chemistry.* **2011**, *50,* 8850-8860.
72. Knoll, J. D.; Higgins, S. L. H.; White, T. A.; Brewer, K. J., Subunit variation to uncover properties of polyazine-bridged Ru(II), Pt(II) supramolecules with low lying charge separated states providing Insight into the functioning as H_2O reduction photocatalysts to produce H_2 *Inorganic Chemistry.* **2013**, *52,* 9749-9760.
73. Sakai, K.; Ozawa, H.; Yamada, H.; Tsubomura, T.; Hara, M.; Higuchi, A.; Haga, M.-a., A tris(2,2'-bipyridine)ruthenium(II) derivative tethered to a cis-$PtCl_2(amine)_2$ moiety: syntheses, spectroscopic properties, and visible-light-induced scission of DNA *Dalton Transactions.* **2006**, 3300-3305.
74. Zhu, J.; Prussin, R.; Dominijanni, A.; Brewer, K. J.; Robertson, J. L., Exploring cellular activity of a polyazine bridged Ru(II)–Pt(II) supramolecule in rat malignant glioma F98 *Manuscript in progress.* **2015**.
75. Holder, A. A.; Zigler, D. F.; Tarrago-Trani, M. T.; Storrie, B.; Brewer, K. J., Photobiological impact of $[\{(bpy)_2Ru(dpp)\}_2RhCl_2]Cl_5$ and $[\{(bpy)_2Os(dpp)\}_2RhCl_2]Cl_5$ [bpy = 2,2‘-Bipyridine; dpp = 2,3-Bis(2-pyridyl)pyrazine] on vero cells *Inorganic Chemistry.* **2007**, *46,* 4760-4762.
76. Yam, V. W. W.; Lee, V. W. M.; Cheung, K. K., Synthesis, photophysics, electrochemistry, and reactivity of ruthenium(II) polypyridine complexes with organoplatinum(II) moieties. crystal structure of $[Ru(bpy)_2(\mu\text{-}2,3\text{-}dpp)PdCl_2]^{2+}$ *Organometallics.* **1997**, *16,* 2833-2841.
77. Creutz, C.; Chou, M.; Netzel, T. L.; Okumura, M.; Sutin, N., Lifetimes, spectra, and quenching of the excited states of polypyridine complexes of iron(II), ruthenium(II), and osmium(II) *Journal of the American Chemical Society.* **1980**, *102,* 1309-1319.

78. Meyer, T. J., Photochemistry of metal coordination complexes: metal to ligand charge transfer excited states. In *Pure and Applied Chemistry*, 1986; Vol. 58, p 1193.
79. Damrauer, N. H.; McCusker, J. K., Ultrafast dynamics in the metal-to-ligand charge transfer excited-state evolution of $[Ru(4,4'\text{-diphenyl-}2,2'\text{-bipyridine})_3]^{2+}$ *Journal of Physical Chemistry A.* **1999**, *103,* 8440-8446.
80. McClenaghan, N. D.; Barigelletti, F.; Maubert, B.; Campagna, S., Towards ruthenium(II) polypyridine complexes with prolonged and predetermined excited state lifetimes *Chemical Communications.* **2002**, 602-603.
81. Ford, W. E.; Rodgers, M. A. J., Reversible triplet-triplet energy transfer within a covalently linked bichromophoric molecule *Journal of Physical Chemistry.* **1992**, *96,* 2917-2920.
82. Tyson, D. S.; Henbest, K. B.; Bialecki, J.; Castellano, F. N., Excited state processes in ruthenium(II)/pyrenyl complexes displaying extendedlifetimes *Journal of Physical Chemistry A.* **2001**, *105,* 8154-8161.
83. Pittau, R.; Baba, A. I.; Shaw, J. R.; Simon, J. A.; Thummel, R. P.; Schmehl, R. H., The photophysical behavior of complexes having nearly isoenergetic MLCT and ligand localized excited states *Coordination Chemistry Reviews.* **1998**, *171,* 43-59.
84. McClenaghan, N. D.; Leydet, Y.; Maubert, B.; Indelli, M. T.; Campagna, S., Excited-state equilibration: a process leading to long-lived metal-to-ligand charge transfer luminescence in supramolecular systems *Coordination Chemistry Reviews.* **2005**, *249,* 1336-1350.
85. Reichardt, C.; Pinto, M.; Wächtler, M.; Stephenson, M.; Kupfer, S.; Sainuddin, T.; Guthmuller, J.; McFarland, S. A.; Dietzek, B., Photophysics of Ru(II) dyads derived from pyrenyl-substitued imidazo[4,5-f][1,10]phenanthroline ligands *Journal of Physical Chemistry A.* **2015**, *119,* 3986-3994.
86. Stephenson, M.; Reichardt, C.; Pinto, M.; Wächtler, M.; Sainuddin, T.; Shi, G.; Yin, H.; Monro, S.; Sampson, E.; Dietzek, B.; McFarland, S. A., Ru(II) dyads derived from 2-(1-pyrenyl)-1H-imidazo[4,5-f][1,10]phenanthroline: versatile photosensitizers for photodynamic applications *Journal of Physical Chemistry A.* **2014**, *118,* 10507-10521.
87. Wilson, G. J.; Launikonis, A.; Sasse, W. H. F.; Mau, A. W. H., Excited-state processes in ruthenium(II) bipyridine complexes containing covalently bound arenes *Journal of Physical Chemistry A.* **1997**, *101,* 4860-4866.
88. Kercher, M.; König, B.; Zieg, H.; De Cola, L., Photoinduced energy- and electron-eransfer processes within dynamic self-assembled donor−acceptor arrays *Journal of the American Chemical Society.* **2002**, *124,* 11541-11551.
89. Schoonover, J. R.; Dattelbaum, D. M.; Malko, A.; Klimov, V. I.; Meyer, T. J.; Styers-Barnett, D. J.; Gannon, E. Z.; Granger, J. C.; Aldridge, W. S.; Papanikolas, J. M., Ultrafast energy transfer between the 3MLCT state of $[RuII(dmb)_2(bpy\text{-}an)]^{2+}$ and the covalently appended anthracene *Journal of Physical Chemistry A.* **2005**, *109,* 2472-2475.
90. El-ghayoury, A.; Harriman, A.; Khatyr, A.; Ziessel, R., Intramolecular triplet energy transfer in metal polypyridine complexes bearing ethynylated aromatic groups *Journal of Physical Chemistry A.* **2000**, *104,* 1512-1523.
91. Albano, G.; Balzani, V.; Constable, E. C.; Maestri, M.; Smith, D. R., Photoinduced processes in 4′ -(9-anthryl)-2,2′ :6′ ,2″ -terpyridine, its protonated forms and Zn(II), Ru(II) and Os(II) complexes *Inorganica Chimica Acta.* **1998**, *277,* 225-231.

92. Serroni, S.; Campagna, S.; Pistone Nascone, R.; Hanan, G. S.; Davidson, G. J. E.; Lehn, J.-M., Controlling the eirection of photoinduced energy transfer in multicomponent species *Chemistry- A European Journal.* **1999**, *5,* 3523-3527.
93. Castellano, F. N., Altering molecular photophysics by merging organic and inorganic chromophores *Accounts of Chemical Research.* **2015**, *48,* 828-839.
94. Zigler, D. F.; Elvington, M. C.; Heinecke, J.; Brewer, K. J., Luminescently tagged 2,2‘-bipyridine complex of FeII: synthesis and photophysical studies of 4-[N-(2-anthryl)carbamoyl]-4‘-methyl-2,2‘-bipyridine *Inorganic Chemistry.* **2006**, *45,* 6565-6567.
95. Nazarov, A. A.; Risse, J.; Ang, W. H.; Schmitt, F.; Zava, O.; Ruggi, A.; Groessl, M.; Scopelitti, R.; Juillerat-Jeanneret, L.; Hartinger, C. G.; Dyson, P. J., Anthracene-tethered ruthenium(II) arene complexes as tools to visualize the cellular localization of putative organometallic anticancer compounds *Inorganic Chemistry.* **2012**, *51,* 3633-3639.
96. Azumaya, I.; Kagechika, H.; Fujiwara, Y.; Itoh, M.; Yamaguchi, K.; Shudo, K., Twisted intramolecular charge-transfer fluorescence of aromatic amides: conformation of the amide bonds in excited states *Journal of the American Chemical Society.* **1991**, *113,* 2833-2838.
97. Lewis, F. D.; Liu, W., Luminescence of N-arylbenzamides in low-temperature glasses *Journal of Physical Chemistry A.* **1999**, *103,* 9678-9686.
98. del Valle, J. C.; Turek, A. M.; Tarkalanov, N. D.; Saltiel, J., Distortion of the fluorescence spectrum of anthracene with increasing laser pulse excitation energy *Journal of Physical Chemistry A.* **2002**, *106,* 5101-5104.
99. Ghazy, R.; Zim, S. A.; Shaheen, M.; El-Mekawey, F., Energy transfer and excited state lifetime of some anthracene laser dyes *Optics & Laser Technology.* **2004**, *36,* 463-469.
100. Basu, U.; Khan, I.; Hussain, A.; Kondaiah, P.; Chakravarty, A. R., Photodynamic effect in near-IR light by a photocytotoxic iron(III) cellular imaging agent *Angewandte Chemie International Edition.* **2012**, *51,* 2658-2661.
101. Simon, J. A.; Curry, S. L.; Schmehl, R. H.; Schatz, T. R.; Piotrowiak, P.; Jin, X.; Thummel, R. P., Intramolecular electronic energy transfer in ruthenium(II) diimine donor/pyrene acceptor complexes linked by a single C−C bond *Journal of the American Chemical Society.* **1997**, *119,* 11012-11022.
102. Weinheimer, C.; Choi, Y.; Caldwell, T.; Gresham, P.; Olmsted Iii, J., Effect of a steric spacer on chromophoric interactions of ruthenium complexes containing covalently bound anthracene *Journal of photochemistry and photobiology A.* **1994**, *78,* 119-126.
103. Wilson, G. J.; Sasse, W. H. F.; Mau, A. W. H., Singlet and triplet energy transfer processes in ruthenium(II) bipyridine complexes containing covalently bound arenes *Chemical Physics Letters.* **1996**, *250,* 583-588.
104. C.A., P., Photoluminescence of solutions *Elsevier, Amsterdam.* **1968**.
105. de Carvalho, I. M. M.; de Sousa Moreira, Í.; Gehlen, M. H., Synthesis, characterization, and photophysical studies of new bichromophoric ruthenium(II) complexes *Inorganic Chemistry.* **2003**, *42,* 1525-1531.
106. Zigler, D. F.; Brewer, K. J., Toward photodynamic therapy of cancer with platinum group metal polyazine complexes *Wiley-Blackwell: Oxford, UK,.* **2009**.
107. Vinograd, J.; Lebowitz, J., Physical and topological properties of circular DNA *Journal of General Physiology.* **1966**, *49,* 103-125.

108. Ravanat, J.-L.; Cadet, J., Reaction of singlet oxygen with 2'-deoxyguanosine and DNA. Isolation and characterization of the main oxidation products *Chemical Research in Toxicology.* **1995**, *8,* 379-388.
109. Garner, R. N.; Joyce, L. E.; Turro, C., Effect of electronic structure on the photoinducedligand exchange of Ru(II) polypyridine complexes *Inorganic Chemistry.* **2011**, *50,* 4384-4391.
110. Wang, J.; Arachchige, S.; Brewer, K. J., Supramolecular complex design and function for photodynamic therapy and solar energy conversion via hydrogen production. Common requirements for molecular architectures for varied light-activated processes *Boca Raton, FL : CRC Press, US.* **2012**.
111. Clarke, M. J.; Zhu, F.; Frasca, D. R., Non-platinum chemotherapeutic metallopharmaceuticals *Chemical Reviews.* **1999**, *99,* 2511-2534.
112. Prussin Ii, A. J.; Zigler, D. F.; Jain, A.; Brown, J. R.; Winkel, B. S. J.; Brewer, K. J., Photochemical methods to assay DNA photocleavage using supercoiled pUC18 DNA and LED or xenon arc lamp excitation *Journal of Inorganic Biochemistry.* **2008**, *102,* 731-739.
113. Jain, A.; Slebodnick, C.; Winkel, B. S. J.; Brewer, K. J., Enhanced DNA photocleavage properties of Ru(II) terpyridine complexes upon incorporation of methylphenyl substituted terpyridine and/or the polyazine bridging ligand dpp (2,3-bis(2-pyridyl)pyrazine) *Journal of Inorganic Biochemistry.* **2008**, *102,* 1854-1861.
114. Wachter, E.; Heidary, D. K.; Howerton, B. S.; Parkin, S.; Glazer, E. C., Light-activated ruthenium complexes photobind DNA and are cytotoxic in the photodynamic therapy window *Chemical Communications.* **2012**, *48,* 9649-9651.
115. Mongelli, M. T.; Heinecke, J.; Mayfield, S.; Okyere, B.; Winkel, B. S. J.; Brewer, K. J., Variation of DNA photocleavage efficiency for [(TL)2Ru(dpp)]Cl2 complexes where TL = 2,2′ -bipyridine, 1,10-phenanthroline, or 4,7-diphenyl-1,10-phenanthroline *Journal of Inorganic Biochemistry.* **2006**, *100,* 1983-1987.
116. Jin, Y.; Cowan, J. A., DNA cleavage by copper complexes. Factors influencing cleavage mechanism and linearization of dsDNA *Journal of the American Chemical Society.* **2005**, *127,* 8408-8415.
117. Huang, C. H.; Mirabelli, C. K.; Mong, S.; Crooke, S. T., Intermolecular cross-linking of DNA through bifunctional intercalation of an antitumor antibiotic *Cancer Research.* **1983**, *43,* 2718-2724.
118. Breslin, D. T.; Yu, C.; Ly, D.; Schuster, G. B., Structural modification changes the DNA binding mode of cation-substituted anthraquinone photonucleases: association by Iintercalation or minor groove binding determines the DNA cleavage efficiency *Biochemistry.* **1997**, *36,* 10463-10473.
119. Kumar, C. V.; Tan, W. B.; Betts, P. W., Hexamminecobalt(III) chloride assisted, visible light induced, sequence dependent cleavage of DNA *Journal of Inorganic Biochemistry.* **1997**, *68,* 177-181.
120. Blackburn, G. M.; Taussig, P. E., The photocarcinogenicity of anthracence: photochemical binding to deoxyribonucleic acid in tissue culture *Biochemical Journal.* **1975**, *149,* 289-291.
121. Sinha, B. K.; Chignell, C. F., Binding of anthracene to cellula macromolecules in the presence of light *Photochemistry and Photobiology.* **1983**, *37,* 33-37.
122. Armitage, B., Photocleavage of nucleic acids *Chemical Reviews.* **1998**, *98,* 1171-1200.

123. Mariappan, M.; Maiya, B. G., Effects of anthracene and pyrene units on the interactions of novel polypyridyl ruthenium(II) mixed-ligand complexes with DNA *European Journal of Inorganic Chemistry*. **2005**, *2005,* 2164-2173.

Chapter 2 Pushing the limits of structurally-diverse light-harvesting Ru(II) metal-organic chromophores for photodynamic therapy

Roberto Padilla[a]*, William A. Maza[a], Anthony J. Dominijanni[c], Brenda S. J. Winkel[b], Amanda J. Morris[a], and Karen J. Brewer[a†]

[a]Department of Chemistry, Virginia Tech, Blacksburg, VA 24061-0212 VA 24061-0212.

[b]Department of Biological Sciences, Virginia Tech, Blacksburg, VA 24061-0406.

[c]Department of Biomedical Engineering and Mechanics, Virginia Tech, Blacksburg, VA 24061-0442

* Corresponding author e-mail: rpadill4@vt.edu (Roberto Padilla)
† Deceased October 24, 2014

Keywords: Photodynamic therapy, metal-organic Ru(II), anthracene, photocytotoxicity, bichromatic

Foreword. This chapter represents a stand-alone manuscript that was submitted to *The Journal of Photochemistry and Photobiology A* currently accepted and under revision. The work presented in this manuscript was done by Roberto Padilla with the assistance of William A. Maza for emission lifetimes and Anthony J. Dominijanni for phototoxicity assays. This was supervised by Professors Brenda S. J. Winkel[b], Professors Amanda J. Morris[a], and Professors Karen J. Brewer[a†].

2.1 Abstract

The synthesis of Ru(II) derivatives $[(AnthbpyMe)(bpy)Ru(dpp)]^{2+}$ **(2)** and $[(AnthbpyMe)_2Ru(dpp)]^{2+}$ **(3)**, and the analysis of their excited state properties as well as their photocytotoxicity against glioma cells are reported. Complexes **2** and **3** absorb visible light with metal-to-ligand charge transfer (MLCT) transitions at λ_{max} = 459 nm (16,000 $M^{-1}cm^{-1}$) and λ_{max} = 461 nm (21,000 $M^{-1}cm^{-1}$), respectively. The complexes exhibit bichromatic properties with the ^{3}MLCT emission centered at λ_{em} = 661 nm and λ_{em} = 663 nm for **2** and **3**, respectively, while the anthracene motif(s) has emission from 450 – 560 nm. The anthracene unit(s) quench the ^{3}MLCT

to give quantum yields (lifetime, τ) of $\Phi_{em} = 0.0059$ (τ = 398 ns) and $\Phi_{em} = 0.0011$ (τ = 414 ns) for **2** and **3**, respectively. The quenching rates were found to be 6.61×10^5 s^{-1} for **2** and 5.64×10^5 s^{-1} for **3**. Electrochemistry reveals an irreversible anthracene oxidation at 1.23 – 1.28 V, while the $Ru^{III/II}$ oxidation process occurs at a potential of 1.53 – 1.55 V. The complexes displayed a quasi-reversible reduction couple attributed to $dpp^{0/-1}$ at 0.98 V. Cytotoxicity of both complexes towards F98 glioma cells was moderate in the absence of light and substantially enhanced with visible light.

2.2 Introduction

Ruthenium(II) tris(2,2'-bipyridine), $[Ru(bpy)_3]^{2+}$ (bpy = 2, 2'-bipyridine), and its derivatives have been extensively studied due to their rich ground and excited state properties.[1-5] These photoactive molecules can be appended with rigid, highly conjugated, and planar organic chromophores through an insulating spacer to tune the photo-chemical and physical properties.[6-14] These metal-organic Ru(II) complexes are known to modify vital biological macromolecules, such as DNA, through oxygen-mediated processes and show promising anticancer activity *in vitro*.[15-21] However, the oxygen-dependence of these Ru(II) PDT agents limit their effectiveness against aggressive, highly-invasive, and neurologically-destructive brain cancers (i.e. malignant gliomas) due to the hypoxic environments that commonly characterize these tumors.[22-24] Thus, there is an urgent need for new molecular architectures of metal-organic Ru(II) PDT agents offering versatile photomodification pathways of vital cellular components (DNA, RNA, and proteins), independent of reactive oxygen species, to treat MGs and other intractable cancers.

Ruthenium PDT agents of the form $[(TL)_2Ru(BL)]^{2+}$ (TL = 2,2'-bipyridine (bpy), 1,10-phenanthroline (phen), 4,7-diphenyl-1,10-phenanthroline (Ph_2phen), and BL = 2,3-bis(2-pyridyl)pyrazine (dpp)) are known to photooxidize DNA by $^1O_2$ generated through excited state

energy transfer between the $[(TL)_2Ru(BL)]^{2+}$ triplet metal-to-ligand, ^{3}MLCT, excited state and molecular oxygen.[25] Covalent coupling of known oxygen-independent DNA oxidizing agents through insulating amide bonds may offer an attractive approach for generating novel metal-organic Ru(II) chromophores to treat MG brain cancer through visible light activation.[26-29] Ru(II) chromophores containing dpp ligands possess the unique added advantage of being able to chelate biologically-relevant cations (i.e. Na^+, K^+, Ca^{2+}, etc.), leading to disruption of cell homeostasis.[30] Ru(II) complexes that incorporate a π-expansive organic unit, such as anthracene, through diverse organic linkers demonstrate that photophysical properties and photodynamic potency can be influenced by controlling excited state dynamics.[8,31] The [Ru]-anthracene hybrid arrangement provides multiple pathways, singlet-singlet, triplet-triplet, and/or singlet-triplet, for deactivation of excited states through energy or electron transfer, which can increase the photoreactivity with biological molecules. Therefore, the proposed molecular architecture of the form anthracene-Ru(II)-dpp is a type of metal-organic Ru(II) complex that can offer multifunctional reactivity to enhance photodynamic potency against aggressive and invasive brain cancers.

Reported herein are two metal-organic Ru(II) complexes based on anthracene tethered via bpyMe (AnthbpyMe = 4-[N-(2-anthryl)carbamoyl]-4′-methyl-2,2′-bipyridine) to $[(bpy)_2Ru(dpp)]^{2+}$ (1). The metal complexes, $[(AnthbpyMe)(bpy)Ru(dpp)]^{2+}$ (2) and $[(AnthbpyMe)_2Ru(dpp)]^{2+}$ (3), were synthesized and their ground and excited states characterized (Figure 2.1). The complexes were also tested for photocytotoxicity against F98 rat glioma cells. The results of these studies indicate that these Ru(II)-anthranyl complexes have promise for the development of multifunctional PDT agents.

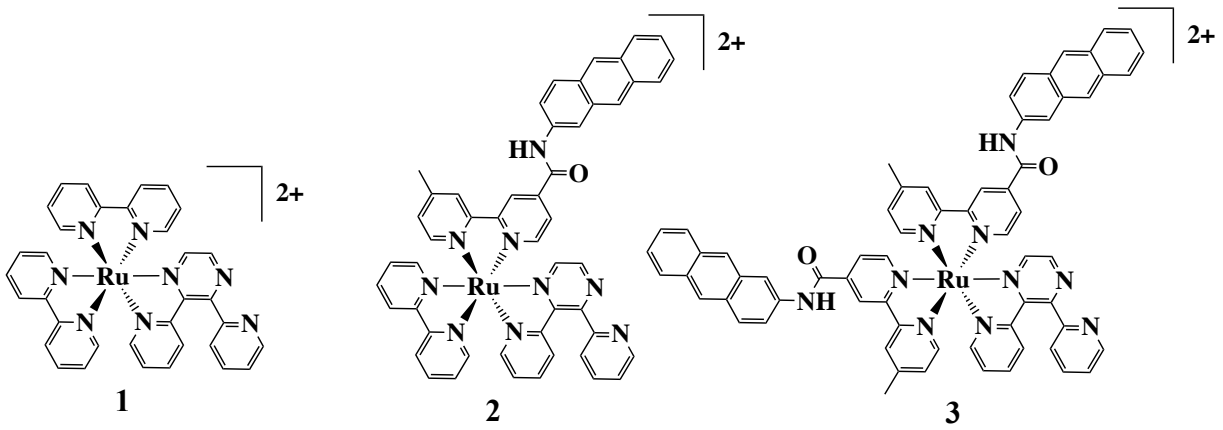

Figure 2.1. Chemical structures of $[(bpy)Ru(dpp)]^{2+}$ (**1**), $[(AnthbpyMe)(bpy)Ru(dpp)]^{2+}$ (**2**), and $[(AnthbpyMe)_2Ru(dpp)]^{2+}$ (**3**), where bpy = 2,2'-bipyridine, dpp = 2,3-bis(2-pyridyl)pyrazine, and AnthbpyMe = 4-[N-(2-anthryl)carbamoyl]-4′-methyl-2,2′-bipyridine.

2.3 Materials and Methods

Materials: All solvents/chemicals were used as received unless otherwise noted and reactions were carried out under $Ar_{(g)}$. $RuCl_3 \bullet 3H_2O$ was purchased from Alfa Aesar. The ligands 2,2'-bipyridine (bpy), 2–aminoanthracene, and 2,3-bis(2-pyridyl)pyrazine (dpp) were obtained from Aldrich, while the compounds $[(bpy)_2Ru(dpp)](PF_6)_2$ 4-[N-(2-anthryl)carbamoyl]-4′-methyl-2,2′-bipyridine (AnthbpyMe), and $[(AnthbpyMe)Ru(bpy)_2](PF_6)_2$ were prepared as described previously.[7,32,33] Spectral grade acetonitrile was obtained from Burdick and Jackson. Tetrabutylammonium hexafluorophosphate (Bu_4NPF_6) was purchased from Fluka. Sephadex LH-20 was purchased from GE Healthcare Biosciences Corporation. Alumina (80 – 200 mesh) and silica (230 – 400 mesh) were purchased from Fisher Scientific.

Synthesis of $[(AnthbpyMe)(bpy)RuCl_2]_{(s)}$: To a solution of DMF:$H_2O$ (70 ml, 6:1) with 0.5 g of LiCl, was added 0.090 g (2 equiv.) of bpy and 0.150 g (1 equiv.) of previously synthesized $[(\eta^6\text{-}C_6H_6)_2RuCl_2Ru(\eta^6\text{-}C_6H_6)_2]$.[34,35]The solution was then heated at 80°C under $Ar_{(g)}$ and after 6 h 0.230 g of AnthbpyMe was added and the heating was continued at 110°C for an additional 6 h. The solution was then cooled to room temperature and then the crude product was precipitated

from 100 ml of ether. The precipitate was collected by vacuum filtration and washed with 50 ml of H_2O and acetone, followed by drying in an oven overnight. The crude product was dissolved in a minimal amount of $CHCl_3$ (1% MeOH) and then purified using two sequential chromatography columns. The sample was first loaded onto a 6–inch silica column, which was flushed with 100% ethyl acetate to elute organic impurities. The crude purple product band was then eluted using a CH_2Cl_2 (≈1% MeOH) as the mobile phase. The volume was reduced and the sample then loaded onto a 24 inch LH-20 column with $CHCl_3$ as the mobile phase. The purple band was collected to give 0.200 g of the desired product in 47% yield. The compound was characterized by HPLC-MS and absorption spectroscopy (Figures 2.7 and 2.8).

Synthesis of $[(AnthbpyMe)_2RuCl_2](s)$: A solution of 1,4–Dioxane:DMF:H_2O (3:2:1) was charged with 0.250 g (1 equiv.) of $RuCl_3 \bullet 3H_2O$ and 0.100 g (2.0 equiv.) AnthbpyMe. To the solution mixture 0.5 g of LiCl was added and set to reflux for 4 h. The complex was then collected and purified by the same procedure described above to give 0.130 g in 54% yield. The compound was characterized by HPLC-MS and absorption spectroscopy (Figures 2.9 and 2.10).

Synthesis of $[(AnthbpyMe)(bpy)Ru(dpp)](PF_6)_2$, (2): $(AnthbpyMe)(bpy)RuCl_{2(s)}$, 0.100 g (1.0 equiv.), was suspended in a 100 ml round bottom flask containing 0.036 g (1.1 equiv.) of dpp and 30 ml of (1, 4–dioxane, DMF, H_2O; 3:2:1). The mixture was then refluxed for 6 h in the dark under $Ar_{(g)}$ after which it was allowed to cool to room temperature and transferred into a saturated aqueous solution of $NH_4PF_{6(aq)}$. The precipitate was collected by vacuum filtration and washed with H_2O to remove any excess salt and then dried overnight. Purification was done by loading the crude product with a minimal amount of acetonitrile onto a 6-inch alumina column (prepared with 100% ethyl acetate). The yellow/orange product band was then eluted with a 1:1 solvent mixture of acetonitrile:ethyl acetate containing 1% MeOH. The product was then loaded

onto a 3–inch silica column, which was flushed with acetonitrile, chloroform, and H_2O. The yellow/orange product band was then eluted with 100 ml solution of acetonitrile containing 10 ml of concentrated HCl containing 1% MeOH. To the collected product was added 25 ml of $NH_4PF_{6(aq)}$ solution and the volume of the acetonitrile was reduced to induce precipitation. The solid was then collected by vacuum filtration and allowed to dry overnight after washing with water. The solid was then dissolved with a minimum amount of DMF and precipitated with diethyl ether. The solid was collected and dried to give 0.090 g of desired product in 55% yield. Spectral data: HPLC-MS (Figure 2.11), ESI-MS (Figure 2.12), ^{1}H NMR (CD_3CN); δ 2.59-261 (3H, m4′-CH3), 7.22-7.24 (1H, d), 7.31-741 (2H, m), 7.45-7.57 (4H, m), 7.65-7.82 (6H, m), 7.87-7.97 (4H, m), 8.02-8.15 (6H, m), 8.21-8.25 (1H, t), 8.52-8.56 (5H, m), 8.63-8.69 (3H, dd), 8.98-8.99 (1H, d) 9.33-9.38(1H, m) (Figures 2.13, 2.14, and 2.15).

Synthesis of $[(AnthbpyMe)_2Ru(dpp)](PF_6)_2$, (3): (AnthbpyMe)(bpy)$RuCl_2$ 0.100 g (1 equiv.) was suspended in a 100 ml round bottom flask containing 0.027 g (1.1 equiv.) of dpp and 30 ml of (1, 4–dioxane, DMF, H_2O; 3:2:1). The mixture was refluxed for 6 h, and then allowed to cool to room temperature. It was then transferred into a saturated solution of $NH_{4(aq)}$. The precipitant was collected by vacuum filtration and washed with H_2O to remove any remaining salt. The crude product was dried overnight. Purification was accomplished using the procedure described in section 2.1.3 to give 0.095 g, 64% yield. Spectral data: HPLC-MS (Figure 2.16), ESI-MS (Figure 2.17), ^{1}H NMR (CD_3CN): δ 2.59-261 (3H, m), 7.22-7.24 (1H, m), 7.31-741 (2H, m), 7.45-7.57 (2H, m), 7.58-7.70 (2H, m), 7.71-7.75 (1H,m), 7.76-7.85 (1H,m), 7.86-8.00 (3H, m), 8.01-8.10 (2H, m), 8.11-8.15 (1H,m), 8.51-8.54 (2H, m) 8.65-8.68(2H, s) 8.98-9.04 (1H, dd) 9.35-9.45(1H, dd) (Figures 2.18, 2.9, and 2.20).

Electrochemistry: Cyclic voltammograms were obtained using a Bioanalytical Systems (BASI) Epsilon electrochemical analyzer using a three-electrode configuration and a single-compartment cell. The supporting electrolyte was a 0.1 M solution of tetrabutylammonium hexafluorophosphate (Bu_4NPF_6) in CH_3CN; sample solutions were deoxygenated by purging with argon before each experiment. A platinum disk and platinum wire were used as the working electrode and the auxiliary electrode, respectively. The reference electrode was Ag/AgCl in 3 M NaCl, which was calibrated against the ferrocene/ferrocenium couple ($FeCp^{2+/0}$ = 0.46 V vs Ag/AgCl 3M NaCl) as an internal standard.[36].

Electronic Absorption: An Agilent 8453 diode array spectrophotometer with 2 nm resolution was used to obtain the electronic absorption spectra. Extinction coefficients were determined at room temperature in a 1 cm quartz cell using solutions prepared gravimetrically in Burdick and Jackson UV-grade acetonitrile and are reported as an average of three measurements.

Excitation Spectra: Excitation spectra were recorded using a modified Photon Technology, Inc. QuantaMaster Model QM-200-45E. The system was modified to use a 150 W cooled xenon arc lamp excitation source with emission collected at a 90° angle relative to the incident excitation by a thermoelectrically cooled Hamamatsu 1527 photomultiplier tube operating in photon counting mode. The emission intensities as a function of excitation wavelength were obtained at 660 nm with samples that were deoxygenated by bubbling through ultra-high purity argon for 10 min.

Emission spectroscopy: The room temperature emission spectra were recorded in the same manner with the same instrumentation as used to obtain the excitation spectra. Air saturated samples were prepared, and the samples were then deoxygenated by bubbling through ultra high purity argon for 5-10 min. The quantum yields of emission (Φ_{em}) were obtained by the ratio

method using $[Ru(bpy)_3](PF_6)_2$ with $\Phi_{em} = 0.062$ in deoxygenated conditions as the standard (SI equation 2.1).[7,37-39]

Emission Lifetimes: Emission lifetimes were obtained either by the time correlated single photon counting technique or pulse method.[39-41]. Time-correlated single photon counting measurements were obtained using a QuantaMaster QM-200-45E (PTI) equipped with a LED light source (510 nm, FWHM ~ 20nm, PTI) and PM-20 TCSPC module SPC-130. Those emission lifetime decay profiles obtained by the pulse method were done so using a home built system in which the samples were excited with the output of Sirah Cobra Stretch dye laser equipped with Exalite 417 dye in dioxane tuned to 420 nm output. The dye laser was pumped by the third harmonic (355 nm) output of a Spectra Physics Indi-HG-10S Nd:YAG laser (10 Hz, 6 ns pulse width). The signals were detected using an EOT ET-2030A amplified silicon detector equipped with a 420 nm notch filter to minimize any contribution of scattered excitation to the observed signal. The signals were digitized using a Tektronix TDS 754C 500 MHz (2GS/s) oscilloscope. Emission lifetime decay measurements were made at 90° relative to the incident excitation pulse. Emission lifetime values were obtained using the DecayFit (www.fluortools.com) software package by a deconvolution/reconvolution process with the instrument response function (IRF).[42] When necessary, additional scatter from the substrate/sample was accounted for in the deconvolution process.

High performance liquid chromatography-mass spectroscopy (HPLC-MS): A Luna C_{18} column (Phenomenox, Torance, CA), 150 × 2.0 mm with 5 μm particles was used in all separations. The mobile phase was acetonitrile and water (containing 1% formic acid, v/v). The gradient began at 95% water for 3 min, then increased to 95% acetonitrile over the next 10 min and then held for 5 min. The system was then ramped down to 95%/5% (H_2O/acetonitrile) in 1

min and then equilibrated for an additional 5 min for a total analysis time of 22 min. All samples were injected using a Thermo Survey Autosampler. Injection volume was 20 μL at a concentration of 100 ng/μL. The HPLC column effluent was pumped directly without any split into a Thermo Instrument TSQ triple quadrupole mass spectrometer (Thermo Finnigan, San Jose, CA) equipped with ESI source, which was used in positive ion MS mode.

Electron spray ionization-mass spectrometry: Mass spectrometry was recorded on an Agilent Technologies 6220 Accurate Mass TOF-LCMS with a dual ESI source in acetone or acetonitrile with 3.5 kV electrospray voltage, 31 V cone voltage, 120°C source temperature, N_2 nebulizing gas (20 L/h), and scan range 250−700 m/z.

Nuclear magnetic resonance (NMR): ^{1}H NMR and ^{1}H–^{1}H COSY spectra were recorded on a JEOL 500 MHz NMR spectrometer at 298 K.

Cell culture: The F98 glioma cell line was obtained from ATCC and maintained in Dulbecco's Modified Eagle's Medium (DMEM, ATCC) supplemented with 10% fetal bovine serum (FBS, ATCC) and 1 % penicillin/streptomycin at 37ºC with 5 % CO_2.

Photolysis: For photolysis treatments, 6-well plates were seeded with ~0.4×10^6 cells per well in 3.0 mL of DMEM and incubated at 37 ºC and 5 % CO_2 for 24 h. The medium was then evacuated from each well and replaced with 1.5 mL of the desired concentration of complex dissolved in DMSO (≤ 5 % v/v) and diluted in DMEM. A control was prepared by mixing the calculated amount of DMSO in the experimental samples with DMEM. The cells were then incubated at 37ºC and 5% CO_2 for 15 min. Each well was then evacuated and the cells were washed with PBS several times before incubating in DMEM without phenol red for 12 h. Before the cells were photolyzed, each LED in the array was calibrated to ~2.50 mW based on readings from a photodiode meter.[43] The array was placed in an incubator at 37ºC and 5% CO_2. A

thermocouple was placed inside the array to monitor the temperature around the cells. One at a time, each 6-well plate, except for the dark controls, was placed in the LED array for 1 h.

Cell viability: Forty-eight hours after photolysis, each well was evacuated and replaced with a mixture of cold AlamarBlue (10 % v/v) and DMEM to perform an indirect viability assay.[44] The cells were incubated for 1.5 h with the AlamarBlue mixture. After incubation, 100 μL from each mixed well was placed in 3 wells of a 96 well plate for each well to ensure more accurate readings. The 96 well plate was sealed with parafilm and kept in the dark at 4ºC for 1-2 h prior to measuring the absorption at 570 and 600 nm with a SpectraMax M2 spectrometer. Cell viability was calculated relative to the control for each of the samples (SI equation 2.2).

LED array: A LED array was designed to insure that only specifically characterized light was administered to the cell environment during treatment. The power source input was 120 volts AC with an output of 13.5 volts DC. A circuitry box was used to calibrate the output of each LED separately prior to the treatment. Two 5 Ω resistors, wiring, a voltage controlling knob, and a LED were placed together for six LED channels with one light source per well in the treatment containers. The six LEDs were placed on a separate board from the circuitry to avoid excessive heating of the plates during treatment. The LED head board was placed on a mount designed to fit the dimensions of the well plates used in treatment and not let light either enter or escape to interrupt the photolysis.

2.4 Results and discussions

Synthesis

The metal-organic Ru(II) chromophores were synthesized and purified as detailed in the methods section (*vida supra*) and the supporting information (SI), with yields between 50-60%.

Characterization of **1**, **2**, and **3** was done by ^{1}H NMR, HPLC-MS, CV, steady-state emission and absorption spectroscopy, and ESI-MS.

Electrochemistry

Electrochemical analysis was used to identify relative ground state redox potentials of **1**, **2**, and **3**. For comparison, both $[Ru(bpy)_3]^{2+}$ and anthracene were also characterized and were found to display oxidation potentials at $E_{1/2}$ of +1.25 and E_p of +1.24 V vs. Ag/AgCl, respectively. These correspond to the $Ru^{(III/II)}$ reversible $1e^-$ oxidation and irreversible anthracene oxidation, respectively.[7,32] Complex **1** displays a characteristic $Ru^{(III/II)}$ reversible $1e^-$ oxidation with an $E_{1/2}$ of 1.45 V (Ag/Ag^+, 3 M NaCl) and a reversible reduction with an $E_{1/2}$ of –1.02 V (Ag/Ag^+, 3 M NaCl) attributed to the 1 e^- $dpp^{0/-1}$ redox couple, Figure 2.2.[45]

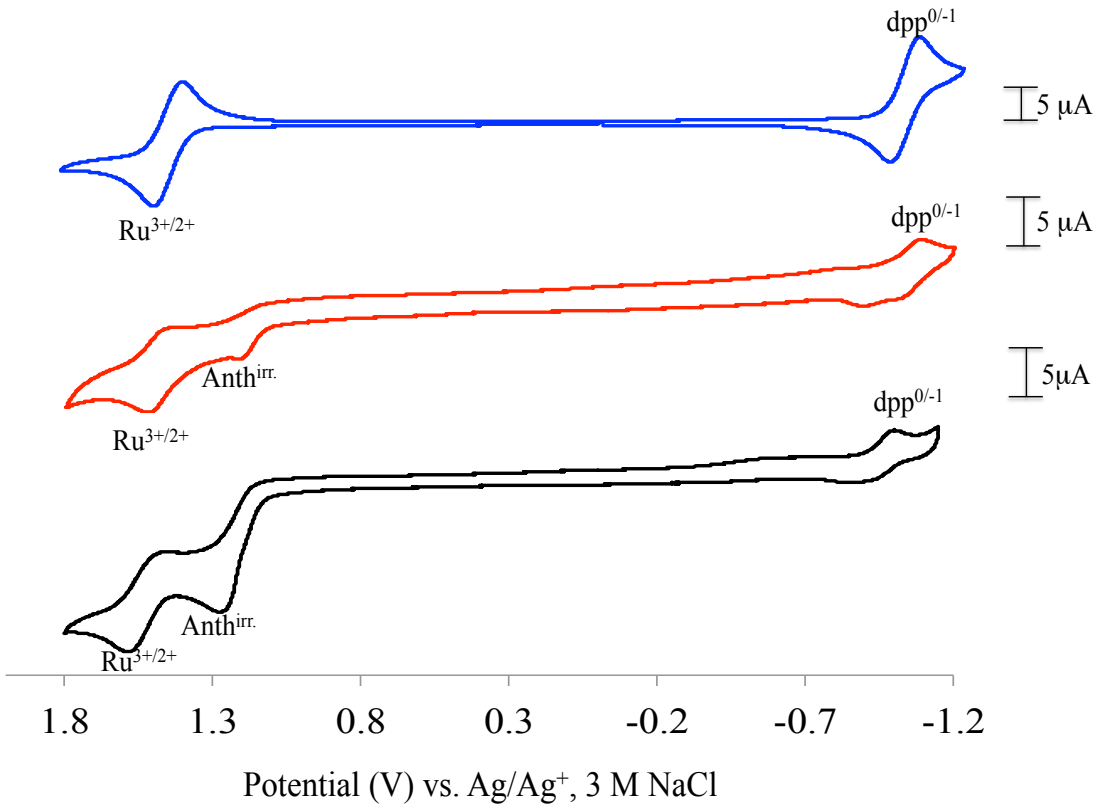

Figure 2.2. Cyclic voltammograms of $[(bpy)Ru(dpp)](PF_6)_2$ (blue, 1), $[(AnthbpyMe)(bpy)Ru(dpp)](PF_6)_2$ (red, 2), and $[(AnthbpyMe)_2Ru(dpp)](PF_6)_2$ (black, 3), in 0.1 M Bu_4NPF_6 CH_3CN, reported vs Ag/AgCl (3 M NaCl, scan rate 100 mV/sec).

Complexes **2** and **3** display reversible 1 e^- oxidation couples with an $E_{1/2}$ of 1.52 V and 1.55 V (Ag/Ag^+, 3 M NaCl, ± 0.01 V), respectively, which are assigned to the reversible oxidations of the $Ru^{(III/II)}$ centers. The irreversible oxidations at 1.24 and 1.28 V (± 0.01 V) are attributed to the anthracene oxidation, which have been shown to undergo irreversible $2e^-$ oxidation to form a di-cation product or nucleophilic attack by CH_3CN.[46,47] The quasi-reversible 1 e^- reduction couple at $E_{1/2}$ = – 0.99 V (Ag/Ag^+, 3 M NaCl) is assigned to the $dpp^{0/-1}$ couple which is consistent with that of the parent complex (*vida supra*) (Figures 2.21 and 2.22). The observed anomalies between – 0.8 and – 0.9 V (Ag/Ag^+, 3 M NaCl, ± 0.01 V) are thought to be due to the irreversible reduction of the anthracene and/or amide linker units.[46,48] Alternatively, these anomalies may be due to adsorption of the molecule onto the electrode. The small changes in the redox potential of the $Ru^{(III/II)}$ and $dpp^{0/-1}$ are also consistent with the spectroscopic results for the lowest lying MLCT transition.

Photophysical properties

Electronic absorption spectroscopy was used to determine the absorption properties of the reported complexes. Compound **1** displays a prominent electronic absorption band at ~ 286 nm with a shoulder centered ~ 325 nm attributed to overlapping bpy and dpp $\pi \rightarrow \pi^*$ transitions, and a broad absorption between 360 nm and 550 nm with a maxima ~ 450 nm characteristic of population of a singlet metal-to-ligand charge transfer, ^{1}MLCT, state from the ground state (Figure 2.3).[49,50] These results are in relatively good agreement with previously published values of $Ru(bpy)_2(dpp)$ in water.[50,51] Assignment of the electronic configuration of the ^{1}MLCT state as being either $Ru(d_\pi^5)bpy(\pi^*)$ or $Ru(d_\pi^5)dpp(\pi^*)$, where the promoted electron is localized on one of the bpy ligands or the dpp respectively, is difficult given the degree of overlap between the two transitions between 360 nm and 550 nm. From the cyclic voltammetry, however, it is likely

that the ^{3}MLCT generated by very fast intersystem crossing resides on the lower energy dpp ligand based on the lower reduction potential of dpp relative to bpy.[52,53]

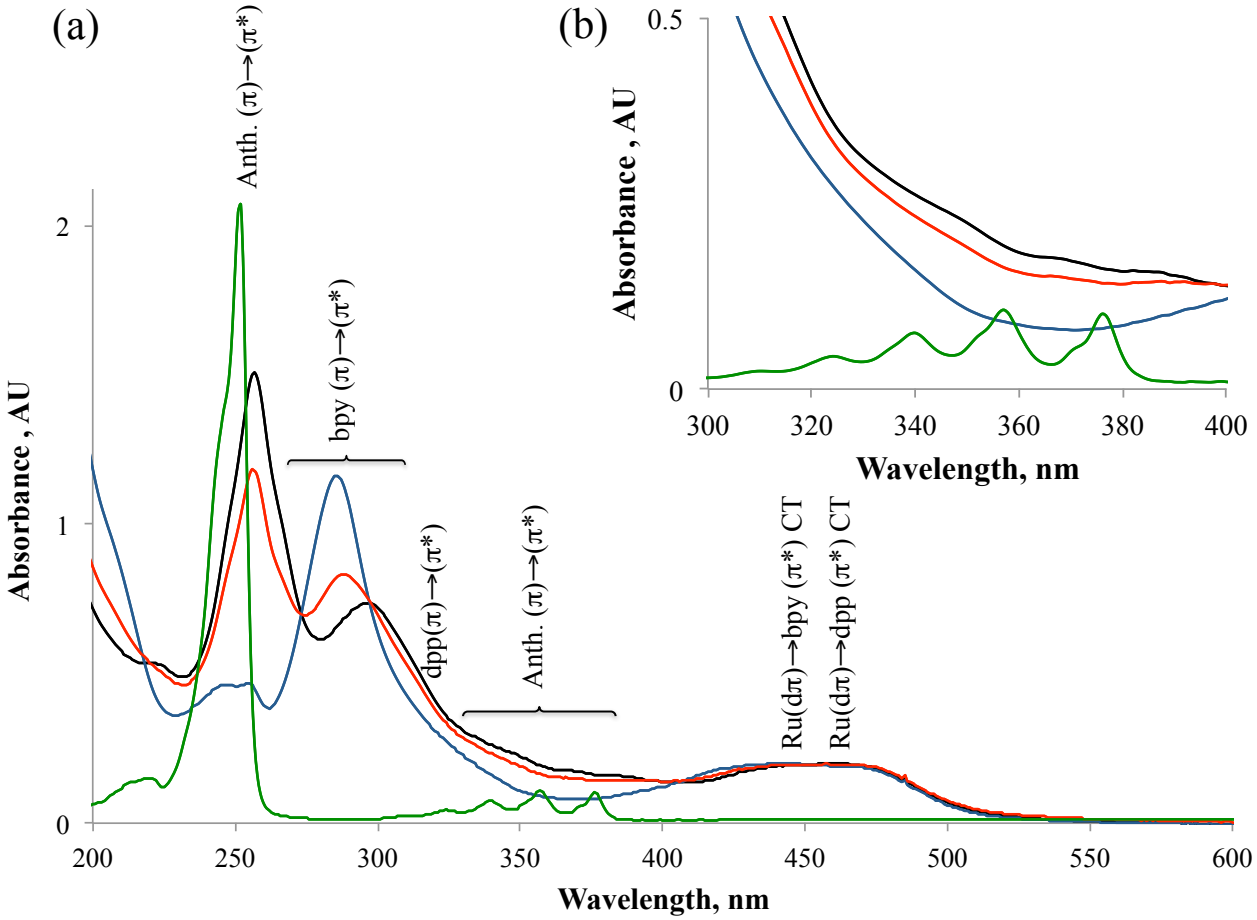

Figure 2.3. (a) Electronic absorption of anthracene (green), $[(bpy)_2Ru(dpp)](PF_6)_2$ (blue, **1**), $[(AnthbpyMe)(bpy)Ru(dpp)](PF_6)_2$ (red), and $[(AnthbpyMe)_2Ru(dpp)](PF_6)_2$ (black) in acetonitrile and (b) scale expansion of electronic absorption spectra.

Complexes **2** and **3** exhibit strong absorption at 256 nm that is attributed to the short axis polarized anthracene π→π* transition.[54] The observed bathochromic shift of the bpy π→π* transition for complex **2** and **3** from ~ 286 nm to ~ 300 nm is believed to arise from inductive effects due to functionalization of the bpy ligands at the 4 and 4′ positions.[55] In addition, the increased absorption observed between ~ 325 nm to ~ 425 nm is believed to arise from underlying transitions characteristic of anthracene absorption in the range of 350 – 400 nm corresponding to a $S_o \rightarrow S_1$ transition polarized along the long axis of the anthracene.[54,56] The

visible region displays absorption maxima centered at 459 nm for **2** (ε = 16,000 $M^{-1}cm^{-1}$) and 461 nm for **3** (ε = 21,000 $M^{-1}cm^{-1}$). These are attributed to ^{1}MLCT transitions corresponding to $Ru(d_\pi) \rightarrow bpy(\pi^*)$, $dpp(\pi^*)$ with the dpp transition assigned the lowest lying MLCT transition (*vide supra*).[57] The increase in the molar absorptivity as a function of anthracene subunits is a result of the interaction of the increase in ring current, which interacts significantly with the transition dipole moment of the ^{1}MLCT transitions.[4,58] Excitation spectra for the complexes were used to determine the contributions of the anthracene and Ru(II) core transitions to the emission intensity of the ^{3}MLCT transition (Figure 2.23). The results corroborate interchromophoric interactions between the appended aromatic anthracene subunit, which give rise to phosphorescence from the ^{3}MLCT. Parent complex **1** demonstrated a transition from 250 – 350 nm speculated to be from the bpy and dpp ligands. Complexes **2** and **3** present similar transitions, but with a bathochromatic shift and an additional transition from 350 – 400 nm attributed to the anthracene.

Steady state emission shows that the excited state energies of the anthracene and Ru(II) core are not significantly perturbed by the covalent attachment of anthracene to the Ru complex. Excitation of complex **1** at 340 nm yields no emission within the near-UV region, while excitation at λ_{ex} = 450 nm gives rise to an emission band centered at 668 nm, characteristic of the emissive ^{3}MLCT state common to ruthenium polypyridyl and polyazine complexes.[45] Conversely, excitation of **2** and **3** with λ_{ex} = 340 nm gives rise to emissive high energy transitions with maxima located at 480 nm and a shoulder at 495 nm arising from anthracene singlet excited state relaxation (Figure 2.4).

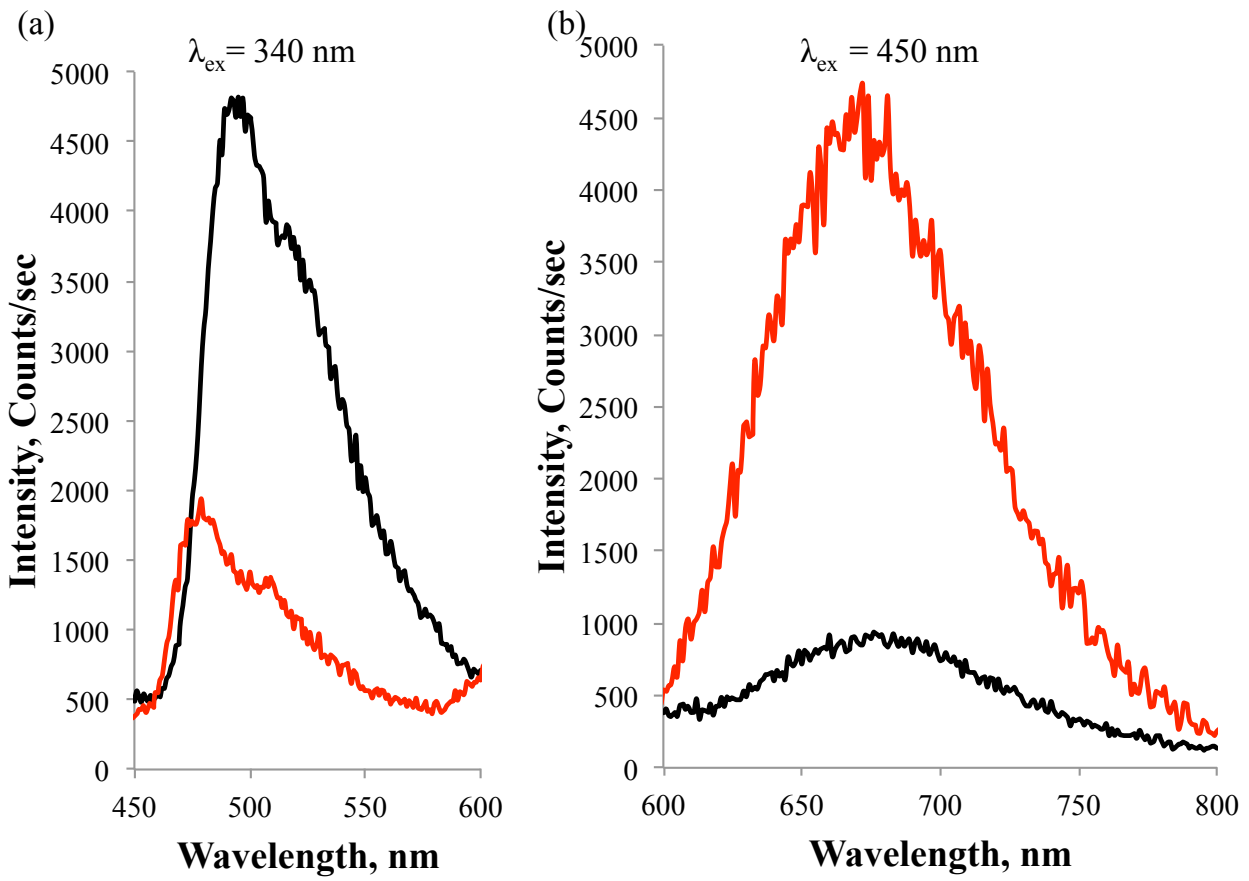

Figure 2.4. Steady state emission of $[(AnthbpyMe)(bpy)Ru(dpp)](PF_6)_2$ (red, **2**), and $[(AnthbpyMe)_2Ru(dpp)](PF_6)_2$ (black, **3**) in acetonitrile, excited at 340 nm (a) and 450 nm (b). Samples were absorbance matched at 450 nm.

The anthracene emission from complexes **2** and **3** displays decreased vibronic structure (compared to the vibronically resolved anthracene emission in solution) between 450 – 580 nm and is red-shifted relative to the anthracene emission (λ_{max} = 394 nm). The red shift in the emission is common to 2-aminoanthracenes due to a twisted intramolecular charge transfer state (TICT).[59,60] The TICT state has been proposed to lead to delocalized e^- density into the $[(bpy)_2Ru(ddp)]^{2+}$ system.[7,58,59]

Excitation of the anthracene moiety results in formation of an anthracene singlet excited state, which is known to undergo intersystem crossing to populate a triplet excited state.[61] Both anthracene singlet and triplet states are depopulated via radiative and non-radiative decay

pathways. The singlet emission lifetime observed for the parent 2-aminoanthracene was ~ 10 ns in CH_3CN. Upon covalent attachment to a bpy of the Ru complex the observed emission lifetime of the pendent anthracene was found to be 4.62 ns and 4.95 ns for complexes **2** and **3**, respectively, upon excitation at 340 nm, Figure 2.5.

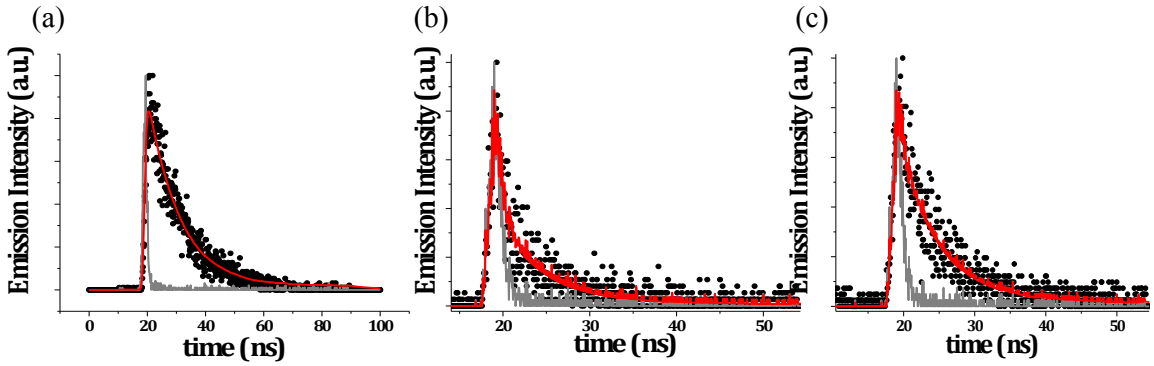

Figure 2.5. Emission lifetime decay (black circles) and corresponding deconvolution fit (red line) using an instrument response function (gray line) and a single exponential decay function for 2-aminoanthracene (a), $[(AnthbpyMe)(bpy)Ru(dpp)](PF_6)_2$ (b), and $[(AnthbpyMe)_2Ru(dpp)](PF_6)_2$ (c) in CH_3CN. Samples were excited at λ_{ex} = 340 nm.

The decreased emission lifetime of the anthracene singlet excited state is presumably due, at least in part, to intra- or inter- molecular energy transfer between the anthracene and the ruthenium core as evidenced by the presence of characteristic Ru emission upon excitation of the anthracene (*vida supra*).[7] Similar results (i.e. quenching of the anthracene singlet excited state by a Ru-polypyridyl core) have been observed in other Ru(II)-polypyridyl-anthracenyl systems.[8] The observed decay rate of the anthracene ligands of complexes **2** and **3** can be summarized as the sum of radiative (k_r) and non-radiative (k_{nr}) terms including a quenching rate constant (k_q) (SI equation 2.3). From the fits of the anthracene emission lifetime decays, Figure 2.5, the quenching rates were found to be 1.16×10^8 s^{-1} and 1.02×10^8 s^{-1} for compounds **2** and **3** corresponding to quenching efficiencies (Φ_q) of 0.538 and 0.505, respectively, (SI equation

2.3). These values assume that the radiative and non-radiative rate constants of the

anthracene emission in complexes **2** and **3** are the same as the anthracene moiety in the absence of the Ru(II)-polypyridyl core.

The parent complex **1** has been reported as having a Φ_{em} of 0.023 and found here to have a τ_{em}, of 540 ± 1 ns upon generating the ^{3}MLCT state.[45] Emission from the Ru(II) ^{3}MLCT state of **2** is centered at 661 nm (λ_{ex} = 450 nm) and was found to have a Φ_{em} of 0.0059, and an emission lifetime, τ_{em}, of 398 ± 1 ns whereas **3** displayed an emission centered at 663 nm, a Φ_{em} of 0.0011, and τ_{em} of 414 ± 1.0 ns. It is evident from the observed Φ_{em} and τ_{em} for **1**, **2**, and **3** that covalent attachment of anthracene ligands to **1** is accompanied by quenching of the Ru(II) ^{3}MLCT. It has been argued for similar compounds that functionalization of both the Ru(II) core and anthracene perturb the triplet energies of each in such a way that they become nearly isoenergetic.[7]

Förster theory of resonance energy transfer (FRET) was used to assess the contribution of excited state energy transfer to the quenching of the anthracene singlet state.[62,63] The Förster overlap integral, *J*, Förster distance, R_o, refractive index, n, donor lifetime, τ_D, and fluorescence quantum yield of the donor Φ_D, were determined to be 3.45×10^{-14} cm^6, 37 Å, 1.344, 10 ns, and 0.41, respectively, (Figure 2.24, SI equations 3 – 7). From the former values a k_{FRET} of 1.7×10^{11} s^{-1} was estimated assuming the distance between the Ru(bpy)$_2$(dpp) and anthracene transition dipoles are approximately 11 Å (obtained from cursory molecular modeling geometry optimizations using Arguslab, www.arguslab.com). The experimental FRET rate constants obtained are less characteristic of intramolecular FRET rates which are known to occur on vibrational timescales, i.e. 10^{10} – 10^{12} s^{-1}, and more characteristic of intermolecular (or diffusional) excited state electron transfer reactions.[64,65]

A Rhem-Weller analysis of the ground state redox energies and anthracene-excited state energy

indicates that a mechanism in which the anthracene undergoes an excited state oxidative electron transfer to the dpp is thermodynamically downhill by at least 300 meV (equation 2.8).[66-68] These observations (e.g. ^{3}MLCT emission upon anthracene excitation and the disparity between the experimental and predicted quenching rate constants via FRET) suggest that although excited state quenching of the anthracene singlet state is partially facilitated by FRET type mechanism, quenching by oxidative excited state electron transfer of the anthracene to the dpp ligand is possible according to Scheme 1.

Scheme 1. Mechanisms of Anthracene

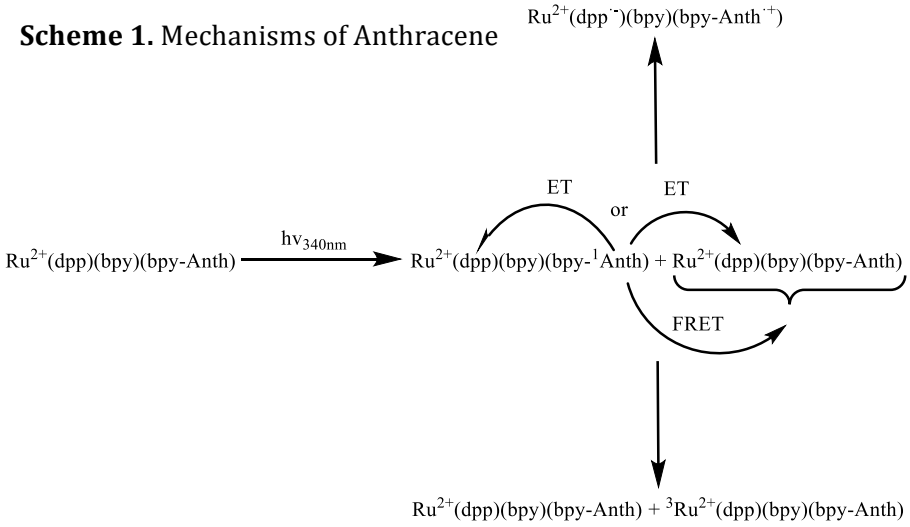

It should be noted that similar singlet energy transfer rates have been reported previously with Ru(II)(bpy)$_3$.[69-71]

Neither oxidative nor reductive excited state electron transfer are energetically favorable between the Ru(II) ^{3}MLCT and anthracene ground state so that the most reasonable mechanism of ^{3}MLCT quenching likely involves energy transfer between the Ru(II) ^{3}MLCT and the anthracene triplet excited state. The Ru(II) triplet quenching rate obtained by subtracting the observed decay rate of **1** from the observed decay rate of **2** and **3** (assuming that the rate of decay of **1** adequately approximates the rate of decay of **2** or **3** in the absence of the appended anthracene) were found to be approximately 6.61×10^5 s^{-1} for **2** and 5.64×10^5 s^{-1} for **3**. These

values are consistent with those obtained in similar Ru(II)-anth systems (SI, equations 9 – 11, Figure 2.26).[7]

Analysis of the Ru(II) emission lifetime decay of **2** and **3** was performed using a model for the Dexter exchange mechanism of energy transfer where the critical distance values, R_o, do not differ significantly between **2** and **3** and lie ~ 8 – 10 Å (SI, equation 2.6).[72] Together with the calculated energy transfer efficiencies, the results are consistent with triplet energy transfer between the lowest ^{3}MLCT and one of the anthracene ligands resulting in an anthracene in its triplet excited state.

In summary, depopulation of an excited anthracene subgroup occurs via competing pathways. Upon formation, the singlet excited state of anthracene may 1) undergo intersystem crossing to form a triplet excited state anthracene followed by decay to the ground state through predominately non-radiative pathways, 2) participate in inter-molecular Förster resonance energy transfer, or 3) participate in inter- or intra- electron transfer with the Ru(II)$(bpy)_2$(dpp). The quenching of the ^{3}MLCT also occurs by competing pathways: the ^{3}MLCT state can undergo 1) inter- or intra- molecular resonance energy transfer by the Dexter exchange mechanism to populate ^{3}anthracene, and/or 2) repopulate the ground state through radiative and non-radiative decay pathways inherent to the Ru(II)$(bpy)_2$(dpp).

Photocytotoxicity and cytotoxicity toward MG cells

To test the potential photocytotoxicity of the reported complexes for the treatment of brain cancers, F98 glioma cells were employed. This cell line is a widely-used rat brain tumor model with biological characteristics resembling those of human glioblastoma.[70] Toxicity assays were conducted to test the effect of compounds **1**, **2**, and **3** against F98 glioma cells, with and

without light activation. In brief, cells were treated with the complexes at a concentration of 75 μM for 1 h, washed to remove excess complex remaining in the medium, and then incubated for 1 h in the dark or under illumination at 455 nm for which a custom-designed photoarray apparatus was employed.[43,73] An AlamarBlue assay was used to quantify cell viability 48 h after treatment. In an effort to explore structure-function relationships in these compounds, anthracene (**4**), $[Ru(bpy)_3](PF_6)_2$ (**5**), and $[(AnthbpyMe)Ru(bpy)_2](PF_6)_2$ (**6**) were also tested in parallel with the title complexes.[7]

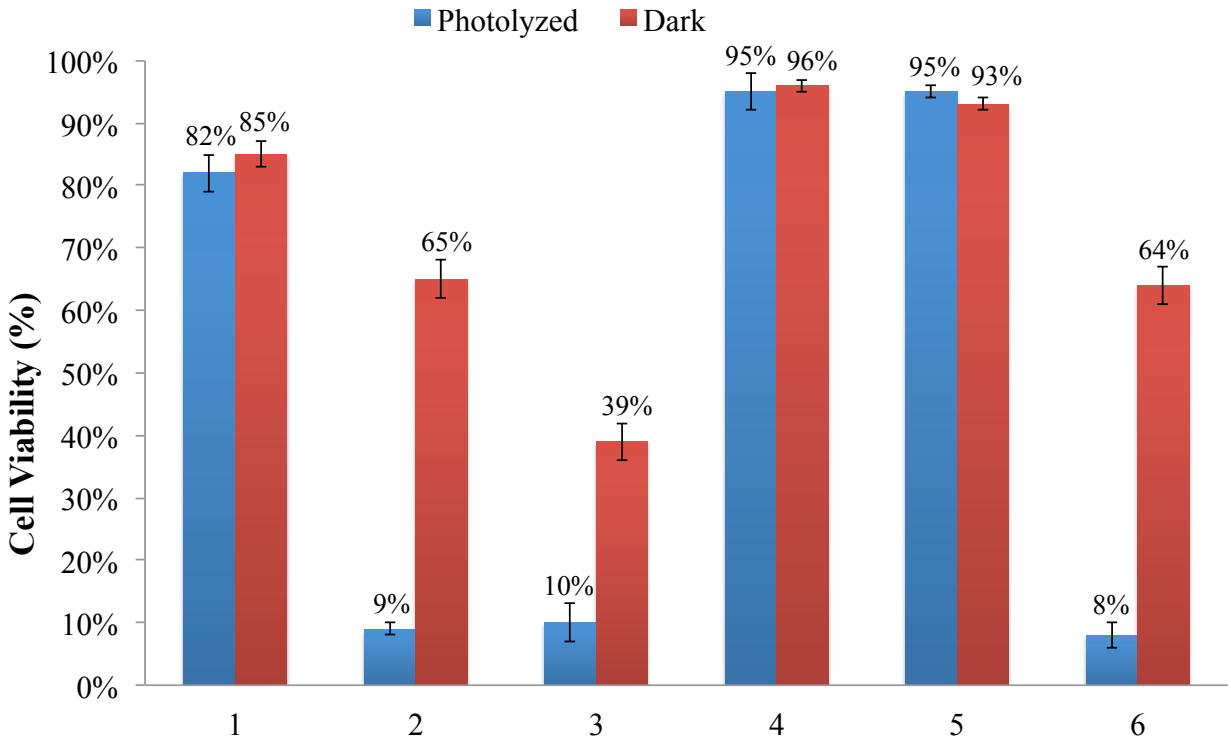

Figure 2.6. Effects of $[(bpy)_2Ru(dpp)](PF_6)_2$ (1), $[(AnthbpyMe)(bpy)Ru(dpp)](PF_6)_2$ (2), $[(AnthbpyMe)_2Ru(dpp)](PF6)_2$ (3), anthracene (4), $[Ru(bpy)_3](PF_6)_2$ (5), and $[(AnthbpyMe)Ru(bpy)_2](PF_6)_2$ (6) against F98MG cells 48 h after photolysis (viability counts were performed in triplicate; bars are standard error).

The cell viability at 48 h post-photolysis revealed that the parent molecules, anthracene (**4**) and $[Ru(bpy)_3]^{2+}$ (**5**), exhibited relatively little cytotoxicity in either the absence or presence of light, while $[(bpy)_2Ru(dpp)]$ (**1**) was moderately cytotoxic under both dark and light conditions. In contrast, the complexes with appended anthracene moieties (**2**, **3**, and **6**) displayed

moderate toxicity in the dark, which was substantially enhanced by exposure to light. This photocytotoxicity is speculated to arise from the multiple deactivation pathways through energy and/or electron transfer processes, which can facilitate redox reactions and result in cell stress/death upon light activation.

2.5 Conclusion

Appending anthracene chromophores to the $[(bpy)_2Ru(dpp)]^{2+}$ framework through amide linkers has resulted in structurally-diverse metal-organic Ru(II) complexes that exhibit unique photophysical properties and enhanced photodynamic potency against F98 glioma cells. Metal organic Ru(II) complexes, $[(AnthbpyMe)(bpy)Ru(dpp)]^2$ and $[(AnthbpyMe)_2Ru(dpp)]^{2+}$, were prepared in moderate yields and characterized for their photophysical properties. Initial evaluation was also made of the phototoxicity of these compounds using the F98 rat glioma cell line. The complexes exhibit efficient light absorption throughout the UV region via ligand-based transition, while the visible region is dominated by MLCT transitions. The addition of the anthryl motif was shown to increase the efficiency with which the complexes absorb visible light, proposed to be caused by the interactions of the induced ring current with the induced dipole moment of the MLCT transitions. The excited-state properties (lifetimes and quantum yields) of the reported complexes were significantly perturbed relative to the parent complex $[(bpy)_2Ru(dpp)]^{2+}$ due to additional deactivation pathways provided by the appended anthracene(s). The excited state dynamics of the reported systems indicate that there is significant interchromophoric communication upon excitation of the anthracene and Ru(II) subunits. It is proposed that excitation of the anthracene subunit can be deactivated through direct electron transfer into the dpp bridging ligand or participate through a Dexter type energy transfer mechanism to populate the ^{3}MLCT state. The ^{3}MLCT excited state is also speculated to

be depopulated through a Dexter type mechanism with efficient quenching between the triplet states of the anthracene. The dynamic excited state properties that are exhibited by these systems suggest that they have propensity for being novel agents for photodynamic therapy against highly invasive and aggressive forms of brain cancer that are intractable to conventional chemotherapeutic therapies. The complexes were shown to be moderately cytotoxic towards F98 rat glioma cells in the dark, an effect that was substantially enhanced upon illumination with visible light. This photocytotoxicity is hypothesized to arise from the unique excited state dynamics that are facilitated by appending an anthracene to the $[(bpy)_2Ru(dpp)]^{2+}$ system. Studies are currently underway to understand the photoreactivity of the proposed systems against cellular substrates such as DNA and protein and to examine the distribution of these complexes within exposed cells.

2.6 Acknowledgements

The authors are grateful to the National Science Foundation (grant CHE–1301131) for financial support. Roberto Padilla received additional support from the National Institutes of Health IMSD Program (grant VT–IMSD-GM072767).

2.7 Supplementary information: Pushing the limits of structurally-diverse light-harvesting Ru(II) metal-organic chromophores for photodynamic therapy

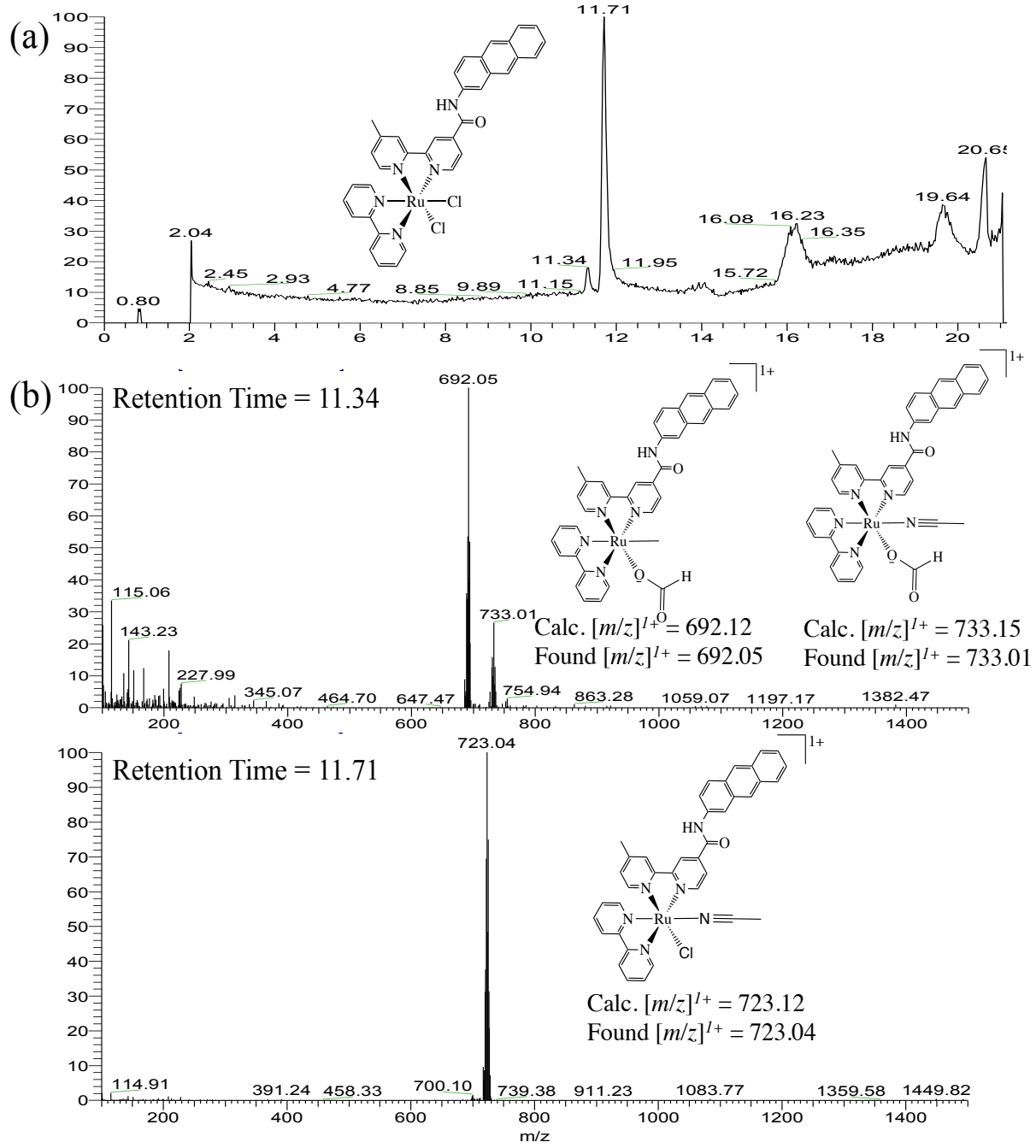

Figure 2.7. (a) HPLC chromatogram of (AnthbpyMe)(bpy)$RuCl_2$(s) displaying the retention times of the compounds. (b) Total mass spectrum of the peaks at the given retention times (R.T) (bpy = 2,2'-bipyridine and AnthbpyMe = 4-[N-(2-anthryl)carbamoyl]-4′-methyl-2,2′-bipyridine).

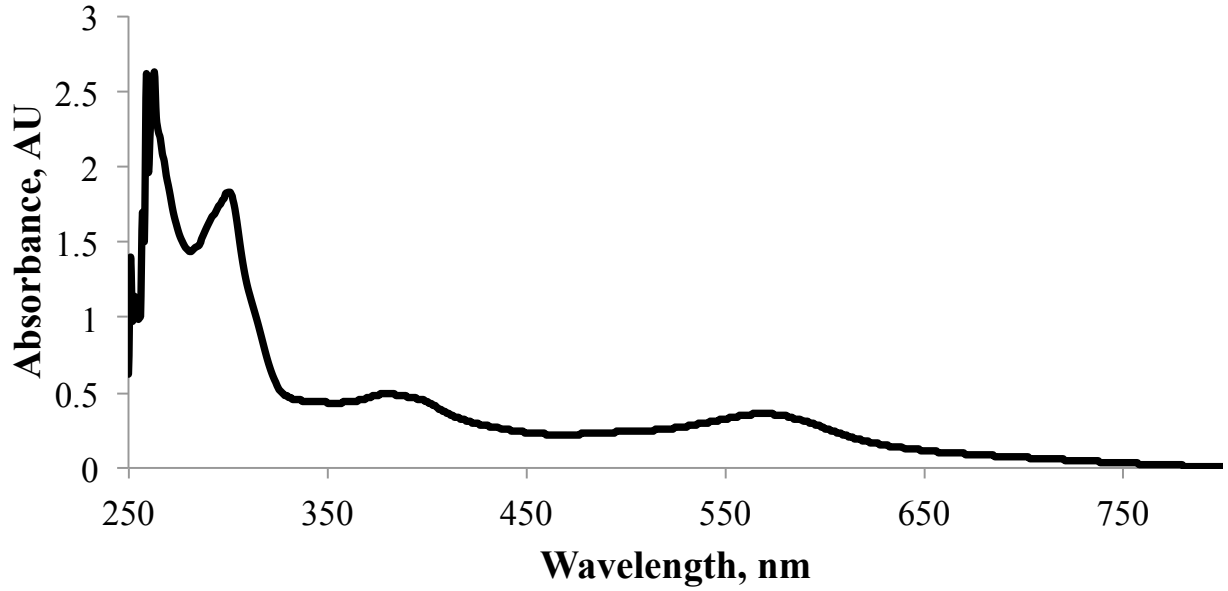

Figure 2.8. Electron absorption of (AnthbpyMe)(bpy)$RuCl_2$(s) in chloroform (bpy = 2,2'-bipyridine and AnthbpyMe = 4-[N-(2-anthryl)carbamoyl]-4′-methyl-2,2′-bipyridine).

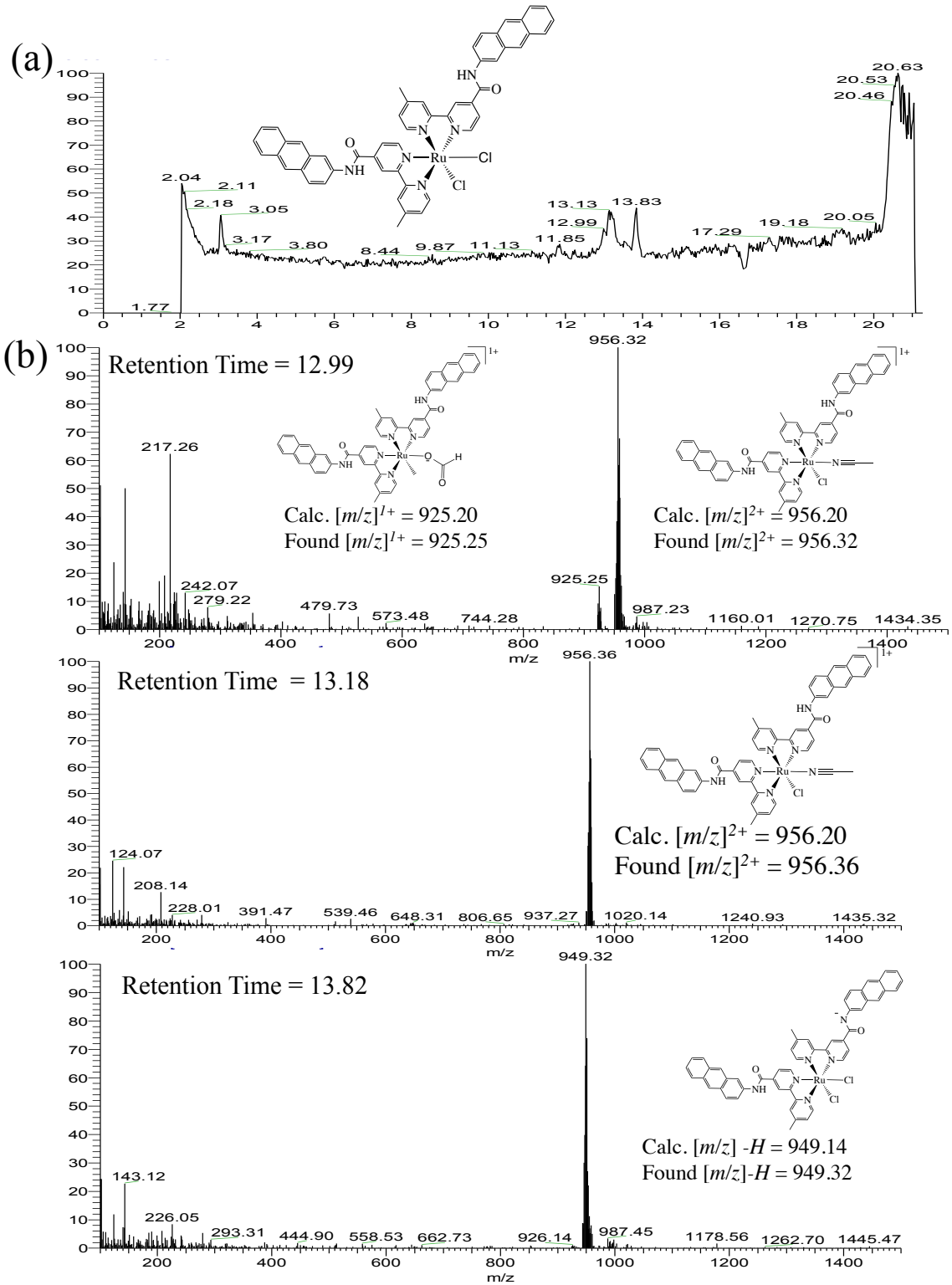

Figure 2.9. (a) HPLC chromatogram of $(AnthbpyMe)_2RuCl_2$(s) displaying the retention times of the compounds. (b) Total mass spectrum of the peaks at the given retention times (R.T) (AnthbpyMe = 4-[N-(2-anthryl)carbamoyl]-4′-methyl-2,2′-bipyridine).

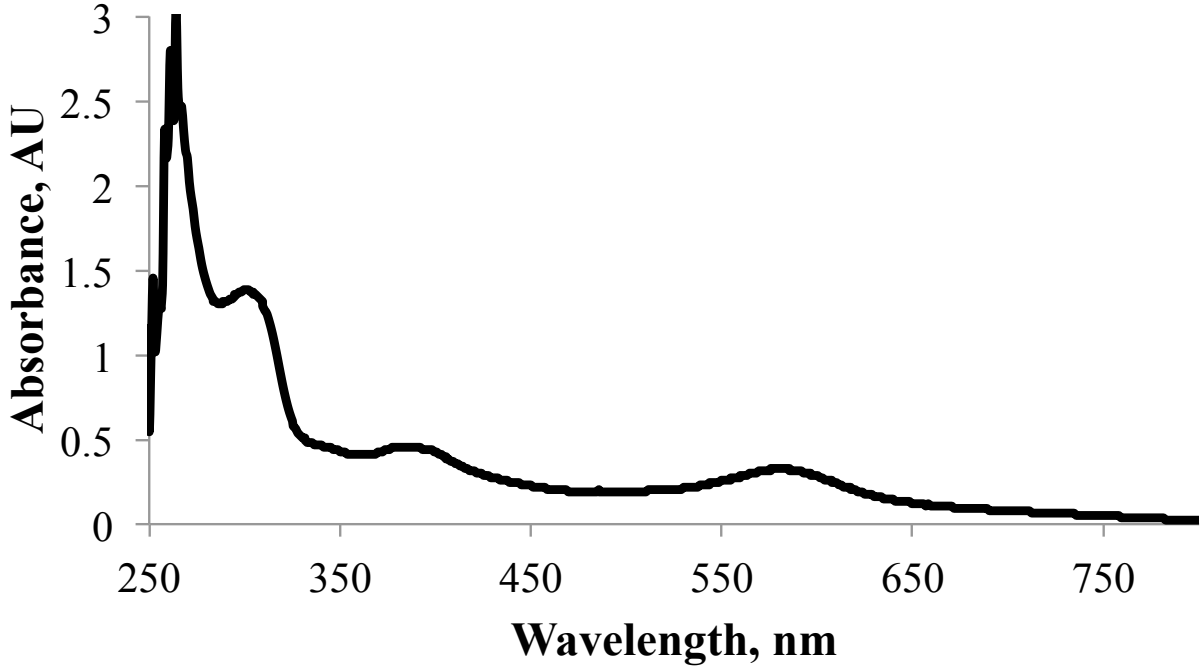

Figure 2.10. Electron absorption of $(AnthbpyMe)_2RuCl_{2(s)}$ in chloroform (bpy = 2,2'-bipyridine and AnthbpyMe = 4-[N-(2-anthryl)carbamoyl]-4′-methyl-2,2′-bipyridine).

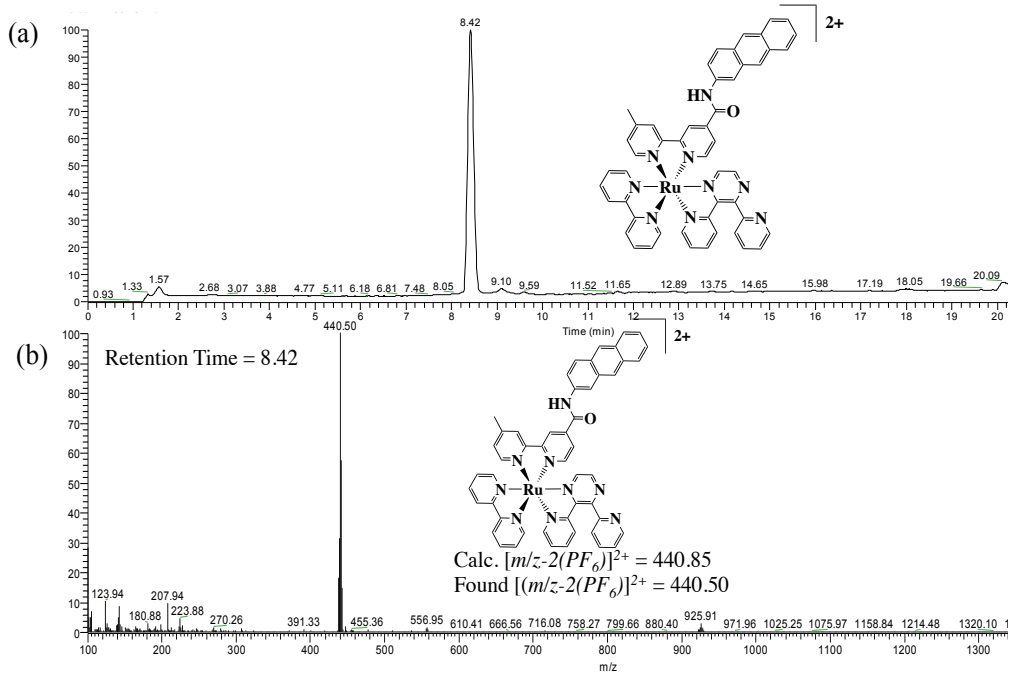

Figure 2.11. (a) HPLC chromatogram of $[(AnthbpyMe)(bpy)Ru(dpp)]^{2+}$ retention times. (b) Total mass spectrum of the peaks at the given retention time (bpy = 2,2'-bipyridine, dpp = 2,3-bis(2-pyridyl)pyrazine, and AnthbpyMe = 4-[N-(2-anthryl)carbamoyl]-4′-methyl-2,2′-bipyridine).

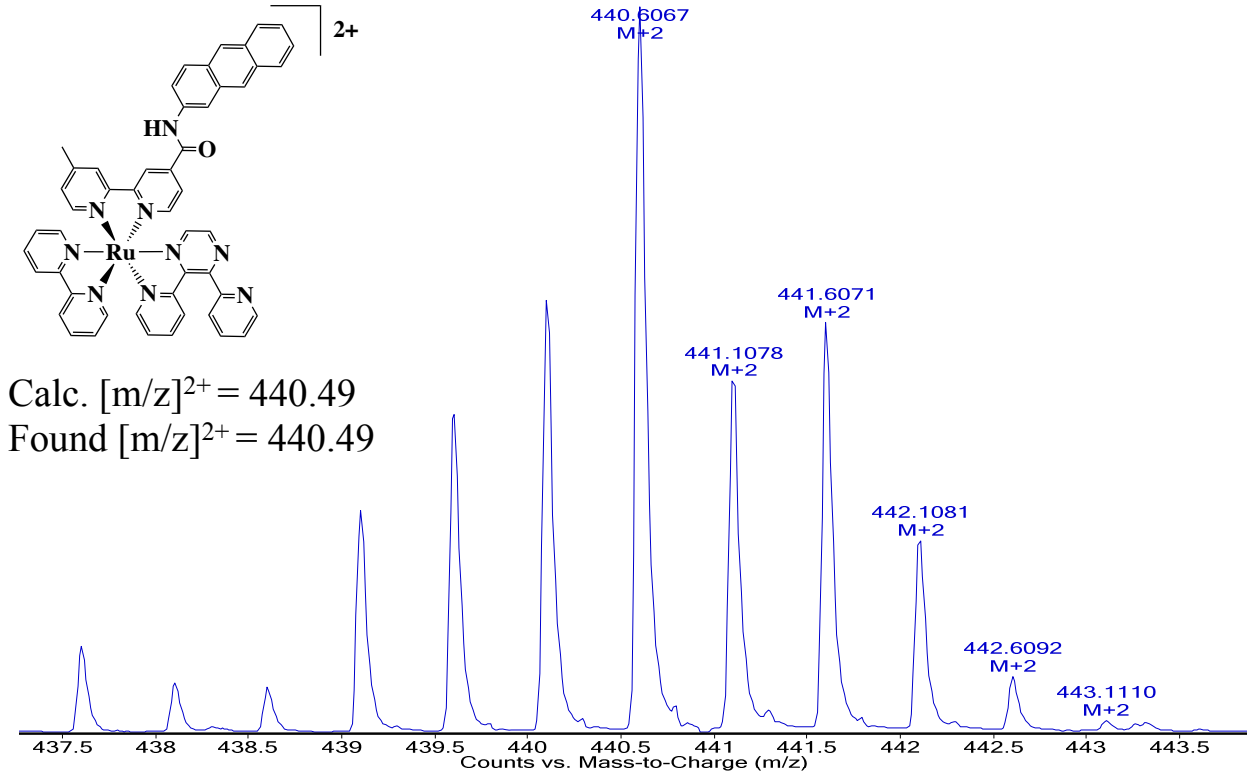

Figure 2.12. Exact mass spectrum of [(AnthbpyMe)(bpy)Ru(dpp)]$(PF_6)_2$ showing the isotopic distribution pattern (bpy = 2,2'-bipyridine, dpp = 2,3-bis(2-pyridyl)pyrazine, and AnthbpyMe = 4-[N-(2-anthryl)carbamoyl]-4′-methyl-2,2′-bipyridine).

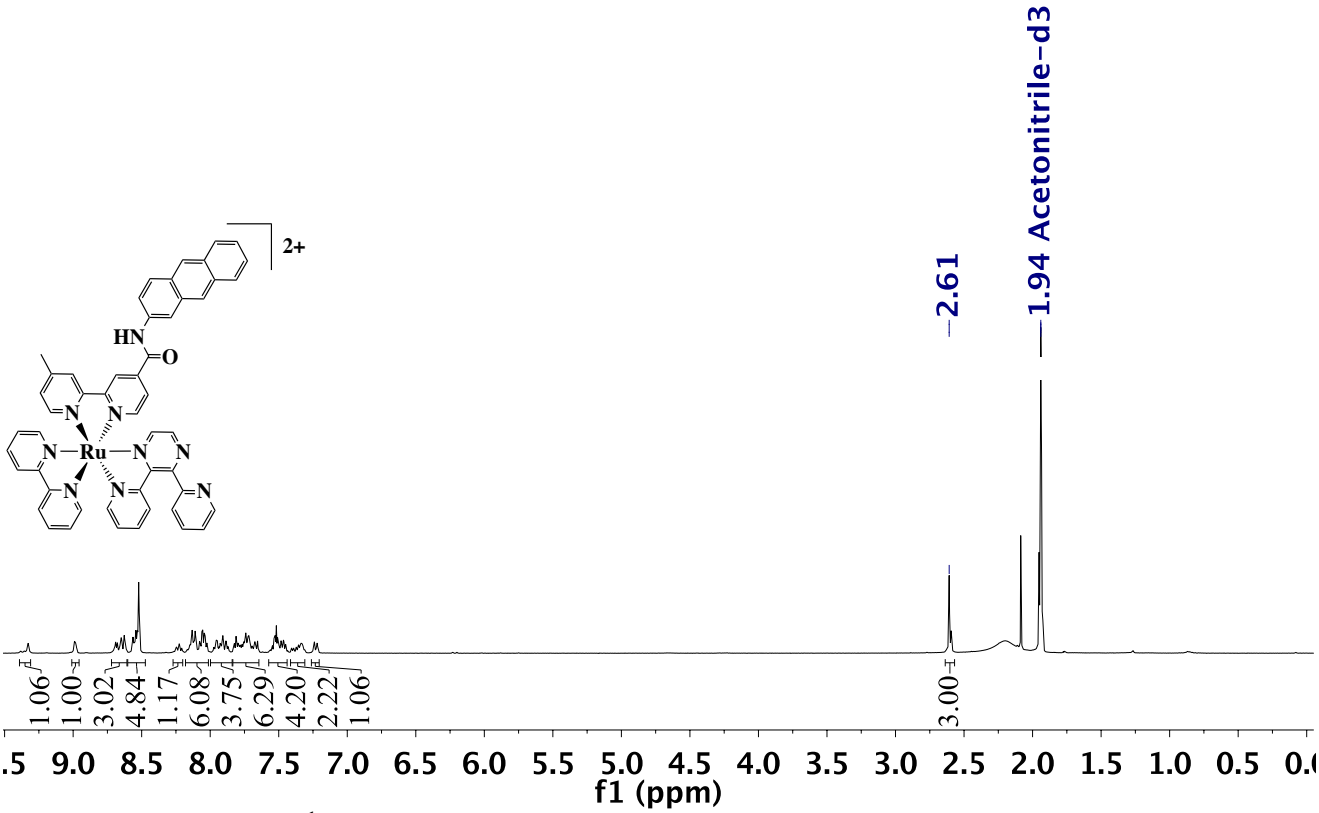

Figure 2.13. Complete ^{1}H-NMR spectrum of [(AnthbpyMe)(bpy)Ru(dpp)]$(PF_6)_2$ in CD_3CN (bpy = 2,2'-bipyridine, dpp = 2,3-bis(2-pyridyl)pyrazine, and AnthbpyMe = 4-[N-(2-anthryl)carbamoyl]-4′-methyl-2,2′-bipyridine).

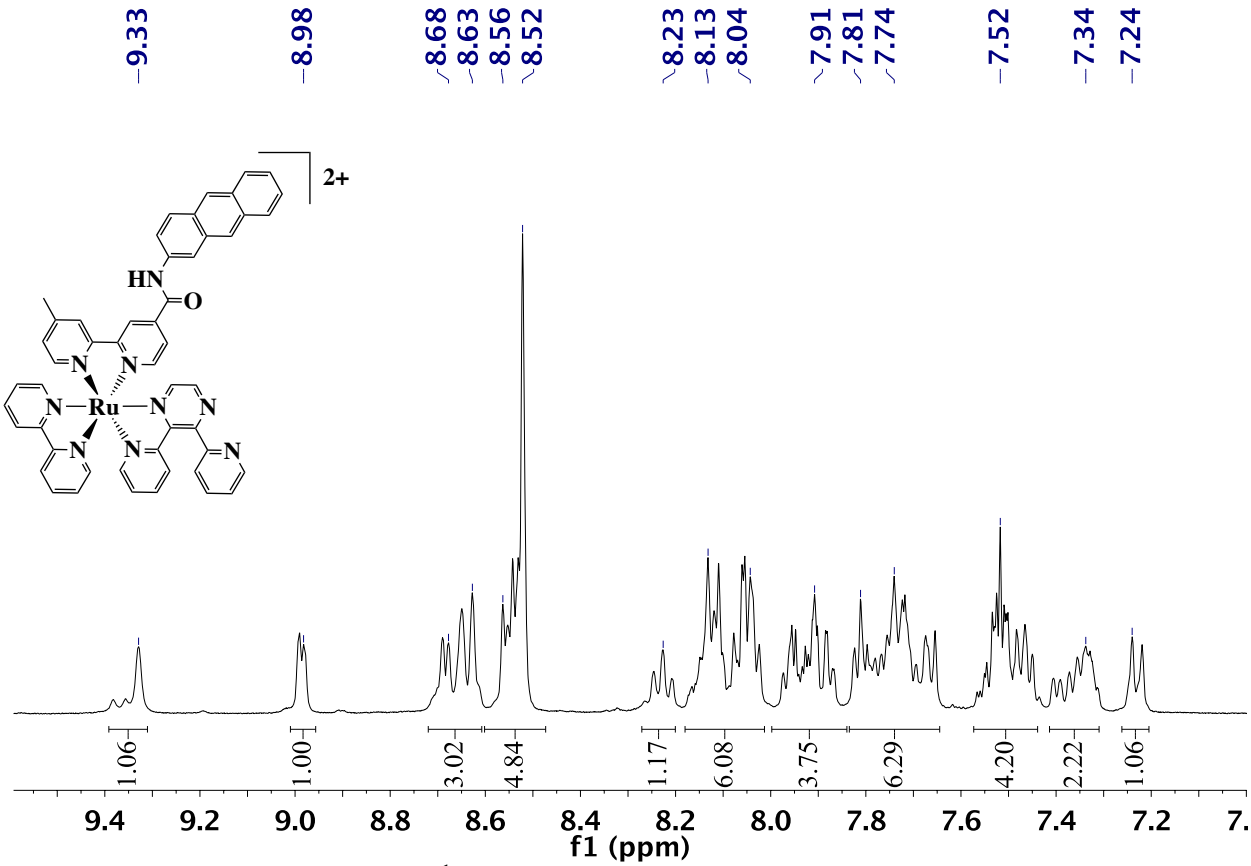

Figure 2.14. Aromatic region of ^{1}H-NMR spectrum for [(AnthbpyMe)(bpy)Ru(dpp)]$(PF_6)_2$ in CD_3CN with chemical shifts (bpy = 2,2'-bipyridine, dpp = 2,3-bis(2-pyridyl)pyrazine, and AnthbpyMe = 4-[N-(2-anthryl)carbamoyl]-4′-methyl-2,2′-bipyridine).

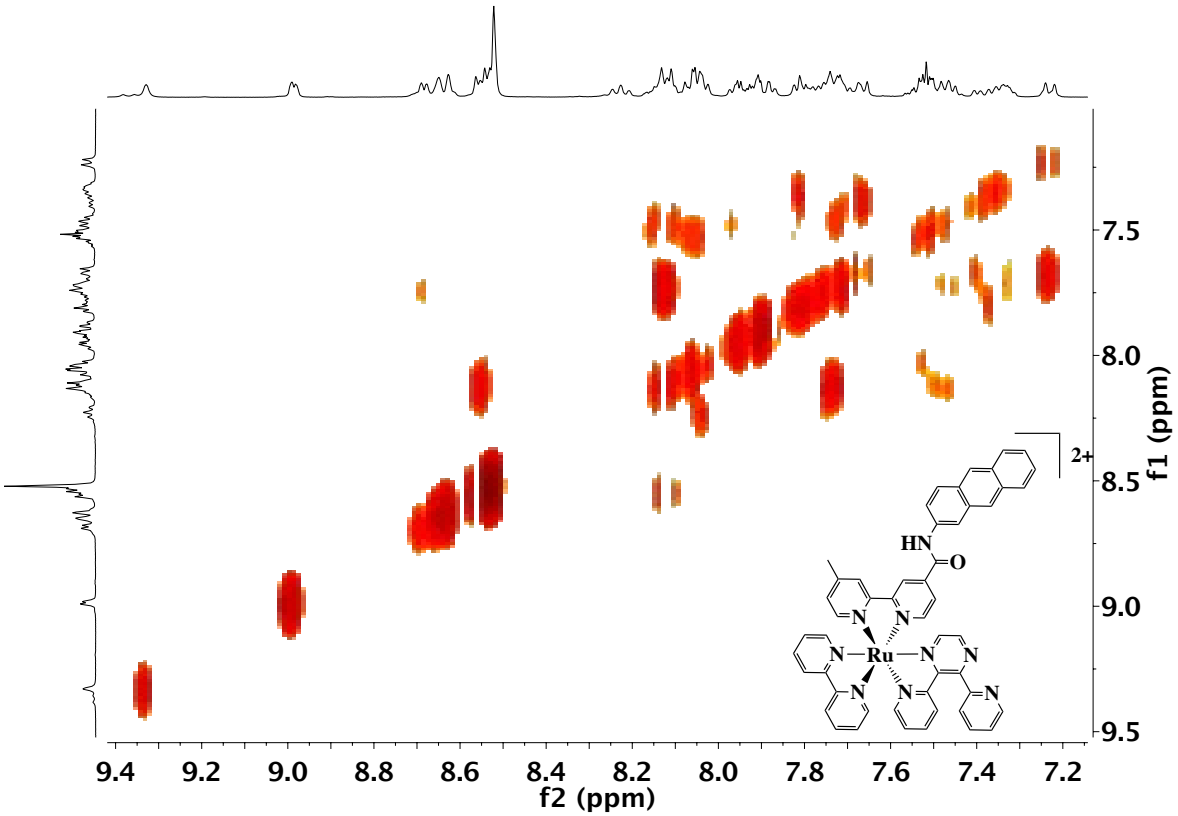

Figure 2.15. ^{1}H-^{1}H COSY spectra of [(AnthbpyMe)(bpy)Ru(dpp)]$(PF_6)_2$ in CD_3CN (bpy = 2,2'-bipyridine, dpp = 2,3-bis(2-pyridyl)pyrazine, and AnthbpyMe = 4-[N-(2-anthryl)carbamoyl]-4′-methyl-2,2′-bipyridine).

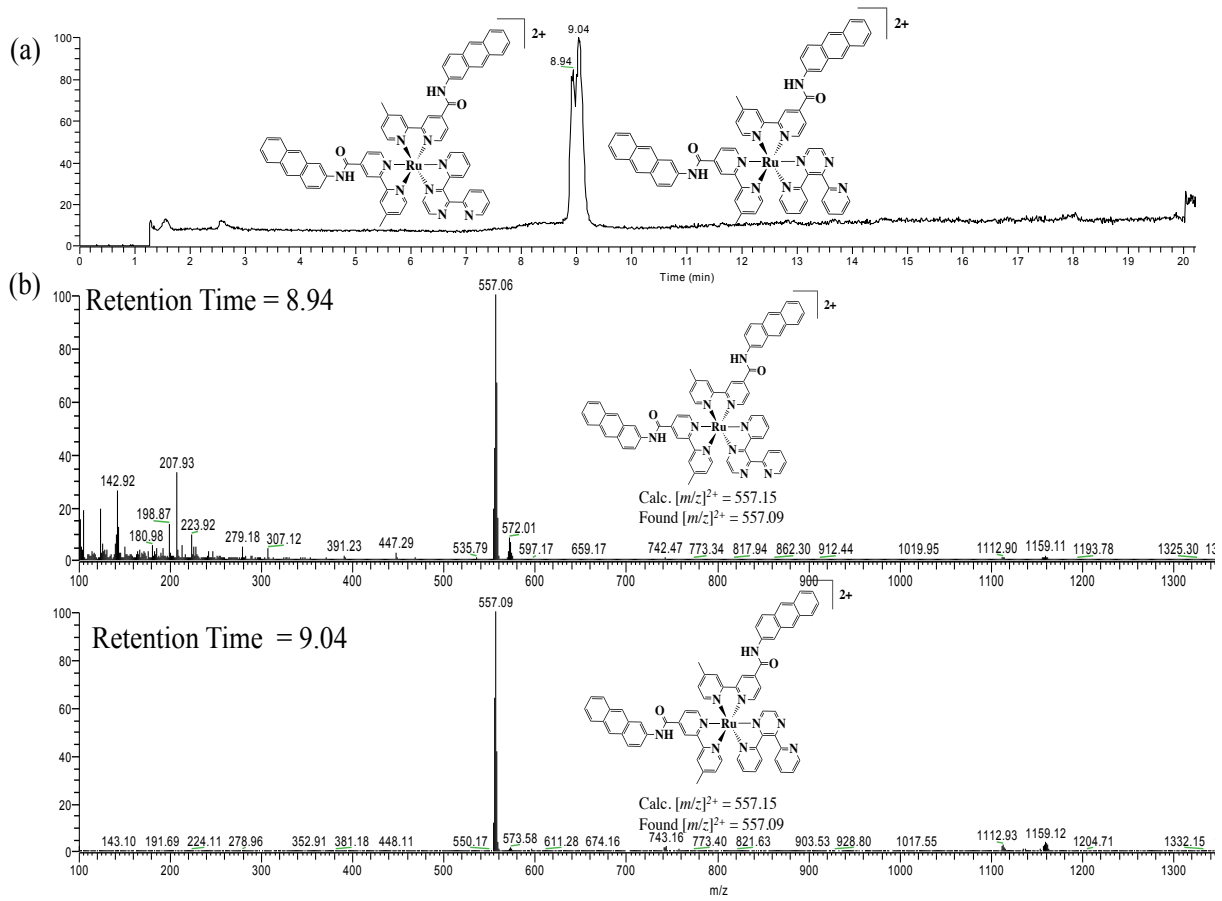

Figure 2.16. (a) HPLC chromatogram of $[(AnthbpyMe)_2Ru(dpp)]^{2+}$ displaying retention times (dpp = 2,3-bis(2-pyridyl)pyrazine, and AnthbpyMe = 4-[N-(2-anthryl)carbamoyl]-4′-methyl-2,2′-bipyridine). (b) Total mass spectrum of the peaks at the given retention times.

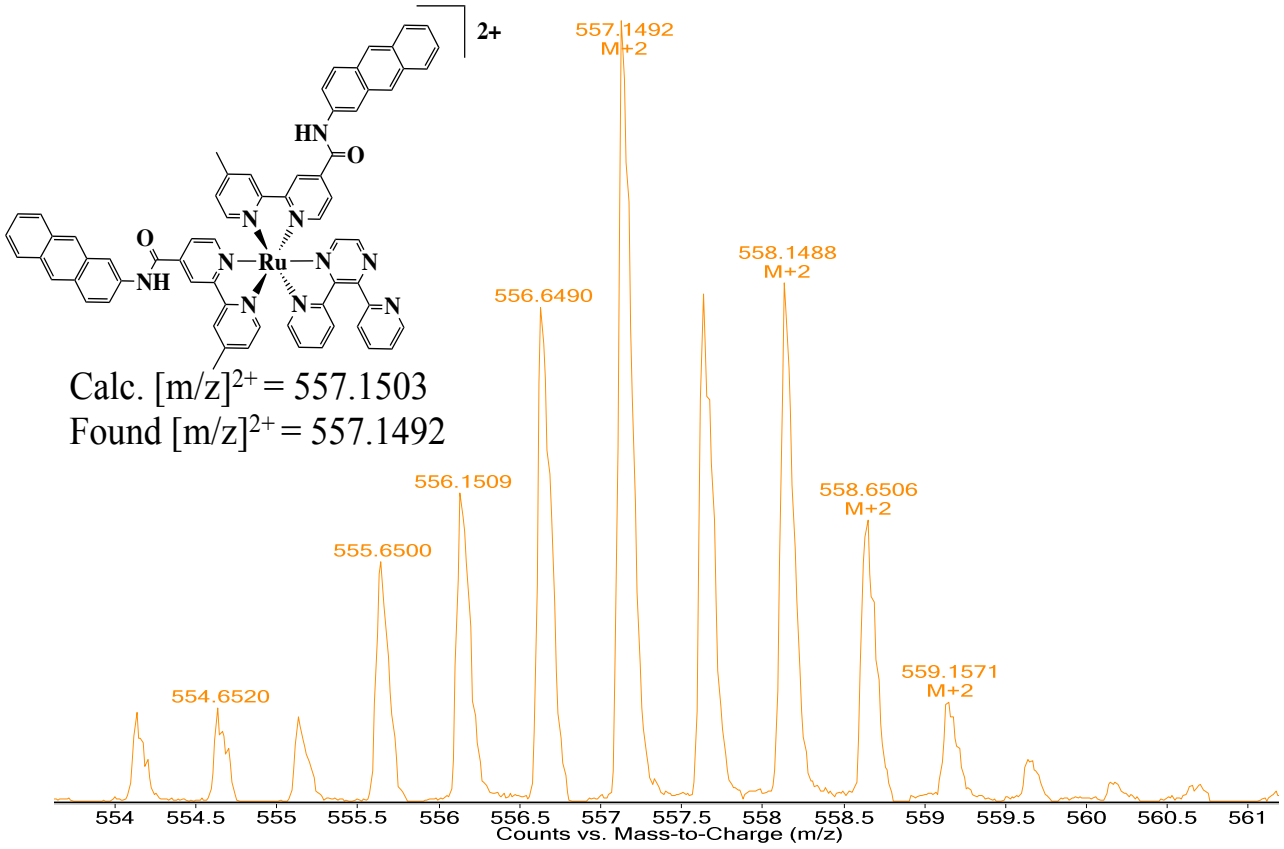

Figure 2.17. Exact mass spectrum of $[(AnthbpyMe)_2Ru(dpp)](PF_6)_2$ showing isotopic distribution pattern (dpp = 2,3-bis(2-pyridyl)pyrazine, and AnthbpyMe = 4-[N-(2-anthryl)carbamoyl]-4′-methyl-2,2′-bipyridine).

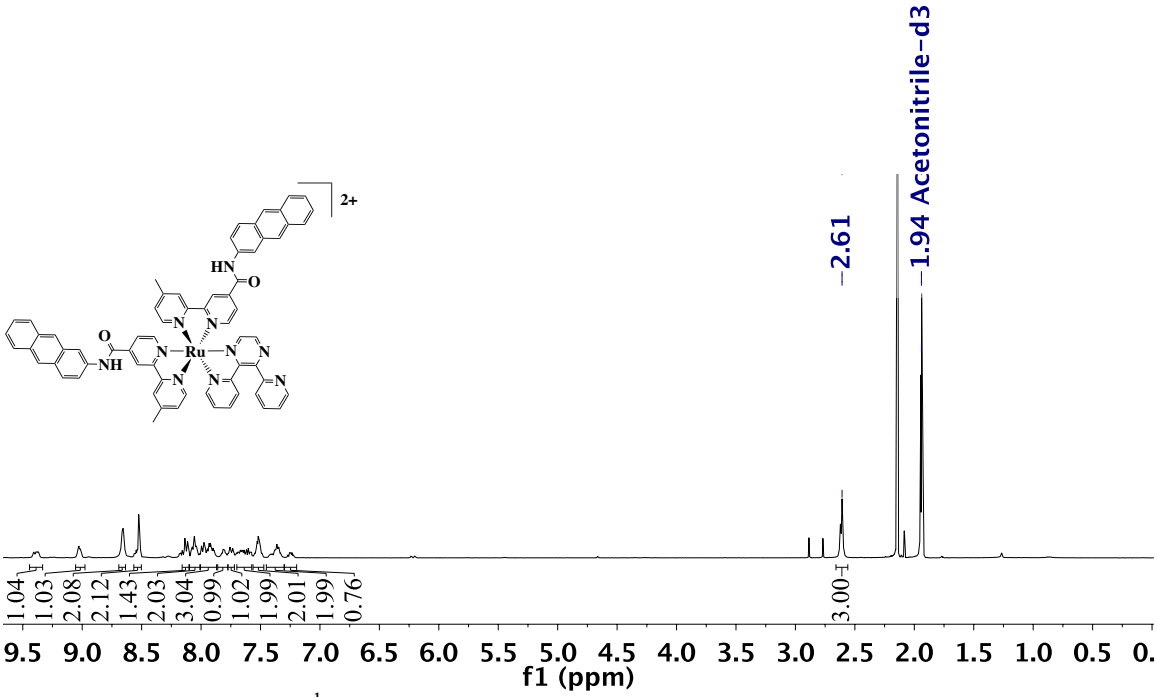

Figure 2.18. Complete ^{1}H-NMR spectrum of $[(AnthbpyMe)_2Ru(dpp)](PF_6)_2$ saturated solution in CD_3CN with chemical shifts (dpp = 2,3-bis(2-pyridyl)pyrazine, and AnthbpyMe = 4-[N-(2-anthryl)carbamoyl]-4′-methyl-2,2′-bipyridine).

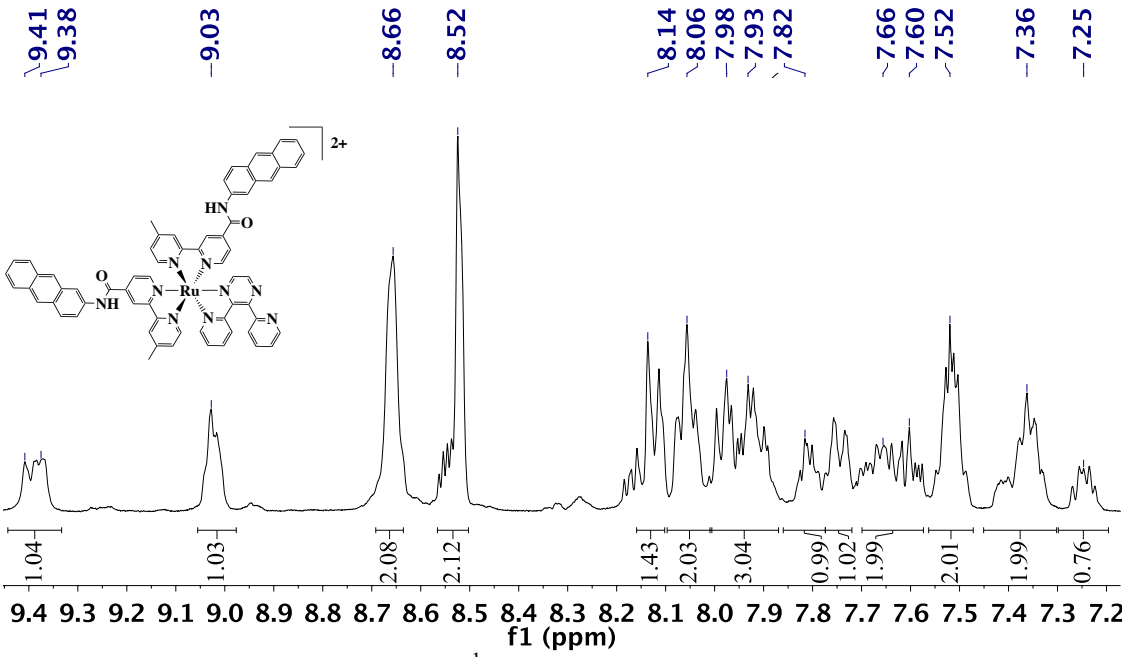

Figure 2.19. Aromatic region of ^{1}H-NMR spectrum for $[(AnthbpyMe)_2Ru(dpp)](PF_6)_2$ in CD_3CN (dpp = 2,3-bis(2-pyridyl)pyrazine, and AnthbpyMe = 4-[N-(2-anthryl)carbamoyl]-4′-methyl-2,2′-bipyridine).

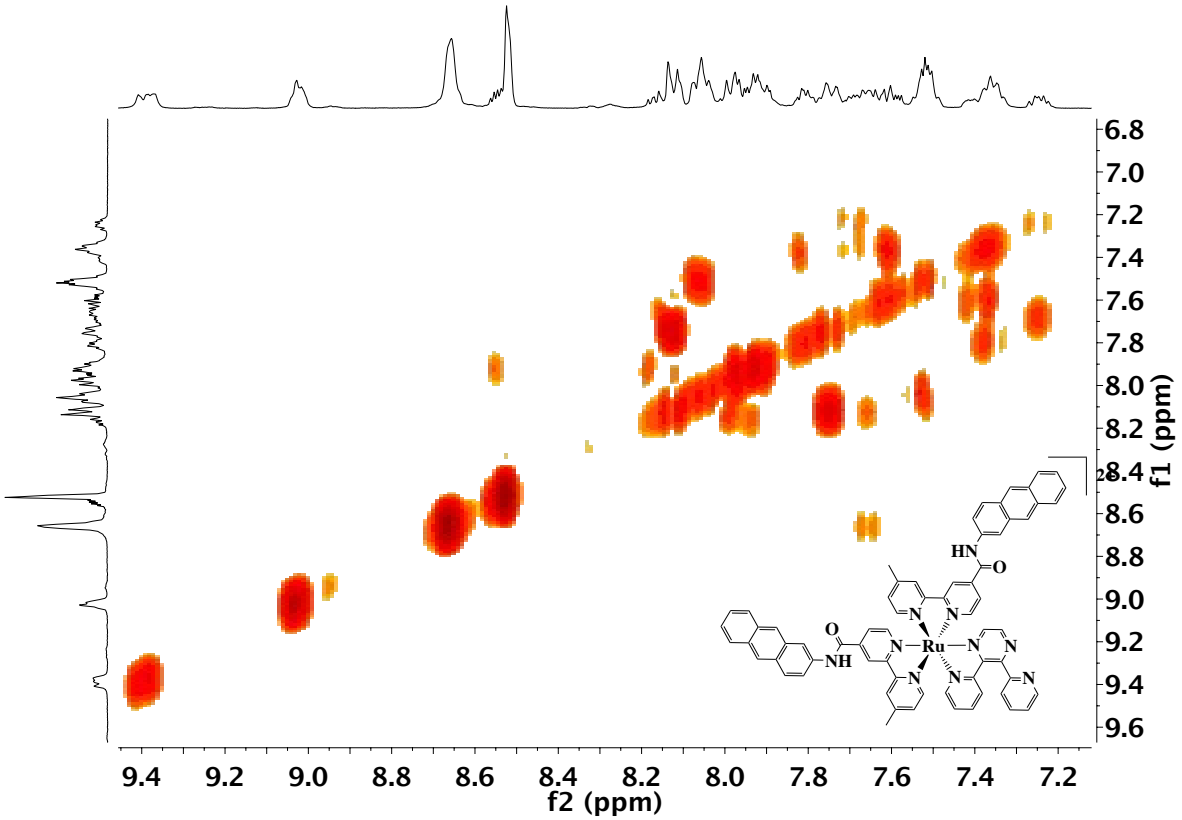

Figure 2.20. ^{1}H-^{1}H COSY spectra of $[(AnthbpyMe)_2Ru(dpp)](PF_6)_2$ in CD_3CN (dpp = 2,3-bis(2-pyridyl)pyrazine, and AnthbpyMe = 4-[N-(2-anthryl)carbamoyl]-4′-methyl-2,2′-bipyridine).

Quantum yields. The quantum yields of emission were obtained by the ratio method (equation 2.1).[7,37-39]

$$\Phi_s = \Phi_r \left(\frac{\int F_s(\lambda_{em})\, d\lambda}{1 - 10^{-A_s(\lambda_{exc})}} \right) \left(\frac{1 - 10^{-A_r(\lambda_{exc})}}{\int F_r(\lambda_{em})\, d\lambda} \right) \left(\frac{n_s^2}{n_r^2} \right) \qquad (2.1)$$

Here the subscripts *s* and *r* correspond to sample and reference compounds whereas *em* and *exc* designate the emission and excitation wavelengths, respectively. The Φ_i is the emission quantum yield, n_i is the index of refraction of the solvent medium, $F_i(\lambda)$ is the emission intensity, and $A_i(\lambda)$ is the optical density at the excitation wavelength.

Cell viability. Viability was calculated as the percent reduction value for each experimental sample divided by the percent reduction value for the matched control as follows (Equation 2.2).

$$\frac{Experimental\ Percent\ Reduction}{Control\ Percent\ Reduction} = Cell\ Viability \qquad (2.2)$$

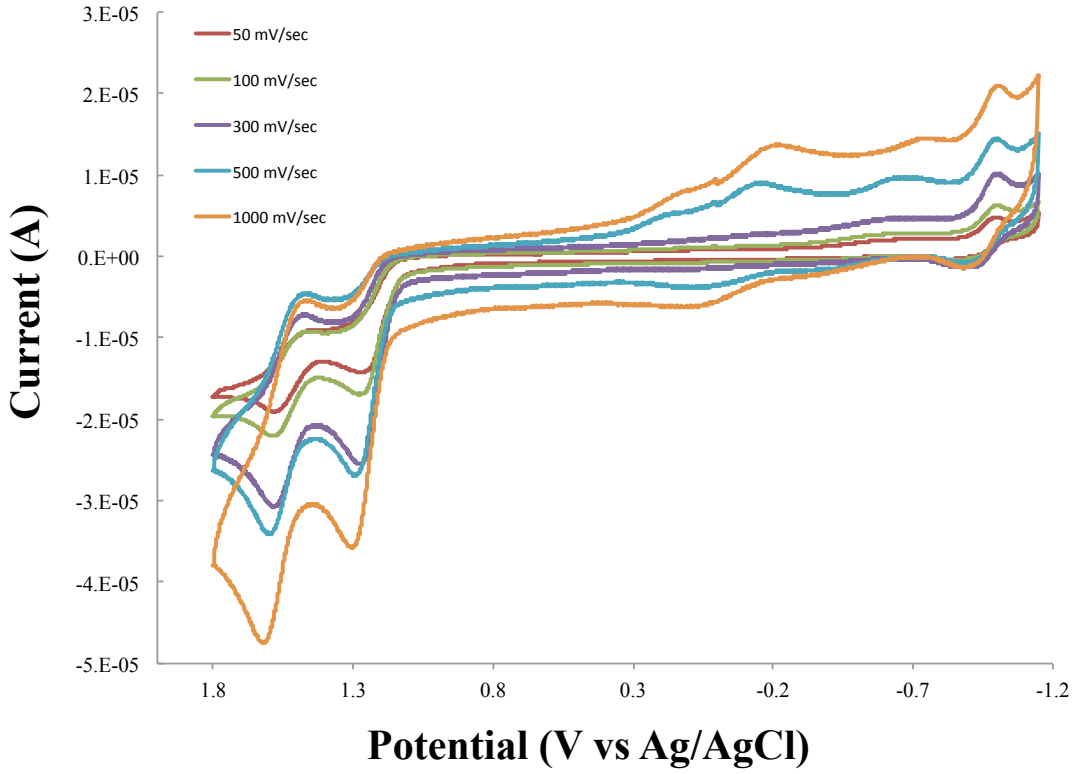

Figure 2.21. Cyclic voltammogram and scan rate dependence plots of [(AnthbpuyMe)(bpy)Ru(dpp)]$(PF_6)_2$ in 0.1 M Bu_4NPF_6 from +1.80 V to –1.2 V vs. Ag/AgCl at various scan rates (50 mV/sec to 1000 mV/sec).

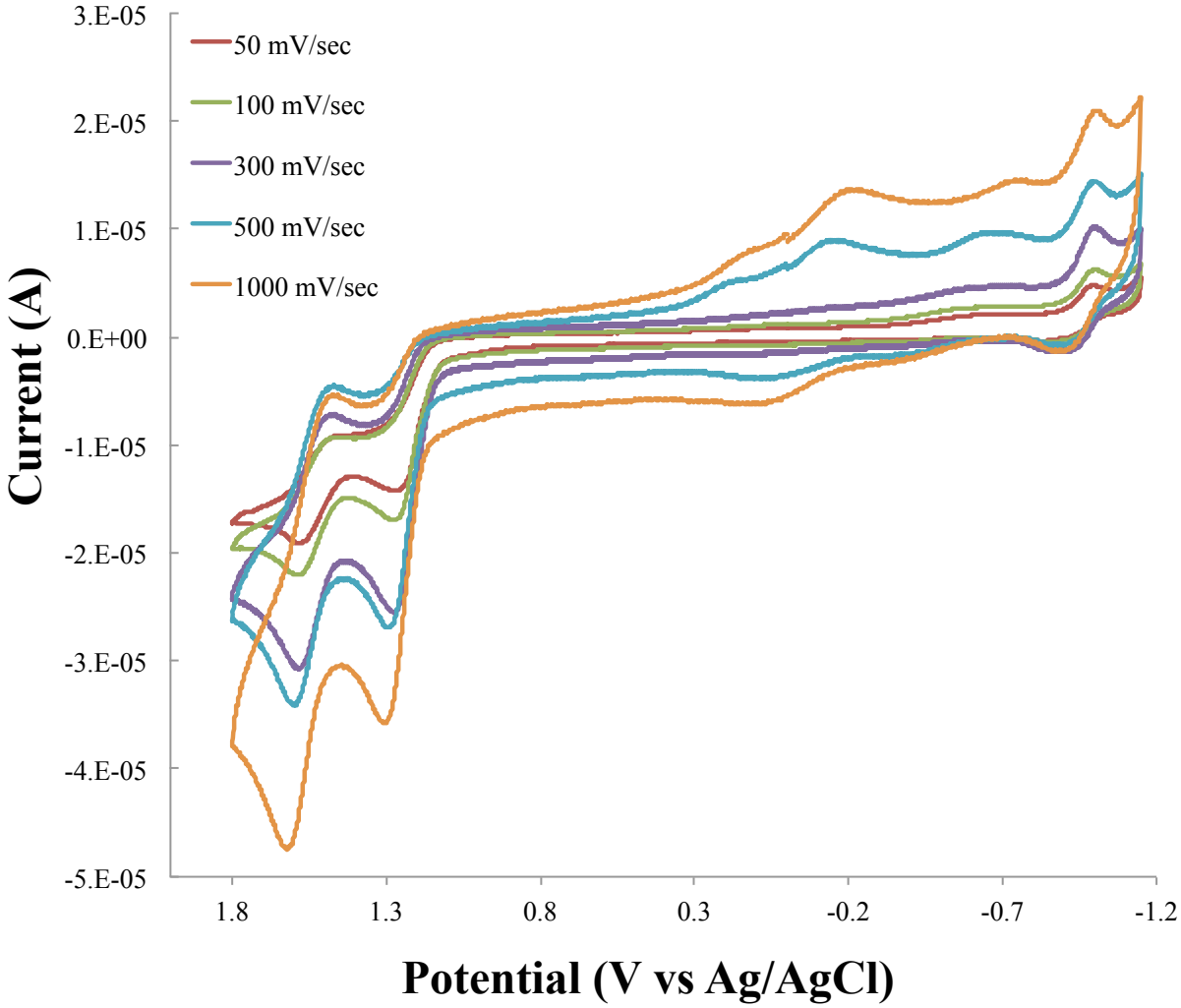

Figure 2.22. Cyclic voltammogram and scan rate dependence plots of $[(AnthbpuyMe)_2Ru(dpp)](PF_6)_2$ in 0.1 M Bu_4NPF_6 from +1.80 V to –1.2 V vs. Ag/AgCl at various scan rates (50 mV/sec to 1000 mV/sec).

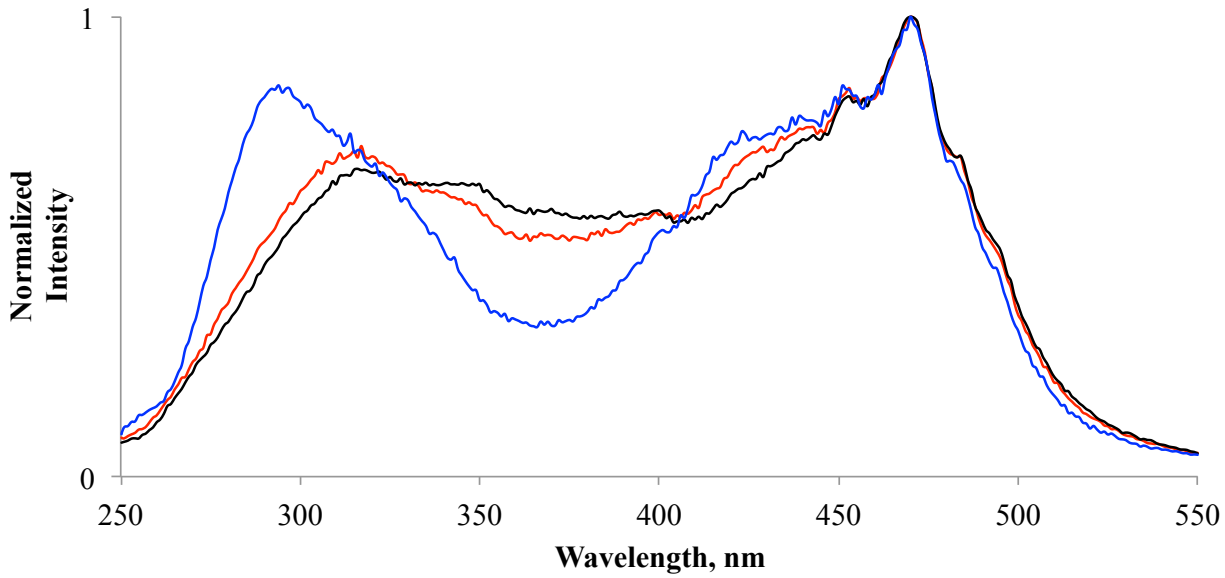

Figure 2.23. Normalized excitation spectra of $[(bpy)_2Ru(dpp)](PF_6)_2$ (blue), $[(AnthbpyMe)(bpy)Ru(dpp)](PF_6)_2$ (red), and $[(AnthbpyMe)_2Ru(dpp)](PF_6)_2$ (black) in acetonitrile.

Emission lifetime decays. The emission lifetimes were obtained using either the time-correlated single photon counting method or laser pulse method as described in the materials and methods section of the main text. It is assumed that the observed decay rates of the bichromophoric complexes are comprised of radiative, k_r, and non-radiative, k_{nr}, rate constants corresponding to the donor in the absence of the tethered acceptor and an additional quenching rate constant, k_q, in the presence of the tethered acceptor (equation 2.3):

$$\boldsymbol{k_{obs} = (\tau_{obs})^{-1} = k_r + k_{nr} + k_q} \qquad (2.3)$$

Quenching Efficiency. Fluorescence quenching efficiencies, Φ_q, were calculated with equation 2.4:

$$\boldsymbol{\Phi_q = 1 - \frac{\Phi_{DA}}{\Phi_D} = 1 - \frac{\tau_{DA}}{\tau_D}} \qquad (2.4)$$

where Φ_{DA} is the fluorescence quantum yield of the donor in the presence of the acceptor (τ_D and τ_{DA} are the fluorescence lifetimes of the donor in the absence and presence of acceptor respectively). The anthracene singlet quenching efficiencies observed for complexes **2** and **3** are

considerably less than the near unity quenching efficiency obtained for similar Ru-polypyridyl-anthracene complex covalently bound through non-insulating bridging bpy-anthracene ligands.[74]

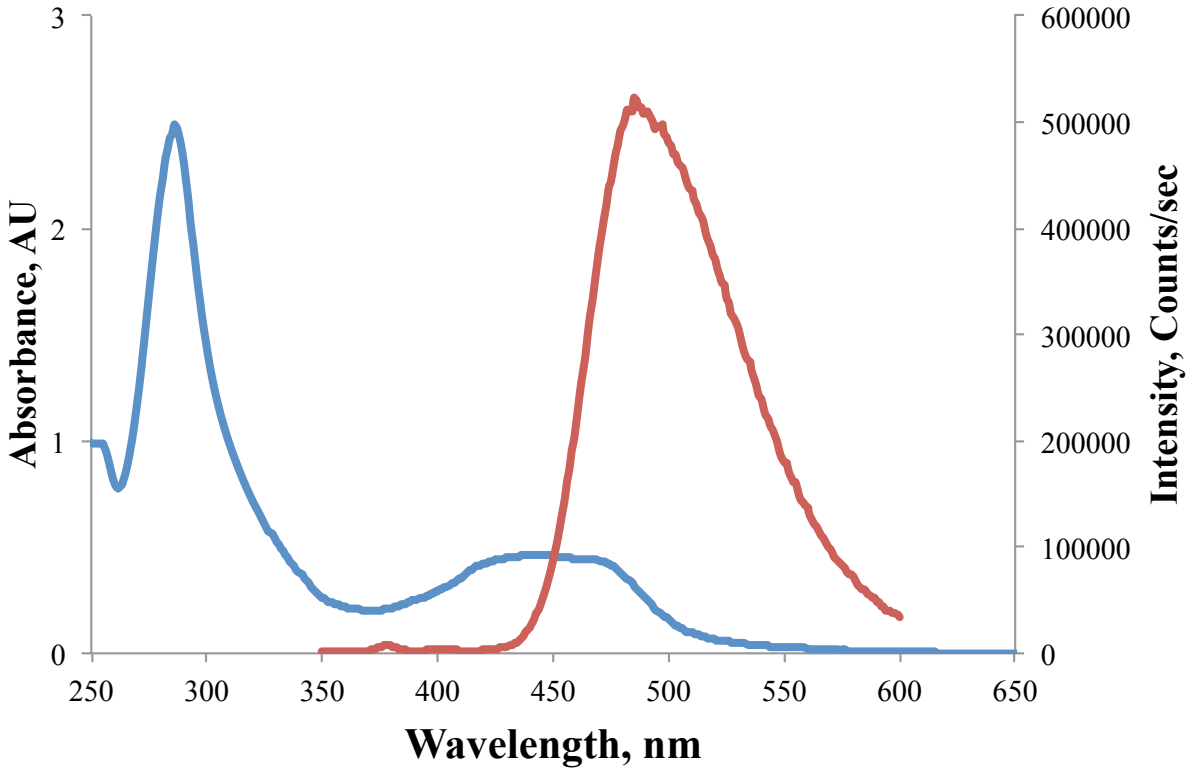

Figure 2.24. Figure 6. Electronic absorption spectrum of $[(bpy)_2Ru(dpp)]^{2+}$ (blue) and steady state emission of 2-aminoanthracene (red, λ_{ex} = 340 nm) in CH_3CN.

The rate of quenching by FRET, k_{FRET}, can be estimated by the relationship (equation 2.5):

$$\boldsymbol{k_{FRET} = \tau_D{}^{-1}\left(\frac{R_o}{R}\right)^6} \qquad (2.5)$$

where τ_D has the same meaning as above, R is the actual distance between the energy donor, anthracene, and acceptor, $Ru(bpy)_2(dpp)$, and R_o, is known as the Förster distance. The latter, R_o, is defined as the distance at which the efficiency of energy transfer is 50% and is directly proportional to the fluorescence quantum yield of the donor in the absence of acceptor, Φ_D, and the Förster overlap integral, J, by the expression (equation 2.6):

$$\boldsymbol{R_o = \left[\frac{9000(\ln 10)\kappa^2 \Phi_D J}{128\pi^5 N_A n^4}\right]^{1/6}} \quad (2.6)$$

where κ^2 is a geometric parameter and describes the relative orientation between the donor and acceptor transition dipole moments, N_A is Avogadro's number, and n is the refractive index of the sample media. For an ensemble in which the donor and acceptor dipole moments are randomly distributed, sampling all possible orientations, the κ^2 parameter averages to 2/3. This value is often substituted for κ^2 in the equation above. However, covalent attachment of anthracene to the bipyridyl ligand(s) via amide linkage restricts the orientation of the anthracene and Ru-core transition dipole moments. Despite this covalent attachment, the anthracene moiety still has room for a range of conformations make a precise estimate of κ^2 difficult, therefore, the 2/3 conventional value is retained. The overlap integral can be quantified by equation 2.7:

$$\boldsymbol{J = \frac{\int_0^\infty I_D(\lambda)\varepsilon_A(\lambda)\lambda^4 d\lambda}{\int_0^\infty I_D(\lambda) d\lambda}} \quad (2.7)$$

where $I_D(\lambda)$ is the emission spectra of the donor and $\varepsilon_A(\lambda)$ is the extinction spectra of the acceptor.

Rhem-Weller analysis. The thermodynamic energy for an excited state oxidative electron transfer is calculated by equation 2.8.[75-77]

$$\Delta G_{ET} = \left(E_{ox,anthracen} - E_{red,dpp}\right) - E_{oo} \quad (2.8)$$

In the expression, ΔG_{ET} represents the free-energy of excited state electron transfer, $E_{ox,dpp}$, $E_{red,anthr}$, and E_{oo} are the one electron oxidation potential of the anthracene, reduction potential of the dpp ligand, and the excited state energy of the anthracene singlet excited state, respectively (*vida supra*).[75-77]

Dexter. Within the framework of the exchange (Dexter) mechanism the observed lifetime decay of D* in the presence of A has been modeled as:[78]

$$I_D(t) = I_D(0)\exp\left[-\frac{t}{\tau_D} - \gamma_D^{-3}\left(\frac{C_A}{C_o}\right)g\left(\frac{e^{\gamma_D}t}{\tau_D}\right)\right] \quad (2.9)$$

where γ_D is related to the Dexter critical transfer distance, R_D, (or the distance at which the probability of energy transfer is 50%) and the average Bohr radius of the interacting species, L, by

$$\gamma_D = \frac{2R_D}{L} \quad (2.10)$$

C_A is the concentration of acceptors and C_o is the critical transfer concentration which is related to R_D. By Taylor expansion and assuming that $e^{\gamma}t/\tau_D$ is sufficiently larger than zero, the function g(z) in equation 2.6 can be approximated by:[78]

$$g(z) = (\ln z)^3 + 1.73(\ln z)^2 + 5.93(\ln z) + 5.44 \quad (11)$$

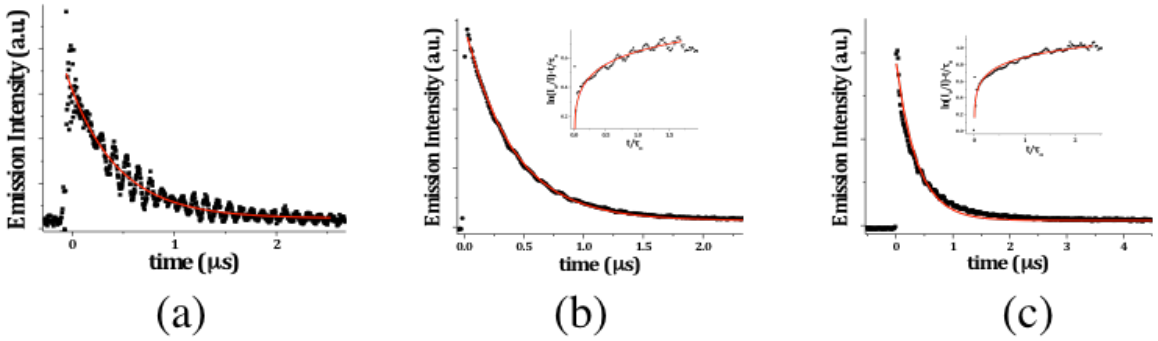

(a) (b) (c)

Figure 2.25. Emission lifetime decays (black circles) and their corresponding single exponential fits (red lines) for $[(bpy)_2Ru(dpp)](PF_6)_2$ (a), $[(AnthbpyMe)(bpy)Ru(dpp)](PF_6)_2$ (b), and $[(AnthbpyMe)_2Ru(dpp)](PF_6)_2$ (c) in acetonitrile. The insets show the best fit of the data to equation 2.11.

2.8 REFERENCES

1. Creutz, C.; Chou, M.; Netzel, T. L.; Okumura, M.; Sutin, N., Lifetimes, spectra, and quenching of the excited states of polypyridine complexes of iron(II), ruthenium(II), and osmium(II) *Journal of the American Chemical Society.* **1980**, *102,* 1309-1319.
2. Meyer, T. J., Photochemistry of metal coordination complexes: metal to ligand charge transfer excited states. In *Pure and Applied Chemistry*, 1986; Vol. 58, p 1193.
3. Damrauer, N. H.; McCusker, J. K., Ultrafast dynamics in the metal-to-ligand charge transfer excited-state evolution of $[Ru(4,4'\text{-diphenyl-}2,2'\text{-bipyridine})_3]^{2+}$ *Journal of Physical Chemistry A.* **1999**, *103,* 8440-8446.
4. McClenaghan, N. D.; Barigelletti, F.; Maubert, B.; Campagna, S., Towards ruthenium(II) polypyridine complexes with prolonged and predetermined excited state lifetimes *Chemical Communications.* **2002**, 602-603.
5. Juris, A.; Balzani, V.; Barigelletti, F.; Campagna, S.; Belser, P.; Von Zelewsky, A., Ru(II) polypyridine complexes: photophysics, photochemistry, eletrochemistry, and chemiluminescence *Coordination Chemistry Reviews.* **1988**, *84,* 85-277.
6. McClenaghan, N. D.; Leydet, Y.; Maubert, B.; Indelli, M. T.; Campagna, S., Excited-state equilibration: a process leading to long-lived metal-to-ligand charge transfer luminescence in supramolecular systems *Coordination Chemistry Reviews.* **2005**, *249,* 1336-1350.
7. de Carvalho, I. M. M.; de Sousa Moreira, Í.; Gehlen, M. H., Synthesis, characterization, and photophysical studies of new bichromophoric ruthenium(II) complexes *Inorganic Chemistry.* **2003**, *42,* 1525-1531.
8. Wilson, G. J.; Launikonis, A.; Sasse, W. H.; Mau, A. W.-H., Excited-state processes in ruthenium(II) bipyridine complexes containing covalently bound arenes *Journal of Physical Chemistry A.* **1997**, *101,* 4860-4866.
9. Kercher, M.; König, B.; Zieg, H.; De Cola, L., Photoinduced Energy- and Electron-Transfer Processes within Dynamic Self-assembled Donor−Acceptor Arrays *Journal of the American Chemical Society.* **2002**, *124,* 11541-11551.
10. Schoonover, J. R.; Dattelbaum, D. M.; Malko, A.; Klimov, V. I.; Meyer, T. J.; Styers-Barnett, D. J.; Gannon, E. Z.; Granger, J. C.; Aldridge, W. S.; Papanikolas, J. M., Ultrafast energy transfer between the 3MLCT state of $[RuII(dmb)_2(bpy\text{-}an)]^{2+}$ and the covalently appended anthracene *Journal of Physical Chemistry A.* **2005**, *109,* 2472-2475.
11. El-ghayoury, A.; Harriman, A.; Khatyr, A.; Ziessel, R., Intramolecular triplet energy transfer in metal polypyridine complexes bearing ethynylated aromatic groups *Journal of Physical Chemistry A.* **2000**, *104,* 1512-1523.
12. Albano, G.; Balzani, V.; Constable, E. C.; Maestri, M.; Smith, D. R., Photoinduced processes in 4′ -(9-anthryl)-2,2′ :6′ ,2″ -terpyridine, its protonated forms and Zn(II), Ru(II) and Os(II) complexes *Inorganica Chimica Acta.* **1998**, *277,* 225-231.
13. Serroni, S.; Campagna, S.; Pistone Nascone, R.; Hanan, G. S.; Davidson, G. J. E.; Lehn, J.-M., Controlling the Direction of Photoinduced Energy Transfer in Multicomponent Species *Chemistry- A European Journal.* **1999**, *5,* 3523-3527.
14. Castellano, F. N., Altering molecular photophysics by merging organic and inorganic chromophores *Accounts of Chemical Research.* **2015**, *48,* 828-839.

15. Mariappan, M.; Maiya, B. G., Effects of Anthracene and Pyrene Units on the Interactions of Novel Polypyridylruthenium(II) Mixed-Ligand Complexes with DNA *European Journal of Inorganic Chemistry.* **2005**, *2005,* 2164-2173.
16. Lincoln, R.; Kohler, L.; Monro, S.; Yin, H.; Stephenson, M.; Zong, R.; Chouai, A.; Dorsey, C.; Hennigar, R.; Thummel, R. P.; McFarland, S. A., Exploitation of long-lived ^{3}IL excited states for metal–organic photodynamic therapy: verification in a metastatic melanoma model *Journal of the American Chemical Society.* **2013**, *135,* 17161-17175.
17. Fleisher, M. B.; Waterman, K. C.; Turro, N. J.; Barton, J. K., Light-induced cleavage of DNA by metal complexes [1] *Inorganic Chemistry.* **1986**, *25,* 3549-3551.
18. Monro, S.; Scott, J.; Chouai, A.; Lincoln, R.; Zong, R.; Thummel, R. P.; McFarland, S. A., Photobiological activity of Ru(II) dyads based on (pyren-1-yl)ethynyl derivatives of 1,10-phenanthroline *Inorganic Chemistry.* **2010**, *49,* 2889-2900.
19. Shi, G.; Monro, S.; Hennigar, R.; Colpitts, J.; Fong, J.; Kasimova, K.; Yin, H.; DeCoste, R.; Spencer, C.; Chamberlain, L.; Mandel, A.; Lilge, L.; McFarland, S. A., Ru(II) dyads derived from α-oligothiophenes: A new class of potent and versatile photosensitizers for PDT *Coordination Chemistry Reviews.* **2015**, *282–283,* 127-138.
20. Liu, J.; Chen, Y.; Li, G.; Zhang, P.; Jin, C.; Zeng, L.; Ji, L.; Chao, H., Ruthenium(II) polypyridyl complexes as mitochondria-targeted two-photon photodynamic anticancer agents *Biomaterials.* **2015**, *56,* 140-153.
21. Mari, C.; Pierroz, V.; Ferrari, S.; Gasser, G., Combination of Ru(II) complexes and light: new frontiers in cancer therapy *Chemical Science.* **2015**, *6,* 2660-2686.
22. Maher, E. A.; Furnari, F. B.; Bachoo, R. M.; Rowitch, D. H.; Louis, D. N.; Cavenee, W. K.; DePinho, R. A., Malignant glioma: genetics and biology of a grave matter *Genes and Development.* **2001**, *15,* 1311-1333.
23. Castro, M. G.; Cowen, R.; Williamson, I. K.; David, A.; Jimenez-Dalmaroni, M. J.; Yuan, X.; Bigliari, A.; Williams, J. C.; Hu, J.; Lowenstein, P. R., Current and future strategies for the treatment of malignant brain tumors *Pharmacology and Therapeutics.* **2003**, *98,* 71-108.
24. Reardon, D. A.; Rich, J. N.; Friedman, H. S.; Bigner, D. D., Recent advances in the treatment of malignant astrocytoma *Journal of Clinical Oncology.* **2006**, *24,* 1253-1265.
25. Mongelli, M. T.; Heinecke, J.; Mayfield, S.; Okyere, B.; Winkel, B. S. J.; Brewer, K. J., Variation of DNA photocleavage efficiency for $[(TL)_2Ru(dpp)]Cl_2$ complexes where TL=2,2'-bipyridine, 1,10-phenanthroline, or 4,7-diphenyl-1,10-phenanthroline *Journal of Inorganic Biochemistry.* **2006**, *100,* 1983-1987.
26. Kumar, C. V.; Punzalan, E. H. A.; Tan, W. B., Adenine-thymine base Pair recognition by an anthryl probe from the DNA minor groove *Tetrahedron.* **2000**, *56,* 7027-7040.
27. Lewis, F. D.; Liu, W., Luminescence of N-arylbenzamides in low-temperature glasses *Journal of Physical Chemistry A.* **1999**, *103,* 9678-9686.
28. Gomer, C. J., Preclinical examination of first and second generation photosensitizers used in photodynamic therapy *Photochemistry and Photobiology.* **1991**, *54,* 1093-1107.
29. Josefsen, L. B.; Boyle, R. W., Photodynamic therapy: novel third-generation photosensitizers one step closer? *British Journal of Pharmacology.* **2008**, *154,* 1-3.
30. Castano, A. P.; Demidova, T. N.; Hamblin, M. R., Mechanisms in photodynamic therapy: part one—photosensitizers, photochemistry and cellular localization *Photodiagnosis and Photodynamic Therapy.* **2004**, *1,* 279-293.

31. Weinheimer, C.; Choi, Y.; Caldwell, T.; Gresham, P.; Olmsted Iii, J., Effect of a steric spacer on chromophoric interactions of ruthenium complexes containing covalently bound anthracene *Journal of photochemistry and photobiology A*. **1994**, *78,* 119-126.
32. Zigler, D. F.; Elvington, M. C.; Heinecke, J.; Brewer, K. J., Luminescently tagged 2,2‘-bipyridine complex of FeII: synthesis and photophysical studies of 4-[N-(2-anthryl)carbamoyl]-4‘-methyl-2,2‘-bipyridine *Inorganic Chemistry*. **2006**, *45,* 6565-6567.
33. Padilla, R.; Corrales, J. A. R.; Donohoe, L. E.; Winkel, B. S. J.; Brewer, K. J., A new class of Ru(II) polyazine agents with potential for photodynamic therapy *Chemical Communicaion.* **2015**, *Just accepted*.
34. Zelonka, R. A.; Baird, M. C., Benzene complexes of ruthenium(II) *Canadian Journal of Chemistry.* **1972**, *50,* 3063-3072.
35. Bennett, M. A.; Huang, T. N.; Matheson, T. W.; Smith, A. K.; Ittel, S.; Nickerson, W., (η6-Hexamethylbenzene)ruthenium complexes. In *Inorganic Syntheses*, John Wiley & Sons, Inc.: 2007; pp 74-78.
36. Bard, A. J.; Faulkner, L. R., *Electrochemical methods : fundamentals and applications*. 2nd ed.; Wiley: New York, 2001; p xxi, 833 p.
37. Wallace, A. W.; Murphy, R. J., W.; Petersen, J. D., Electrochemical and photophysical properties of mono- and bimetallic ruthenium(II) complexes *Inorganica Chimica Acta.* **1989**, *166,* 47-54.
38. Kawanishi, Y.; Kitamura, N.; Tazuke, S., Dependence of spectroscopic, electrochemical, and excited-state properties of tris chelate ruthenium(II) complexes on ligand structure *Inorganic Chemistry.* **1989**, *28,* 2968-2975.
39. Valeur, B.; Berberan-Santos, M. N., *Molecular fluorescence : principles and applications*. Second edition. ed.; Wiley-VCH Verlag GmbH & Co. KGaA: Weinheim, Germany, 2013; p xix, 569 pages.
40. O'Connor, D. V.; Phillips, D., *Time-correlated single photon counting*. Academic Press: London, 1984; p viii, 288 p.
41. Demas, J. N., *Excited state lifetime measurements*. Academic Press: New York, 1983; p xiii, 273 p.
42. Baba, A. I.; Shaw, J. R.; Simon, J. A.; Thummel, R. P.; Schmehl, R. H., The photophysical behavior of d6 complexes having nearly isoenergetic MLCT and ligand localized excited states *Coordination Chemistry Reviews.* **1998**, *171,* 43-59.
43. Zhu, J.; Prussin, R.; Dominijanni, A.; Brewer, K. J.; Robertson, J. L., Exploring cellular activity of a polyazine bridged Ru(II)–Pt(II) supramolecule in rat malignant glioma F98 *Manuscript in progress.* **2015**.
44. O'Brien, J.; Wilson, I.; Orton, T.; Pognan, F., Investigation of the Alamar Blue (resazurin) fluorescent dye for the assessment of mammalian cell cytotoxicity *European Journal of Biochemistry.* **2000**, *267,* 5421-5426.
45. Mongelli, M. T.; Brewer, K. J., Synthesis and study of the light absorbing, redox and photophysical properties of Ru(II) and Os(II) complexes of 4,7-diphenyl-1,10-phenanthroline containing the polyazine bridging ligand 2,3-bis(2-pyridyl)pyrazine *Inorganic Chemistry Communications.* **2006**, *9,* 877-881.
46. Weinberg, N. L.; Weinberg, H. R., Electrochemical oxidation of organic compounds *Chemical Reviews.* **1968**, *68,* 449-523.

47. Wilson, G. J.; Launikonis, A.; Sasse, W. H. F.; Mau, A. W. H., Excited-state processes in ruthenium(II) bipyridine complexes containing covalently bound arenes *Journal of Physical Chemistry A.* **1997**, *101,* 4860-4866.
48. Simon, J. A.; Curry, S. L.; Schmehl, R. H.; Schatz, T. R.; Piotrowiak, P.; Jin, X.; Thummel, R. P., Intramolecular electronic energy transfer in ruthenium(II) diimine donor/pyrene acceptor complexes linked by a single C−C bond *Journal of the American Chemical Society.* **1997**, *119,* 11012-11022.
49. Juris, A.; Balzani, V.; Barigelletti, F.; Campagna, S.; Belser, P. l.; Von Zelewsky, A., Ru (II) polypyridine complexes: photophysics, photochemistry, eletrochemistry, and chemiluminescence *Coordination Chemistry Reviews.* **1988**, *84,* 85-277.
50. Brewer, K. J.; Murphy Jr, W. R.; Spurlin, S. R.; Petersen, J. D., The next generation of (polyazine) ruthenium (II) complexes *Inorganic Chemistry.* **1986**, *25,* 882-884.
51. Braunstein, C. H.; Baker, A. D.; Strekas, T. C.; Gafney, H. D., Spectroscopic and electrochemical properties of the dimer tetrakis (2, 2'-bipyridine)(-2, 3-bis (2-pyridyl) pyrazine) diruthenium (II) and its monomeric analog *Inorganic Chemistry.* **1984**, *23,* 857-864.
52. Lumpkin, R. S.; Kober, E. M.; Worl, L. A.; Murtaza, Z.; Meyer, T. J., Metal-to-ligand charge-transfer (MLCT) photochemistry: experimental evidence for the participation of a higher lying MLCT state in polypyridyl complexes of ruthenium(II) and osmium(II) *Journal of Physical Chemistry.* **1990**, *94,* 239-243.
53. Crosby, G.; Demas, J., Quantum efficiencies on transition metal complexes. II. Charge-transfer luminescence *Journal of the American Chemical Society.* **1971**, *93,* 2841-2847.
54. Klevens, H. B.; Platt, J. R., Spectral resemblances of cata‐condensed hydrocarbons *Journal of Chemical Physics.* **1949**, *17,* 470-481.
55. Mecklenburg, S. L.; Peek, B. M.; Schoonover, J. R.; McCafferty, D. G.; Wall, C. G.; Erickson, B. W.; Meyer, T. J., Photoinduced electron transfer in amino acid assemblies *Journal of the American Chemical Society.* **1993**, *115,* 5479-5495.
56. Mecklenburg, S. L.; McCafferty, D. G.; Schoonover, J. R.; Peek, B. M.; Erickson, B. W.; Meyer, T. J., Spectroscopic study of electron transfer in a trifunctional lysine with anthraquinone as the electron acceptor *Inorganic Chemistry.* **1994**, *33,* 2974-2983.
57. Lumpkin, R. S.; Kober, E. M.; Worl, L. A.; Murtaza, Z.; Meyer, T. J., Metal-to-Ligand Charge-Transfer (Mlct) Photochemistry - Experimental-Evidence for the Participation of a Higher Lying Mlct State in Polypyridyl Complexes of Ruthenium(Ii) and Osmium(Ii) *Journal of Physical Chemistry.* **1990**, *94,* 239-243.
58. Dey, J.; Warner, I. M., Dual fluorescence of 9-(N,N-dimethylamino)anthracene: Effect of solvent polarity and viscosity *Journal of Physical Chemistry A.* **1997**, *101,* 4872-4878.
59. Rettig, W., Photoinduced charge separation via twisted intramolecular charge transfer states. In *Electron Transfer I*, Mattay, J., Ed. Springer Berlin Heidelberg: 1994; Vol. 169, pp 253-299.
60. Suresh, M.; Kar, P.; Das, A., Intramolecular charge transfer aromatic amines and their application towards molecular logic gate *Inorganica Chimica Acta.* **2010**, *363,* 2881-2885.
61. Turro, N. J., *Modern molecular photochemistry*. Benjamin/Cummings Pub. Co.: Menlo Park, Calif., 1978; p 628 p.
62. Forster, T., Zwischenmolekulare energiewanderung und fluoreszenz *Annalen Der Physik.* **1948**, *2,* 55-75.

63. Forster, T., 10th Spiers memorial lecture - transfer mechanisms of electronic excitation *Discussions of the Faraday Society.* **1959**, 7-17.
64. Bock, C. R.; Meyer, T. J.; Whitten, D. G., Electron transfer quenching of the luminescent excited state of tris(2,2'-bipyridine)ruthenium(II). Flash photolysis relaxation technique for measuring the rates of very rapid electron transfer reactions *Journal of the American Chemical Society.* **1974**, *96,* 4710-4712.
65. Ward, M. D., Photo-induced electron and energy transfer in non-covalently bonded supramolecular assemblies *Chemical Society Reviews.* **1997**, *26,* 365-375.
66. Knibbe, H.; Rehm, D.; Weller, A., Formation of electron donor-acceptor complexes in stimulated state *Berichte der Bunsen-Gesellschaft Physical Chemistry Chemical Physics.* **1967**, *71,* 916-&.
67. Knibbe, H.; Rehm, D.; Weller, A., Intermediates and kinetics of fluorescence quenching by electron transfer *Berichte der Bunsen-Gesellschaft Physical Chemistry Chemical Physics.* **1968**, *72,* 257-&.
68. Knibbe, H.; Rehm, D.; Weller, A., Thermodynamics of excited electron donor-acceptor complex formation *Berichte der Bunsen-Gesellschaft Physical Chemistry Chemical Physics.* **1969**, *73,* 839.
69. Mandal, K.; Pearson, T. D. L.; Krug, W. P.; Demas, J. N., Singlet energy transfer from the charge-transfer excited state of tris(2,2'-bipyridine)ruthenium(II) to laser dyes *Journal of the American Chemical Society.* **1983**, *105,* 701-707.
70. Mandal, K.; Pearson, T. D. L.; Demas, J. N., Singlet energy transfer from the charge transfer excited state of tris (2,2′ ‐ bipyridine) ruthenium (II) *Journal of Chemical Physics.* **1980**, *73,* 2507-2509.
71. Mandal, K.; Demas, J. N., Surfactant-enhanced singlet energy transfer from the charge-transfer excited state of tris(2,2-bipyridine) ruthenium(II) *Chemical Physics Letters.* **1981**, *84,* 410-414.
72. Inokuti, M.; Hirayama, F., Influence of energy transfer by the exchange mechanism on donor luminescence *Journal of Chemical Physics.* **1965**, *43,* 1978-1989.
73. Jain, A.; Slebodnick, C.; Winkel, B. S. J.; Brewer, K. J., Enhanced DNA photocleavage properties of Ru(II) terpyridine complexes upon incorporation of methylphenyl substituted terpyridine and/or the polyazine bridging ligand dpp (2,3-bis(2-pyridyl)pyrazine) *Journal of Inorganic Biochemistry.* **2008**, *102,* 1854-1861.
74. Wilson, G. J.; Launikonis, A.; Sasse, W. H.; Mau, A. W.-H., Excited-state processes in ruthenium(II) bipyridine complexes containing covalently bound arenes *The Journal of Physical Chemistry A.* **1997**, *101,* 4860-4866.
75. Knibbe, H.; Rehm, D.; Weller, A., Formation of Electron Donor-Acceptor Complexes in Stimulated State *Berichte Der Bunsen-Gesellschaft Fur Physikalische Chemie.* **1967**, *71,* 916-&.
76. Knibbe, H.; Rehm, D.; Weller, A., Intermediates and Kinetics of Fluorescence Quenching by Electron Transfer *Berichte Der Bunsen-Gesellschaft Fur Physikalische Chemie.* **1968**, *72,* 257-&.
77. Knibbe, H.; Rehm, D.; Weller, A., Thermodynamics of Excited Electron Donor-Acceptor Complex Formation *Berichte Der Bunsen-Gesellschaft Fur Physikalische Chemie.* **1969**, *73,* 839-&.
78. Inokuti, M.; Hirayama, F., Influence of energy transfer by the exchange mechanism on donor luminescence *The Journal of Chemical Physics.* **1965**, *43,* 1978-1989.

Chapter 3 A New Class of Ru(II) Polyazine Agents with Potential for Photodynamic Therapy

Roberto Padilla[a]*, José A. Rodriguez-Corrales[a], Lauren E. Donohoe[a] Brenda S. J. Winkel[b], and Karen J. Brewer[a†]

[a]Department of Chemistry, Virginia Tech, Blacksburg, VA 24061-0212 VA 24061-0212.

[b]Department of Biological Sciences, Virginia Tech, Blacksburg, VA 24061-0406.

* Corresponding author e-mail: rpadill4@vt.edu (Roberto Padilla)
† Deceased October 24, 2014

Keywords: Photodynamic therapy, metal-organic Ru(II), anthracene, photocytotoxicity, bichromatic

Foreword. This chapter represents a stand-alone manuscript that was submitted to *Chemical Communication* currently accepted and pending revisions. The work presented in this manuscript was conducted by Roberto Padilla with the assistance of Jose A. Rodriguez-Corrales (validated DNA shift gel assays) and Lauren E. Donohoe (repeated CT-DN titration studies). This was supervised by Professors Brenda S. J. Winkel[b] and Professors Karen J. Brewer[a†]

3.1 Abstract

Appending anthracene units to $[(bpy)_2Ru(dpp)]^{2+}$ results in Ru(II) agents that exhibit dynamic photoreactivity towards DNA and protein. $[(Anthbpy)(bpy)Ru(dpp)]^{2+}$ and $[(Anthbpy)_2Ru(dpp)]^{2+}$ are the first metal-organic Ru(II) agent with dpp ligands shown to photomodify DNA in the presence or absence of oxygen, while also binding protein in an oxygen-dependent manner.

3.2 Manuscript New Class of Ru(II) Polyazine Agents with Potential for Photodynamic Therapy

Ru(II) photosensitizers (PSs) have been investigated extensively as potential agents for photodynamic anti-cancer therapy (PDT).[1-3]The well-studied $[Ru(bpy)_3]^{+2}$ PS mediates the

oxidation of DNA via quenching of the $[Ru(bpy)_3]^{2+}$ triplet metal-to-ligand charge transfer (^{3}MLCT) excited state by molecular oxygen, $^3O_2$, upon light activation.[4,5]Ru(II) PSs that efficiently sensitize $^3O_2$ have been shown to modify DNA and/or protein within cells, which disrupts cell homeostasis leading to necrotic and/or apoptotic processes.[4,6,7]Although Ru(II) agents that efficiently produce $^1O_2$ are desirable for PDT, Ru(II) systems that exhibit multiple pathways of reactivity are sought in order to improve PDT efficacy.[8] One approach has been to covalently append polycyclic aromatic hydrocarbon (PAH) units that independently intercalate and oxidize DNA.[9-11]The reactivity of these Ru(II) hybrid complexes has been found to be intimately associated with both the nature of the covalent linker and the type of chromophore appended to the Ru(II) unit, thus suggesting new avenues for optimizing the photoreactivity of Ru(II) agents for PDT.[12-18]

We recently described the synthesis and characterization of $[(AnthbpyMe)(bpy)Ru(dpp)]^{2+}$ (**2**) and $[(AnthbpyMe)_2Ru(dpp)]^{2+}$ (**3**) (AnthbpyMe = 4-[N-(2-anthryl)carbamoyl]-4'-methyl-2,2'-bipyridine; bpy = 2,2'-bipyridine; dpp = 2, 3-bis (2′-pyridyl) pyrazine (Figure 1).[19]

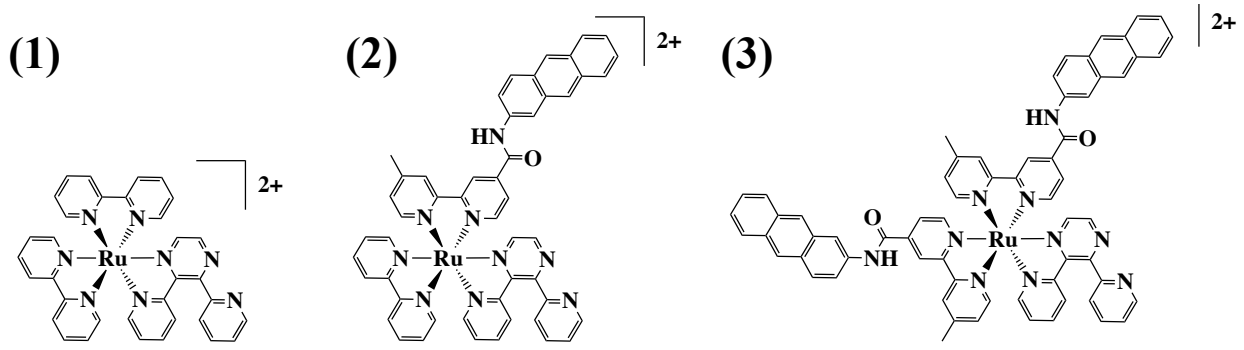

Figure 3.1. Structural representation of the parent molecule, $[(bpy)_2Ru(dpp)]^{2+}$ (**1**), and the anthryl derivatives, $[(AnthbpyMe)(bpy)Ru(dpp)]^{2+}$ (**2**), and $[(AnthbpyMe)_2Ru(dpp)]^{2+}$ (**3**).

The PAH, anthracene, has shown substantial promise for enhancing the PDT reactivity of Ru(II) complexes.[19,20]Anthracene can by itself intercalate into the DNA double helix and, upon

irradiation with UV light, oxidize adjacent sites in the DNA molecule though reactive oxygen species (ROS) or anthracene-derived cation radicals.[21-26]When appended to Ru(II) PSs, anthryl groups have been shown to promote enhanced binding to calf-thymus (CT) DNA by intercalative π-stacking, while facilitating DNA photocleavage by •OH and by sensitized $^3O_2$ mechanisms via the anthracene and Ru(II) units, respectively.[20]We have shown that complexes **2** and **3** efficiently absorb light throughout the visible region, facilitated by several MLCT transitions with λ_{max} = 459 nm (ε = 16,000 $M^{-1}cm^{-1}$) and 461 nm (ε = 21,000 $M^{-1}cm^{-1}$), respectively.[19]Upon excitation the anthracene-[Ru]-dpp hybrid arrangement provides multiple pathways, singlet-singlet, triplet-triplet, and/or singlet-triplet, for deactivation from the ^{3}MLCT excited state through energy/electron transfer, which is speculated to enhance the PDT potency that was observed for these complexes against mammalian cells in preliminary experiments.[19]

In this study, we demonstrate that $[(AnthbpyMe)(bpy)Ru(dpp)]^{2+}$ (**2**) and $[(AnthbpyMe)_2Ru(dpp)]^{2+}$ (**3**) can modify DNA and protein through multifaceted pathways that appear to be unique to the anthracene-[Ru]-dpp systems. Gel shift assays were used to examine the potential reactivity of the title complexes with biomacromolecules under diverse conditions. These assays have been used extensively to monitor the DNA binding propensity of metal-organic complexes, including oxidation of DNA via ROSs, by monitoring the electrophoretic migration of DNA.[27-31]Altered migration of the DNA-complex adduct reflects a change in size, charge, and/or configuration of DNA, the latter involving conversion of supercoiled (SC) plasmid to open circular (OC) and/or linear (L) forms.

Figure 2 compares the effects of the Ru(II) complexes on DNA with and without photolysis and in the presence and absence of oxygen.

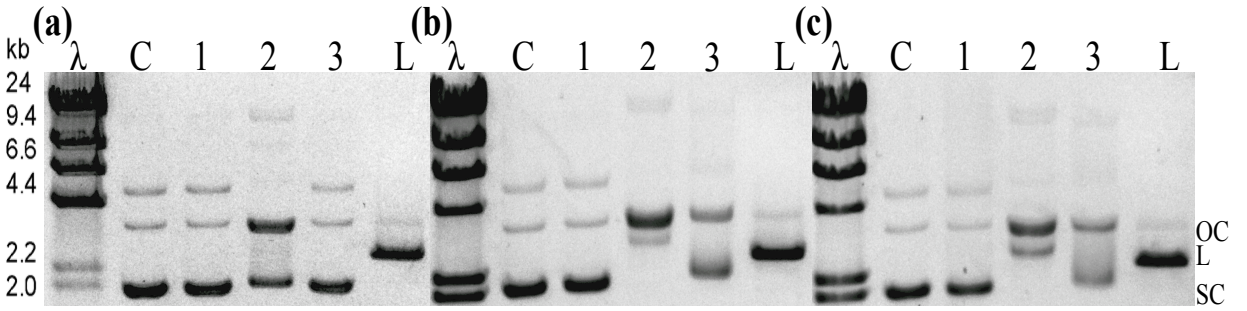

Figure 3.2. DNA gel shift assay for (a) $[(bpy)_2Ru(dpp)](PF_6)_2$ (**1**), (b) $[(AnthbpyMe)(bpy)Ru(dpp)](PF_6)_2$ (**2**), and (c) $[(AnthbpyMe)_2Ru(dpp)](PF_6)_2$ (**3**). λ: DNA weight marker, C: pUC19 DNA, 1 = 5:1 (BP:MC) incubated in the dark for 1 h, 2 = 5:1 (BP:MC) exposed to a 455 nm LED for 1 h,with $^3O_2$ 3 = 5:1 (BP:MC) exposed to a 455 nm LED for 1h without $^3O_2$, L = linearized pUC19 DNA.

Both title complexes, as well as the parent molecule, $[(bpy)_2Ru(dpp)](PF_6)_2$ (**1**), appear to be chemically inert toward DNA in the dark in the presence of oxygen (lane 1), with no detectable change in ethidium bromide fluorescence intensity or migration of the SC DNA. However, upon photolysis at 455 nm for 1 h in the presence of $^3O_2$, all three Ru(II) complexes alter the electrophoretic mobility of plasmid DNA (lanes 2 and 3). As previously reported, the parent complex (**1**) exhibited $^3O_2$-dependent conversion of a substantial proportion of SC DNA to the OC form, but only in the presence of oxygen.[30]The title complexes **2** and **3** modified the plasmid DNA even more efficiently and did so both in the presence and absence of $^3O_2$. Under both conditions these complexes completely converted SC DNA to a mixture of OC DNA and a band with a distinctly different migration rate than either OC and L DNA (control lanes C and L). The primary difference between the two anthracene-[Ru]-dpp systems appears to be in the efficiency of the conversion, with the relative intensities of the OC and intermediate bands differing reproducibly in the presence of **2** versus **3**.

It is hypothesized that the photooxidation of DNA by the anthracene-[Ru]-dpp systems under $^3O_2$ is facilitated independently by the Ru(II) PS (via $^3O_2$) or anthracene (via •OH or anthracene-derived radicals) unit(s) to produce OC DNA. The intermediate band is speculated to

consist of modified forms of OC or L DNA to which the complex is photochemically bound.[32-34] In the absence of $^3O_2$, the DNA modification is speculated to involve a •OH and/or anthracene-derived radical produced by the anthryl unit(s) to form the OC DNA, as has been reported for anthracene alone.[8,26] In this case, the faster migrating band is speculated to consist of cross-linked DNA product(s), as has previously been reported for several other anthracene derivatives.[22,32,33] Samples treated with complex **3** also exhibited a higher degree of smearing of the lower band, which is attributed to the steric constraints from the two-anthryl units which could enhance crosslinking of DNA through the formation of multiple photoadducts by a single Ru(II) complex.[34-36] These results strongly suggest that the anthracene-[Ru]-dpp hybrid systems uniquely modify plasmid DNA via an $^3O_2$-independent mechanism attributed to the appended anthryl unit(s).

To further investigate the mechanism of photooxidation and the participation of •OH radicals in DNA binding and cleavage by these complexes, we examined the effects of the •OH scavengers DMSO, sodium iodide, and sodium benzoate[20,34] on their ability to photomodify DNA (Figure 3). The parent complex (**1**) effectively converted a substantial proportion of the SC DNA to the OC form following 1 h of photolysis at 455 nm, whether or not •OH radical scavengers were present (Figure 3a). The presence of these scavengers also appeared to have little or no effect on the activity of complex **2** (Figure 3b). This supports the hypothesis that $^1O_2$ and anthracene-derived radicals mediate the formation of OC DNA and the band of intermediate mobility. Oxidation of OC DNA is hypothesized to be mediated by an anthracene-derived radical that can occur via a known ^{3}anthracene excited state that readily photooxidizes across the 9,10 position of the anthracene.[19,37]

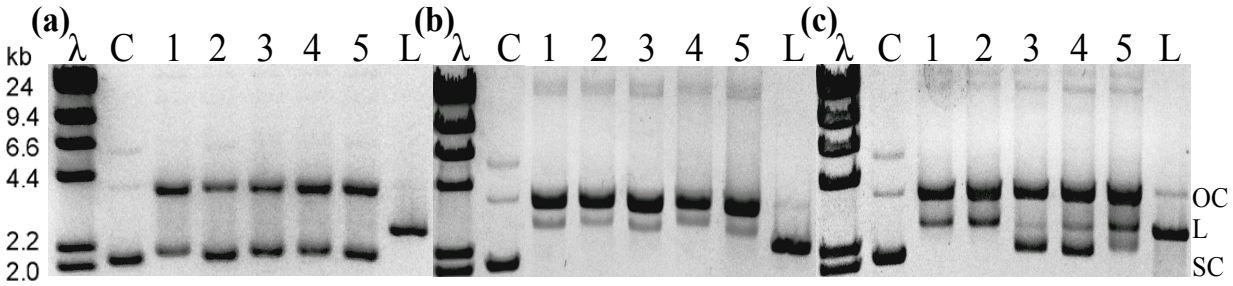

Figure 3.3. DNA gel shift assay for (a) $[(bpy)_2Ru(dpp)](PF_6)_2$, (b) $[(AnthbpyMe)(bpy)Ru(dpp)](PF_6)_2$, and (c) $[(AnthbpyMe)_2Ru(dpp)](PF_6)_2$ using a 5:1 BP:MC ratio. λ: DNA weight marker, C = pUC19 DNA, 1 = MC + hν, 2 = DMSO + MC +hν, , 3 = NaI + MC + hν, 4 = NaCl + MC + hν, 5 = sodium benzoate + MC + hν, L= linearized pUC19 DNA. hν = 455 nm LED irradiation with $^3O_2$.

In contrast, although complex **3** displayed no change in reactivity toward DNA in the presence of DMSO (Figure 3c, lane 2), samples containing sodium-based scavengers exhibited a distinctly different profile (Figure 3c, lanes 3 – 5). In this case, complex **3** converted SC DNA to OC DNA and the intermediate-mobility band, but also produced a third band with accelerated mobility. A salt-induced change in interaction of anthracene with DNA, from intercalative to non-intercalative binding, has previously been hypothesized to facilitate cleavage of the DNA backbone.[23,38]This effect, together with the presence of the second anthryl unit in complex **3,** could facilitate the formation of cross-linked DNA.

To examine the modes of binding in further detail, the apparent DNA binding constants, K_b, of the three complexes were compared. In these experiments, UV-vis spectroscopy was used to monitor the MLCT (λ_{max}) during titration with CT DNA in the dark (Table 1; ESI).[20,39,40] The results suggest that complex **2** can efficiently intercalate into the DNA duplex via the anthracene motif, as indicated by the two orders of magnitude enhancement in K_b relative to the parent complex (**1**). In contrast, complex **3,** with two anthryl units, exhibited a K_b similar to **1**, suggesting that steric constraints may impede intercalation into the DNA duplex. However, the presence of two anthracene units could facilitate inter/intra crosslinking of DNA without

influencing the MLCT transition. The results suggest that appending a second anthryl unit to the Ru(II) PS may negatively impact non-covalent intercalation, while still facilitating other binding modes that allow for DNA crosslinking.

Table 1: Results of absorption titration experiments

Complex	K_b/M^{-1}
$[(bpy)_2Ru(dpp)](PF_6)_2$ (**1**)	4.50×10^3
$[(AnthbpyMe)(bpy)Ru(dpp)](PF_6)_2$ (**2**)	3.50×10^5
$[(AnthbpyMe)_2Ru(dpp)](PF_6)_2$ (**3**)	4.50×10^3

Standard deviation ± 10%

Alternative targets for metal-organic Ru(II) agents are proteins that, like DNA, are abundant and essential cellular macromolecules.[41,42] The disruption of protein functionality within cells can trigger oxidative stress and threaten cell viability.[43,44] The oxidation of proteins can be mediated by Ru(II) PSs through sensitization of $^3O_2$, ROS production, and/or direct attack by protein-derived radicals upon light activation.[45] We therefore tested the propensity of our anthracene-[Ru]-dpp complexes to bind to and disrupt a prototypical protein, bovine serum albumin (BSA), by monitoring effects on electrophoretic migration and/or protein abundance by sodium dodecyl sulfate-polyacrylamide gel electrophoresis (SDS-PAGE).

Figure 4 displays SDS-PAGE analysis of the interaction of complexes **1**, **2**, and **3** with BSA, with and without photolysis and in the presence and absence of oxygen at a 1:1 protein-to-metal complex (P:MC) molar ratio.

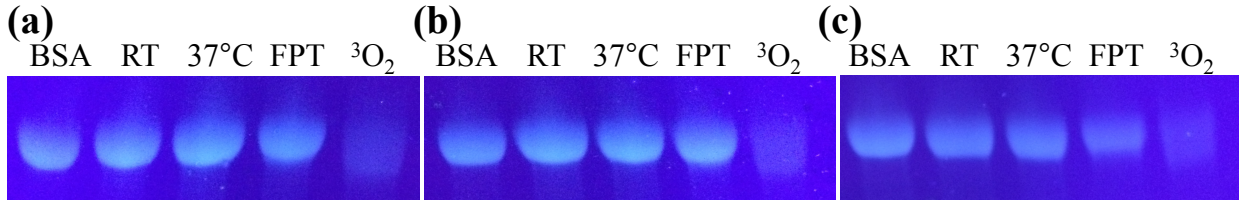

Figure 3.4. SDS-PAGE assay for (a) $[(bpy)_2Ru(dpp)](PF_6)_2$, (b) $[(AnthbpyMe)(bpy)Ru(dpp)](PF_6)_2$, and (c) $[(AnthbpyMe)_2Ru(dpp)](PF_6)_2$. BSA = bovine serum

albumin control, RT = 1:1 (P:MC) solution in the dark for 1 h at room temperature,, 37°C = 1:1 (P:MC) solution in the dark for 1 h at 37°C, and FPT = 1:1 (P:MC) solution under 455 nm irradiation for 1 h without $^3O_2$. $^3O_2$ = 1:1, (P:MC) solutions, under 455 nm irradiation for 1 h with $^3O_2$.

The three complexes displayed very similar behavior under these conditions. The migration and intensity of the bands in the first four lanes of each panel were indistinguishable, suggesting that the complexes do not interact with and/or covalently bind to BSA in the dark at either RT or 37 °C in the presence of $^3O_2$ (lanes RT and 37 °C) or following photolysis in theabsence of $^3O_2$ (lane FPT). However, a substantial decrease in fluorescence intensity was observed when the protein-complex solutions were photolyzed in the presence of $^3O_2$ (lane $^3O_2$). This suggests that the reported complexes can modify BSA via an $^3O_2$-mediated mechanism, resulting in degradation of the protein and/or the production of high-molecular-weight cross-linked products through protein-derived radical reactions.[42,46-48] No high molecular mass products were observed in these experiments, suggesting that the complexes degrade BSA, with absolute dependence on light and $^3O_2$. This is in contrast to the $^3O_2$-independent interaction of (**2**) and (**3**) with DNA, indicating that the anthracene-[Ru]-dpp complexes interact with these two biological macromolecules through different mechanisms.

The light- and $^3O_2$-mediated reactivity of these complexes was further investigated across a range of concentrations. Figure 5 displays the results of SDS-PAGE assays for solutions of protein-to-metal complex (P:MC) at 10:1, 1:1, and 1:10 molar ratios, photolyzed for 1 h in the presence of $^3O_2$.

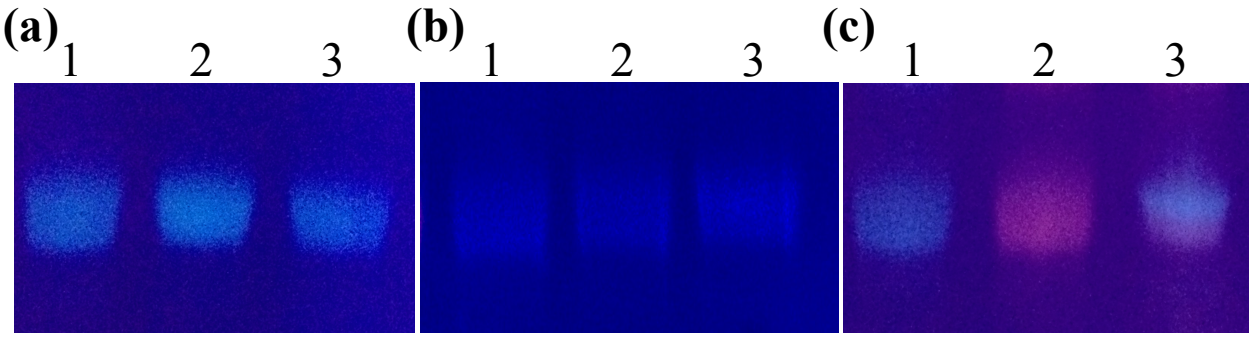

Figure 3.5. Figure 5: SDS-PAGE assay for (a) 10:1 (P:MC), (b) 1:1 (P:MC), and (c) 1:10 (P:MC) solutions containing BSA and (1) $[(bpy)_2Ru(dpp)](PF_6)_2$ (**1**), (2) $[(AnthbpyMe)(bpy)Ru(dpp)](PF_6)_2$ (**2**), or (3) $[(AnthbpyMe)_2Ru(dpp)](PF_6)_2$ (**3**) under 455 nm irradiation for 1 h with $^3O_2$. BSA = BSA control without complex.

At a 10:1 ratio, all three complexes appeared to have a minimal effect on fluorescence of the BSA band in these gels (Figure 5a). However, at ratios of 1:1 and 1:10 P:MC (Figure 5b and c) all of the samples showed evidence of photo-oxidation of the protein. Moreover, the two anthracene-containing complexes showed evidence of covalent binding to the protein, remaining associated with the protein bands even under the denaturing conditions of this assay, indicated by the red fluorescence emanating from the [Ru] core in lanes 2 and 3, Figure 5c. It was also observed that complex **3** displays a lower activity toward BSA as compared to complex **2**, which can be attributed to steric interference from the second anthryl unit, as also observed for binding to DNA.

In summary, DNA gel shift and SDS-PAGE assays established that complexes **2** and **3** mediate DNA and protein damage upon photoactivation. The complexes were shown to bind and efficiently photocleave DNA in the presence or absence of $^3O_2$, while modification of BSA displayed absolute dependence on the presence of light and $^3O_2$. This study also demonstrated that appending a second anthryl unit to the $[(bpy)_2Ru(dpp)]^{2+}$ PS can negatively impact intercalative binding properties and may facilitate the formation of cross-linked DNA. The second anthryl unit also appears to reduce binding affinity for protein. This is the first study to

show metal-organic complexes **2** and **3** are able to modify different biomacromolecules through various modes of interaction. The reported complexes offer versatile photomodification pathways toward biomacromolecules and show promise as potential PDT agents. In addition, the dpp ligands in these complexes offer the potential to chelate additional metals and further diversify their activity.

The authors are grateful to the National Science Foundation (grant CHE–1301131) for funding this work. Roberto Padilla received additional support from the National Institutes of Health (grant VT–IMSD-GM072767). This manuscript is dedicated to the memory of Karen Jenks Brewer and the generous spirit that sustained 22 years of collaboration with the Winkel group.

3.3 Supporting information: A New Class of Ru(II) Polyazine Agents with Potential for PDT

Materials and methods

Materials. All solvents/chemicals were used as received unless otherwise noted. Circular and linear pUC19 plasmid DNA were purchased from Bayou Biolabs. Lambda DNA/*Hin*dIII molecular weight marker was obtained from Promega. Electrophoresis grade (boric acid, agarose), and molecular biology grade glycerol were purchased from Fisher Scientific. Mini-PROTEAN TGX Stain-Free Precast Gels and running buffers were obtained from BioRad.

Biological Procedure

DNA gel assay. DNA-metal complex (MC) solutions were prepared in a 5:1 BP (base pairs):MC ratio in 10 mM phosphate buffer (pH = 7.4) with 16.5 μM metal complex to ensure an absorbance of at least 0.1 at the excitation wavelength (455 nm) in all samples. The complexes were dissolved in 200 μL of DMF and the concentration was determined using known extinction coefficients at the λ_{max} for each complex.[16,19] Anaerobic solutions were deoxygenated with argon

for 15 min prior to photolysis. The former solutions were then blanketed with $Ar_{(g)}$ during photolysis, while aerobic solutions where exposed to atmospheric conditions. Solutions were photolyzed for 1 h with an LED array.[31] A 0.8% w/w gel was prepared and placed in a model B1A stage Owl Separation Systems with 300 ml of 1X TB buffer (90 mM tris base, 90 mM boric acid). Each sample was prepared for loading by adding 2 μl of loading dye to a 10 μl aliquot of sample and then loaded into their respective wells. A potential of 100 V was applied through the gel for 1 h. Following electrophoresis, gels were stained in 0.5 μg/ml ethidium bromide for 0.5 h and washed using double deionized water for 0.5 h. The gels were visualized on a Fisher Biotech UV-transilluminator and images were captured using an Olympus SP-320 camera fitted with an ethidium bromide filter.

Scavenger assay. Concentration of DNA, metal complex, and buffer in the solutions were the same as described above. However, individual ROS scavengers were added before photolysis. Sodium iodide, sodium benzoate, and DMSO were used as hydroxyl radical scavengers. Sodium chloride was utilized as an ionic control in order to determine if the change in the activity of the complexes was due to an ionic component instead of an ROS scavenger effect. Little or no difference was observed between the NaCl ionic control and the sample photolyzed under standard conditions (82.5 μM DNA, 16.5 μM metal complex, 10 mM buffer).

CT-DNA titration. The concentration of CT DNA was calculated by using known extinction coefficient at 260 nm (6,600 $M^{-1}\,cm^{-1}$ per base).[49] The ratio of absorbance for the DNA sample at 260 nm and 280 nm was taken and was always greater than 1.8, indicating that the DNA was substantially free of protein.[50] A solution 5 mM in Tris buffer (pH = 7.0), 50 mM NaCl, and 30 μM in complex was prepared. This solution was titrated with increasing amounts of DNA from 10^{-6} to 10^{-4} M. The solution was incubated in the dark for 5 min prior to each measurement to

allow formation of non-covalent interaction and establishment of equilibrium. Binding constants were determined by triplicate utilizing the model proposed by Schmechel and Crothers (1971) and latter modified by Meehan *et al* (1987).[39,40]

SDS-PAGE assay. A bovine serum albumin (BSA) stock solution was prepared by dissolving 100 mg of BSA in 5 ml of 20 mM NaH_2PO_4 to give a 20 mg/ml solution. The complexes were dissolved in 200 μL of DMF and the concentration was determined by using known extinction coefficient at a λ_{max} for each complex.[16,19] Protein-metal complex solutions were prepared in a 10:1 P:MC ratio in 20 mM phosphate buffer (pH = 7.4) by diluting 50 μL of 20 mg/ml BSA protein with the appropriate amount of complex to a total volume of 500 μL. Anaerobic solutions were deoxygenated through 5 cycle of freeze pump thaw prior to photolysis for 1 h with an LED array.[31]Aerobic solutions where exposed to atmospheric conditions during photolysis for 1 h with an LED array.[31]A 10% precast polyacrylamide Mini-PROTEAN TGX Stain-Free Gels, 8.6 × 6.7 cm (W × L), was used for the SDS-PAGE analysis. Prior to loading, each samples was combined with an equal volume of loading buffer (125 mM Tris, pH 6.8, 4% SDS, 20% glycerol, 0.1% bromophenyl blue, and 2% β-mercaptoethanol) and heated at 95°C for 5 min. A potential of 200 V was applied through the gel for 30 min followed by visualization on a Fisher Biotech UV-transilluminator. The images were captured using an Olympus SP-320 camera.

3.4 References

1. Macdonald, I. J.; Dougherty, T. J., Basic principles of photodynamic therapy *Journal of Porphyrins and Phthalocyanines.* **2001**, *5,* 105-129.
2. Glazer, E. C., Light-activated metal complexes that covalently modify DNA *Israel Journal of Chemistry.* **2013**, *53,* 391-400.
3. Wang, H. t.; Li, H. h.; Huang, M. q.; Huang, W. x.; Ma, C. s.; Wang, M. l.; He, C. x.; Liu, J. h.; Zhang, Q. l., Photocleavage of DNA and adenine–thymine inclined binding by a novel ruthenium(II) complex with 3,4-dibromo-imidazo[4,5-f][1,10]phenanthroline ligand *Inorganic Chemistry Communications.* **2015**, *55,* 30-35.
4. Fleisher, M. B.; Waterman, K. C.; Turro, N. J.; Barton, J. K., Light-induced cleavage of DNA by metal complexes [1] *Inorganic Chemistry.* **1986**, *25,* 3549-3551.

5. Fiers, W.; Beyaert, R.; Declercq, W.; Vandenabeele, P., More than one way to die: apoptosis, necrosis and reactive oxygen damage *Oncogene.* **1999**, *18,* 7719.
6. Liu, Y.; Hammitt, R.; Lutterman, D. A.; Joyce, L. E.; Thummel, R. P.; Turro, C., Ru(II) complexes of new tridentate ligands: Unexpected high yield of sensitized $^1O_2$ *Inorganic Chemistry.* **2009**, *48,* 375-385.
7. Sun, Y.; Joyce, L. E.; Dickson, N. M.; Turro, C., Efficient DNA photocleavage by $[Ru(bpy)_2(dppn)]^{2+}$ with visible light *Chemical Communications.* **2010**, *46,* 2426-2428.
8. Fukuzumi, S.; Ohkubo, K.; Zheng, X.; Chen, Y.; Pandey, R. K.; Zhan, R.; Kadish, K. M., Metal bacteriochlorins which act as dual singlet oxygen and superoxide generators *Journal of Physical Chemistry B.* **2008**, *112,* 2738-2746.
9. Lincoln, R.; Kohler, L.; Monro, S.; Yin, H.; Stephenson, M.; Zong, R.; Chouai, A.; Dorsey, C.; Hennigar, R.; Thummel, R. P.; McFarland, S. A., Exploitation of long-lived ^{3}IL excited states for metal–organic photodynamic therapy: verification in a metastatic melanoma model *Journal of the American Chemical Society.* **2013**, *135,* 17161-17175.
10. Shi, G.; Monro, S.; Hennigar, R.; Colpitts, J.; Fong, J.; Kasimova, K.; Yin, H.; DeCoste, R.; Spencer, C.; Chamberlain, L.; Mandel, A.; Lilge, L.; McFarland, S. A., Ru(II) dyads derived from α-oligothiophenes: A new class of potent and versatile photosensitizers for PDT *Coordination Chemistry Reviews.* **2015**, *282–283,* 127-138.
11. Mari, C.; Pierroz, V.; Ferrari, S.; Gasser, G., Combination of Ru(II) complexes and light: new frontiers in cancer therapy *Chemical Science.* **2015**, *6,* 2660-2686.
12. Ford, W. E.; Rodgers, M. A. J., Reversible triplet-triplet energy transfer within a covalently linked bichromophoric molecule *Journal of Physical Chemistry.* **1992**, *96,* 2917-2920.
13. Tyson, D. S.; Henbest, K. B.; Bialecki, J.; Castellano, F. N., Excited State Processes in Ruthenium(II)/Pyrenyl Complexes Displaying Extended Lifetimes *Journal of Physical Chemistry A.* **2001**, *105,* 8154-8161.
14. Pittau, R.; Baba, A. I.; Shaw, J. R.; Simon, J. A.; Thummel, R. P.; Schmehl, R. H., The photophysical behavior of complexes having nearly isoenergetic MLCT and ligand localized excited states *Coordination Chemistry Reviews.* **1998**, *171,* 43-59.
15. McClenaghan, N. D.; Leydet, Y.; Maubert, B.; Indelli, M. T.; Campagna, S., Excited-state equilibration: a process leading to long-lived metal-to-ligand charge transfer luminescence in supramolecular systems *Coordination Chemistry Reviews.* **2005**, *249,* 1336-1350.
16. de Carvalho, I. M. M.; de Sousa Moreira, Í.; Gehlen, M. H., Synthesis, characterization, and photophysical studies of new bichromophoric ruthenium(II) complexes *Inorganic Chemistry.* **2003**, *42,* 1525-1531.
17. Reichardt, C.; Pinto, M.; Wächtler, M.; Stephenson, M.; Kupfer, S.; Sainuddin, T.; Guthmuller, J.; McFarland, S. A.; Dietzek, B., Photophysics of Ru(II) dyads derived from pyrenyl-substitued imidazo[4,5-f][1,10]phenanthroline ligands *Journal of Physical Chemistry A.* **2015**, *119,* 3986-3994.
18. Stephenson, M.; Reichardt, C.; Pinto, M.; Wächtler, M.; Sainuddin, T.; Shi, G.; Yin, H.; Monro, S.; Sampson, E.; Dietzek, B.; McFarland, S. A., Ru(II) dyads derived from 2-(1-pyrenyl)-1H-imidazo[4,5-f][1,10]phenanthroline: versatile photosensitizers for photodynamic applications *Journal of Physical Chemistry A.* **2014**, *118,* 10507-10521.
19. Padilla, R.; Maza, W. A.; Dominijanni, A. J.; Winkel, B. S. J.; Morris, A. J.; J., B. K., Pushing the limits of structurally-diverse light-harvesting Ru(II) metal-organic

chromophores for photodynamic therapy *Journal of photochemistry and photobiology A.* **2015**, *Under Review*.
20. Mariappan, M.; Maiya, B. G., Effects of Anthracene and Pyrene Units on the Interactions of Novel Polypyridylruthenium(II) Mixed-Ligand Complexes with DNA *European Journal of Inorganic Chemistry.* **2005**, *2005,* 2164-2173.
21. Huang, Y.; Zhang, Y.; Zhang, J.; Zhang, D. W.; Lu, Q. S.; Liu, J. L.; Chen, S. Y.; Lin, H. H.; Yu, X. Q., Synthesis, DNA binding and photocleavage study of novel anthracene-appended macrocyclic polyamines *Organic & Biomolecular Chemistry.* **2009**, *7,* 2278-2285.
22. Modukuru, N. K.; Snow, K. J.; Perrin Jr, B. S.; Bhambhani, A.; Duff, M.; Kumar, C. V., Tuning the DNA binding modes of an anthracene derivative with salt *Journal of photochemistry and photobiology A.* **2006**, *177,* 43-54.
23. Tan, W. B., Recognition, binding and cleavage of DNA by anthracene derivaties and heme proteins *Ph. D. Thesis, University of Connecticut. Recognition, binding and cleavage of DNA by anthracene derivaties and heme proteins.*
24. Kumar, C. V.; Asuncion, E. H., Sequence dependent energy transfer from DNA to a simple aromatic chromophore *Journal of the Chemical Society.* **1992**, 470-472.
25. Kumar, C. V.; Tan, W. B.; Betts, P. W., Hexamminecobalt(III) chloride assisted, visible light induced, sequence dependent cleavage of DNA *Journal of Inorganic Biochemistry.* **1997**, *68,* 177-181.
26. Dong, S.; Hwang, H. M.; Harrison, C.; Holloway, L.; Shi, X.; Yu, H., UVA light-induced DNA cleavage by selected polycyclic aromatic hydrocarbons *Bulletin of environmental contamination and toxicology.* **2000**, *64,* 467-474.
27. Mongelli, M. T.; Heinecke, J.; Mayfield, S.; Okyere, B.; Winkel, B. S. J.; Brewer, K. J., Variation of DNA photocleavage efficiency for $[(TL)_2Ru(dpp)]Cl_2$ complexes where TL=2,2'-bipyridine, 1,10-phenanthroline, or 4,7-diphenyl-1,10-phenanthroline *Journal of Inorganic Biochemistry.* **2006**, *100,* 1983-1987.
28. Jain, A.; Slebodnick, C.; Winkel, B. S. J.; Brewer, K. J., Enhanced DNA photocleavage properties of Ru(II) terpyridine complexes upon incorporation of methylphenyl substituted terpyridine and/or the polyazine bridging ligand dpp (2,3-bis(2-pyridyl)pyrazine) *Journal of Inorganic Biochemistry.* **2008**, *102,* 1854-1861.
29. Wachter, E.; Heidary, D. K.; Howerton, B. S.; Parkin, S.; Glazer, E. C., Light-activated ruthenium complexes photobind DNA and are cytotoxic in the photodynamic therapy window *Chemical Communications.* **2012**, *48,* 9649-9651.
30. Mongelli, M. T.; Heinecke, J.; Mayfield, S.; Okyere, B.; Winkel, B. S. J.; Brewer, K. J., Variation of DNA photocleavage efficiency for [(TL)2Ru(dpp)]Cl2 complexes where TL = 2,2′ -bipyridine, 1,10-phenanthroline, or 4,7-diphenyl-1,10-phenanthroline *Journal of Inorganic Biochemistry.* **2006**, *100,* 1983-1987.
31. Prussin Ii, A. J.; Zigler, D. F.; Jain, A.; Brown, J. R.; Winkel, B. S. J.; Brewer, K. J., Photochemical methods to assay DNA photocleavage using supercoiled pUC18 DNA and LED or xenon arc lamp excitation *Journal of Inorganic Biochemistry.* **2008**, *102,* 731-739.
32. Blackburn, G. M.; Taussig, P. E., The photocarcinogenicity of anthracence: photochemical binding to deoxyribonucleic acid in tissue culture *Biochemical Journal.* **1975**, *149,* 289-291.

33. Sinha, B. K.; Chignell, C. F., Binding of anthracene to cellula macromolecules in the presence of light *Photochemistry and Photobiology.* **1983**, *37,* 33-37.
34. Armitage, B., Photocleavage of nucleic acids *Chemical Reviews.* **1998**, *98,* 1171-1200.
35. Noll, D. M.; Mason, T. M.; Miller, P. S., Formation and repair of interstrand cross-links in DNA *Chemical Reviews.* **2006**, *106,* 277-301.
36. Bhan, P.; Miller, P. S., Photo-cross-linking of psoralen derivatized oligonucleoside methylphosphonates to single-stranded DNA *Bioconjugate Chemistry.* **1990**, *1,* 82-88.
37. Wilson, G. J.; Launikonis, A.; Sasse, W. H. F.; Mau, A. W. H., Excited-state processes in ruthenium(II) bipyridine complexes containing covalently bound arenes *Journal of Physical Chemistry A.* **1997**, *101,* 4860-4866.
38. Terry, C. A.; Fernandez, M. J.; Gude, L.; Lorente, A.; Grant, K. B., Physiologically relevant concentrations of NaCl and KCl Increase DNA photocleavage by an N-substituted 9-aminomethylanthracene dye *Biochemistry.* **2011**, *50,* 10375-10389.
39. Schmechel, D. E. V.; Crothers, D. M., Kinetic and hydrodynamic studies of the complex of proflavine with poly A·poly U *Biopolymers.* **1971**, *10,* 465-480.
40. Wolfe, A.; Shimer, G. H.; Meehan, T., Polycyclic aromatic hydrocarbons physically intercalate into duplex regions of denatured DNA *Biochemistry.* **1987**, *26,* 6392-6396.
41. Dahl, J. U.; Gray, M. J.; Jakob, U., Protein quality control under oxidative stress conditions *Journal of Molecular Biology.* **2015**, *427,* 1549-1563.
42. Davies, M. J., Singlet oxygen-mediated damage to proteins and its consequences *Biochemical and Biophysical Research Communications.* **2003**, *305,* 761-770.
43. Bose, B.; Dube, A., Interaction of Chlorin p6 with bovine serum albumin and photodynamic oxidation of protein *Journal of Photochemistry and Photobiology B.* **2006**, *85,* 49-55.
44. Packer, L.; Kellogg, E. W., Photooxidative damage to mammalian cells and proteins by visible light. In *Chemical deterioration of proteins,photooxidative damage to mammalian cells and proteins by visible light*, ACS: 1980; Vol. 123, pp 83-93.
45. Bose, B.; Dube, A., Interaction of Chlorin p6 with bovine serum albumin and photodynamic oxidation of protein *Journal of Photochemistry and Photobiology B: Biology.* **2006**, *85,* 49-55.
46. Stadtman, E. R., Oxidation of free amino acids and amino acid residues in proteins by radiolysis and by metal-catalyzed reactions *Annual Review of Biochemistry.* **1993**, *62,* 797-821.
47. Wright, A.; Bubb, W. A.; Hawkins, C. L.; Davies, M. J., Singlet oxygen–mediated protein oxidation: Evidence for the formation of reactive side chain peroxides on tyrosine residues *Photochemistry and Photobiology.* **2002**, *76,* 35-46.
48. Silvester, J. A.; Timmins, G. S.; Davies, M. J., Protein hydroperoxides and carbonyl groups generated by porphyrin-induced photo-oxidation of bovine serum albumin *Archives of Biochemistry and Biophysics.* **1998**, *350,* 249-258.
49. Reichmann, M. E.; Rice, S. A.; Thomas, C. A.; Doty, P., A further examination of the molecular weight and size of desoxypentose nucleic acid *Journal of the American Chemical Society.* **1954**, *76,* 3047-3053.
50. Marmur, J., A procedure for the isolation of deoxyribonucleic acid from micro-organisms *Journal of Molecular Biology.* **1961**, *3,* 208-IN201.

Chapter 4 Exploring the Intracellular Localization and Photocytotoxicity of a New Class of Ru(II) Polyazine Complexes for Photodynamic Therapy

Roberto Padilla[a]*, Anthony J. Dominijanni[b], Kristi DeCourcy[c], Brenda S. J. Winkel[d], and Karen J. Brewer[a†]

[a]Department of Chemistry, Virginia Tech, Blacksburg, VA 24061

[b]Department of Biomedical Engineering and Mechanics, Virginia Tech, Blacksburg, VA 24061

[c]Fralin Life Science Institute, Virginia Tech, Blacksburg, VA 24061

[d]Department of Biological Sciences, Virginia Tech, Blacksburg, VA 24061

* Corresponding author e-mail: rpadill4@vt.edu (Roberto Padilla)

† Deceased October 24, 2014

Foreword. This chapter represents a stand-alone manuscript to be submitted to *ChemBioChem*. The work presented in this manuscript was conducted by Roberto Padilla with the assistance of Anthony J. Dominijanni (assisted with photocytotoxicity assays) and Dr. Kristi DeCourcy (assisted with cell images). This was supervised by Professors Brenda S. J. Winkel[b] and Professors Karen J. Brewer[a†].

4.1 Abstract

The cellular localization and photocytotoxicity of three recently-described [Ru]-anthracene hybrid complexes were tested using F98 rat glioma cells. $[(AnthbpyMe)Ru(bpy)_2]^{2+}$, $[(AnthbpyMe)(bpy)Ru(dpp)]^{2+}$, and $[(AnthbpyMe)_2Ru(bpy)]^{2+}$ exhibited IC_{50} values of 72 ± 1 μM, 107 ± 1 μM and 85 ± 1 μM, respectively, with 15 min of exposure followed by 1 h of irradiation at 455 nm. Confocal microscopy showed that the complexes initially localize primarily along the cell membrane and in nucleoli, subsequently becoming associated almost exclusively with discrete dot-like structures within the cytoplasm. Dose response curves demonstrated that all three complexes have substantial toxicity that is highly light-dependent.

These complexes offer a promising platform for further development of novel photodynamic therapy agents.

4.2 Introduction

Photodynamic therapy (PDT) is a promising treatment for a variety of conditions and diseases, including cancer, whereby a photosensitizer (PS) and light are used in combination to generate reactive cytotoxic agents to destroy target cells or tissues.[1-15] Considerable progress has been made in developing metal complexes as potential PDT agents that can function in both oxygen-replete and hypoxic environments to generate toxic agents upon irradiation.[16-24] Ruthenium polyazine complexes comprise a versatile class of anticancer drugs with considerable interest as potential PDT agents due to their favorable absorption, dynamic excited state, and photophysical properties, and reactivity toward biomacromolecules under a various conditions.[15,25-31] The photosensitizer, tris(2,2'-bipyridine) ruthenium(II) $[Ru(bpy)_3]^{2+}$, and its analogs are proven PDT agents that generate reactive triple metal-to-ligand charge transfer (^{3}MLCT) states that are typically long-lived and that efficiently generate $^1O_2$ to mediate the oxidation of biomacromolecules such as DNA upon light activation.[4,32] Although $[Ru(bpy)_3]^{2+}$ has been shown to modify DNA *in vitro*, its potential as a PDT agent is compromised by its inability to traverse the plasma membrane.[33] A potential approach to improving the cellular permeability of Ru(II) polyazine complexes is to increase their lipophilicity by covalently appending polycyclic aromatic hydrocarbons (PAH).[34,35] These appended PAHs may also enhance the PDT potency of the complex.[13,32,36-38] Ru(II) dyads that incorporate pyrene units have been shown to mediate the light-induced cell uptake and oxidation of DNA via oxygen dependent and independent mechanisms, while chemically binding to DNA.[39,40] These [Ru]-pyrene systems exhibit enhanced photobiological potency at submicromolar regimes under short

drug-to-light intervals.[40,41]

Appending anthryl units to the $[(bpy)_2Ru(dpp)]^{2+}$ PS through amide bond(s) generates a [Ru]-PAH system that can bind to and modify DNA in the presence and absence of oxygen upon irradiation (λ_{irr} = 455 nm), while also offering the potential for sequestering biologically-relevant cations (i.e. Fe^{2+}, Na^+, K^+, Ca^{2+}, etc.).[42] The anthryl units afford the added advantage of providing an avenue for coupling known metal-based DNA binding agents (e.g., cisplatin) to the complex.[22-24,42] The anthracene-[Ru]-dpp hybrids, $[(AnthbpyMe)(bpy)Ru(dpp)]^{2+}$ and $[(AnthbpyMe)_2Ru(dpp)]^{2+}$ (bpy = 2, 2′ –bipyridine, dpp = 2,3-bis(2-pyridyl)pyrazine, and AnthbpyMe = 4-[*N*-(2-anthryl)carbamoyl]-4′ -methyl-2,2′ -bipyridine), have recently been shown to modify DNA in the presence and absence of $^3O_2$, while oxidizing protein structures through an $^3O_2$-mediated mechanism, in both cases in a light-dependent manner.[43] Although these anthracene-[Ru]-dpp compounds can generate a burst of reactive cytotoxic agent for PDT applications, their efficiency in modifying biological targets is likely to be highly dependent on the ability to permeate the cell membrane.[32,44-48]

Herein we study and compare the uptake and intracellular distribution of [Ru]-anthracene hybrid systems, $[(AnthbpyMe)Ru(bpy)_2]^{2+}$ (**3**), $[(AnthbpyMe)(bpy)Ru(dpp)]^{2+}$ (**4**), and $[(AnthbpyMe)_2Ru(dpp)]^{2+}$ (**5**), in F98 glial cells with parent Ru(II) PS, $[Ru(bpy)_3]^{2+}$ and $[(bpy)_2Ru(dpp)]^{2+}$, in an attempt to understand their *in vitro* behavior in mammalian cells.[43,49,50] The intrinsic ^{3}MLCT emission properties of these [Ru] hybrid compounds was harnessed to monitor their intracellular distribution by confocal laser scanning microscopy. We also determined the IC_{50} values for these systems with the same cell lines. This is the first reported study of the *in vivo* behavior of Ru(II) complexes that append anthracene unit(s) to the $[Ru(bpy)_3]^{2+}$ and $[(bpy)_2Ru(dpp)]^{2+}$ PSs through amide linkers.

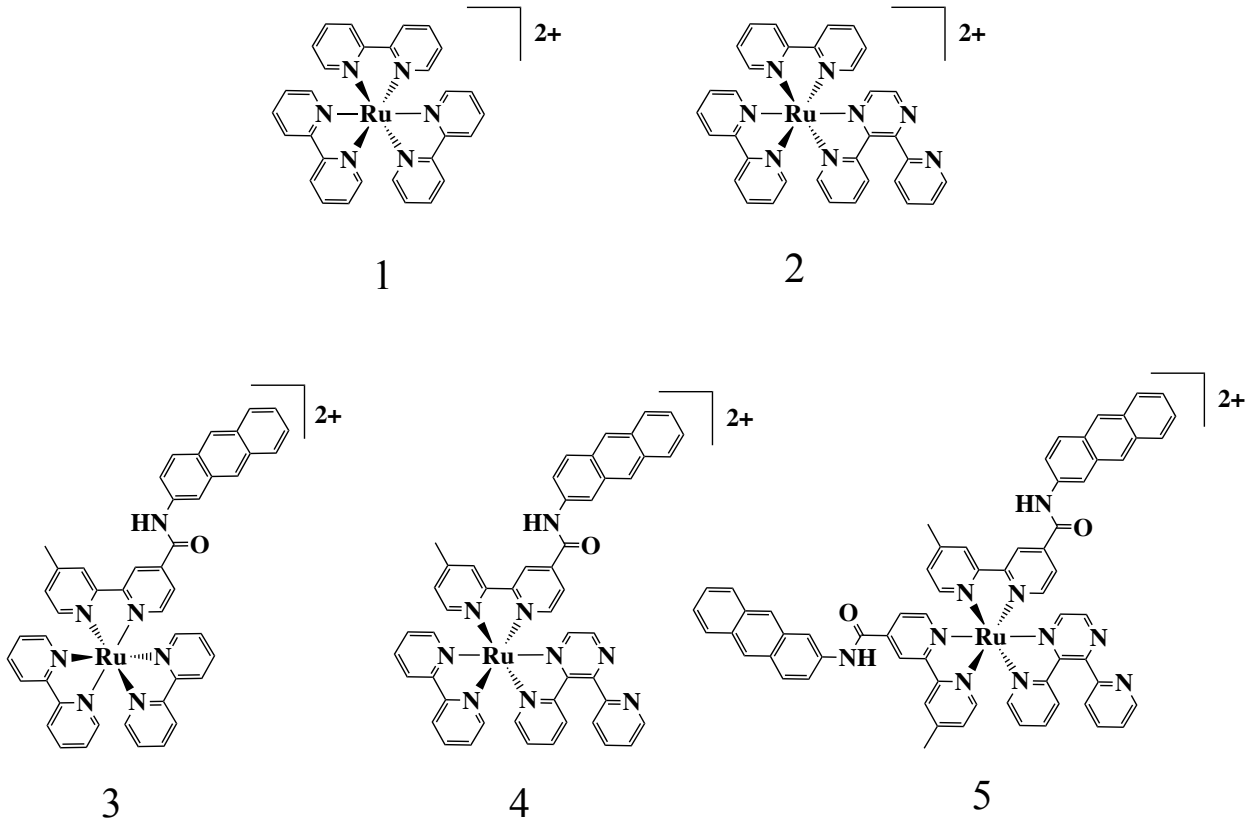

Figure 1. Chemical structures of $[Ru(bpy)_3]^{2+}$ (**1**), $[(bpy)_2Ru(dpp)]^{2+}$ (**2**), $[(AnthbpyMe)Ru(bpy)]^{2+}$ (**3**), $[(AnthbpyMe)(bpy)Ru(dpp)]^{2+}$ (**4**), and $[(AnthbpyMe)_2Ru(dpp)]^{2+}$ (**5**).

4.3 Results and Discussion

The efficiency with which PSs are able to modify biological targets (DNA, RNA, proteins, lipids, etc.) within cells is highly dependent on cellular uptake, which is commonly estimated by their lipophilicity.[34,35] To evaluate the potential of $[(AnthbpyMe)Ru(bpy)]^{2+}$ (**3**), $[(AnthbpyMe)(bpy)Ru(dpp)]^{2+}$ (**4**), and $[(AnthbpyMe)_2Ru(dpp)]^{2+}$ (**5**) to serve as efficient PSs in a biological context, partition coefficients were determined using a modified shake-flask method and compared to those of anthracene and the parent complexes, $[Ru(bpy)_3]^{2+}$ (**1**) and $[(bpy)_2Ru(dpp)]^{2+}$ (**2**) .[52] The results are reported in Table 1.

Table 1. Lipophilicity of compounds 1 – 5.

Compound	Log $P_{o/w}$
Anthracene	+ 4.56*
$[Ru(bpy)_3](PF_6)_2$(**1**)	- 1.21**
$[(bpy)Ru(dpp)](PF_6)_2$ (**2**)	- 2.53
$[(AnthbpyMe)Ru(bpy)_2](PF_6)_2$ (**3**)	+ 0.80
$[(AnthbpyMe)(bpy)Ru(dpp)](PF_6)_2$ (**4**)	+ 0.64
$[(AnthbpyMe)_2Ru(dpp)](PF_6)_2$ (**5**)	+ 1.30
**Ref.[36].*Ref.[50].Standard deviation ± 10%	

Anthracene and $[Ru(bpy)_3]^{2+}$ (**1**) have previously been reported to have substantial positive and negative log$P_{o/w}$ values, respectively.[36,53] Consistent with this, parent complex **2** displayed an even more negative log$P_{o/w}$ value, attributed to the dpp ligand which is speculated to be more hydrophilic than bpy.[33] The [Ru]-anthracene hybrid compounds (**3**, **4**, and **5**) exhibited log$P_{o/w}$ values that were intermediate between anthracene and the respective Ru(II) parent complexes (**1** and **2**), with complex **5** displaying the highest log$P_{o/w}$ value, reflecting the presence of a second anthryl unit.[53] The overall lipophilicity of the three [Ru]-anthracene hybrid systems should enhance the potential for cellular uptake and for therapeutic success.[54] It is noteworthy that the log$P_{o/w}$ value of all three title complexes are within the desired range of + 1.5 ± 1.0 for optimal oral absorption or central nervous system penetration.[34,35,55] These [Ru]-anthracene complexes also demonstrate superior log$P_{o/w}$ values than clinically-approved Pt-based drugs such as cisplatin, carboplatin, and temozolomide, which have reported log$P_{o/w}$ values of - 2.50, - 2.30, and - 0.24, respectively.[54,56,57]

To investigate the potential of the [Ru]-anthracene compounds to be taken up by mammalian cells, we took advantage of the luminescent property of the Ru(II) core to conduct confocal laser scanning microscopy analyses. Parent complexes **1** and **2** give rise to an emission band within the 580 – 700 nm range when excited with l_{ex} = 488 nm (l_{ex} = laser excitation), characteristic of the emissive ^{3}MLCT state common for ruthenium polyazine complexes.[58] The Ru (II) unit within the [Ru] hybrid structure can be excited with l_{ex} = 488 nm independent of the

anthracene unit, as previously reported, giving rise to emission bands within the 580 – 700 nm range similar to the parent complexes.[44]

To examine the interaction of the title compounds with mammalian cells, 6-well glass plates were seeded with F98 glioma cells, a widely-used rat brain tumor model with biological characteristics resembling those of human glioblastoma (Figure S1).[59] The cells were incubated for 24 h to create a monolayer of cells for imaging and a series of concentration assays was then used to determine that 75 μM of the parent and title complexes was optimal for capturing the emission from both the ^{1}anthracene and ^{3}MLCT states in these experiments (data not shown). The results of initial experiments using emission from the Ru(II) unit (580 – 700 nm; l_{ex} = 488 nm) to monitor the ability of the complexes to adsorb to and/or enter F98 cells within a 15 min treatment window are illustrated in Figure 2. Emission from the anthryl unit in these complexes was not detected with the parameters used in these experiments. This was confirmed with cells treated with anthracene alone, which exhibited no detectable emission with l_{ex} = 488 nm (data not shown), although these cells did display an extremely low, but measurable emission with l_{ex} = 408 nm (data not shown) consistent with previous reports of cellular uptake of anthracene labeled systems.[60] Fluorescence was also not detected for cells treated with parent complexes **1** and **2** (Figure 2A and B), despite the presence of [Ru] units in these structures, indicating that these complexes did not adhere to or enter the cells, consistent with the low lipophilicity of these molecules. In marked contrast, cells incubated with the [Ru]-anthracene hybrid complexes, **3**, **4**, and **5,** displayed strong fluorescence that was distributed across the cytoplasm, with the exception of what appeared to be nuclei. This result indicates that the appended anthracene(s) confer enhanced affinity for cells, entirely or in part due to the observed enhancementin lipophilicity, and significantly increase the transport of these molecules across the membrane and

into F98 cells, similar to what has been observed for anthracene-tethered Ru(II) arene complexes with A549 lung carcinoma cells.[61] Anthracene-tagged bidpyridinium amides have also been shown to penetrate the membrane and localize in nuclei of HeLa cells.[60]

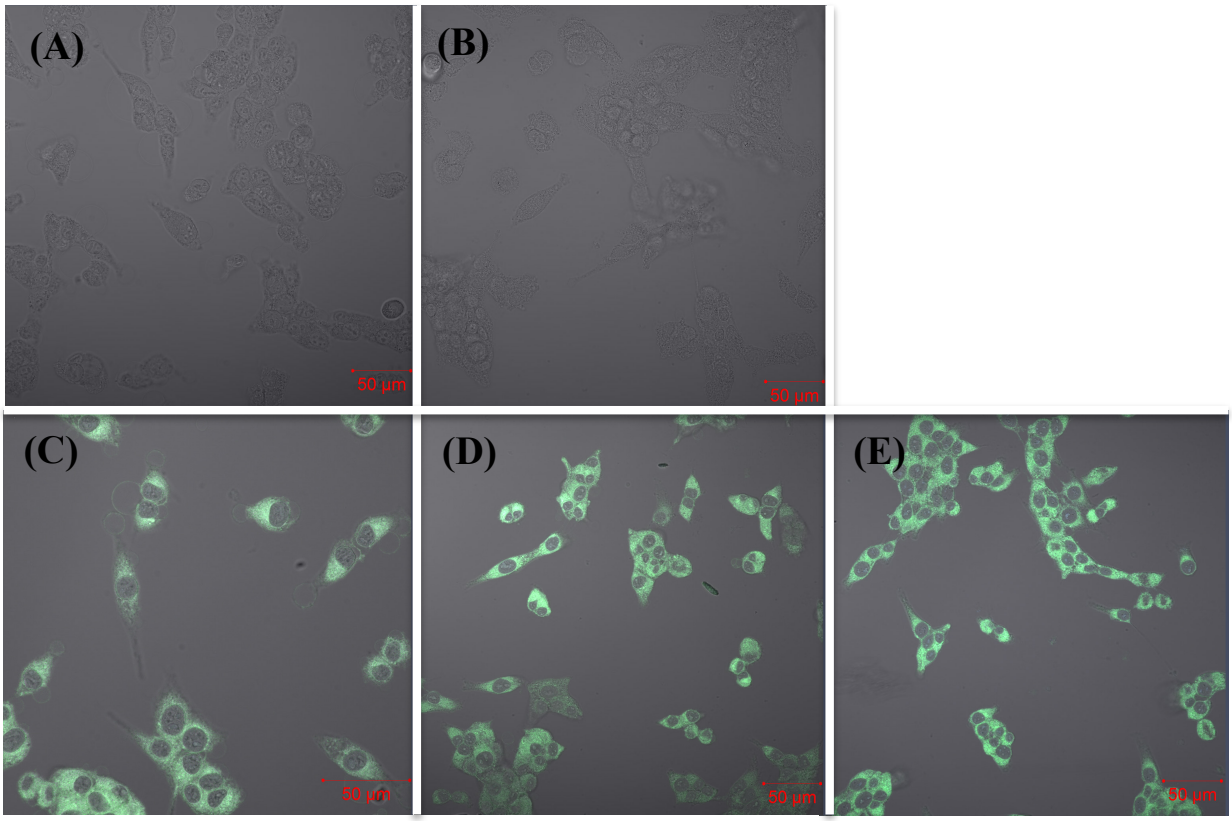

Figure 2. Screening of [Ru] compounds for uptake into F98 MG cells. Cells were incubated with 75 uM of individual compounds for 15 min at 37°C, washed, and emission from Ru(II) monitored by confocal microscopy. (A) $[Ru(bpy)_3]^{2+}$ (**1**), (B) $[(bpy)_2Ru(dpp)]^{2+}$ (**2**), (C) $[(AnthbpyMe)Ru(bpy)_2]^{2+}$ (**3**), (D) $[(AnthbpyMe)(bpy)Ru(dpp)]^{2+}$ (**4**), and (E) $[(AnthbpyMe)_2Ru(dpp)]^{2+}$ (**5**). Images were collected at 630 – 700 nm (right, l_{ex} = 488 nm).

All three complexes appeared to be excluded from spherical structures within the F98 cells, also based on examination of multiple optical slices (Figure 2 and S2). To determine whether these structures were nuclei, cells were treated with the three complexes for 15 min, washed, and allowed to recover for 24 h. The cells were then stained with 4',6-diamidino-2-phenylindole (DAPI), a nuclear and chromosome counterstain that emits blue fluorescence upon binding to AT regions of DNA. Images were collected under conditions specific for DAPI (l_{ex} = 408 nm; l_{em} =

420 – 550 nm) or Ru(II) (l_{ex} = 488 nm; l_{em} = 630 – 700). In all three cases the signal from the Ru(II) had a pattern complementary to that of DAPI, indicating that the three title complexes are indeed present at very low or undetectable levels within nuclei after 15 min of incubation. It also appeared that nuclei in cells exposed to compounds **4** and **5** (Figure 3C and D) were smaller than those in untreated cells (Figure 3A) and those treated with complex **3** (Figure 3B).

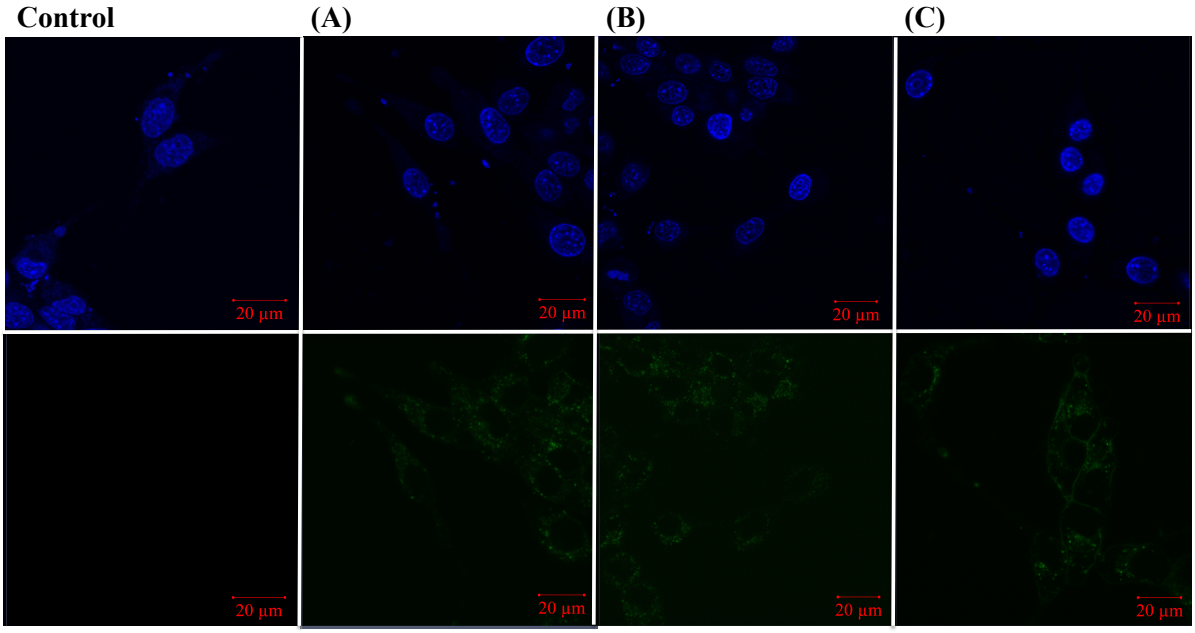

Figure 3. Confirmation of nuclear exclusion of the [Ru]-anthracene complexes. Confocal images of live F98 MG cells incubated for 15 min at 37 °C with complexes, washed, incubated without complex for 24 h prior to staining with DAPI. (A) no complex, (B) $[(AnthbpyMe)Ru(bpy)2]^{2+}$, (c) $[(AnthbpyMe)(bpy)Ru(dpp)]^{2+}$, and (D) $[(AnthbpyMe)_2Ru(dpp)]^{2+}$. Images were collected at 420 – 550 nm (left, l_{ex} = 408 nm) or 630 – 700 nm (right, l_{ex} = 488 nm).

To further investigate the uptake and localization of the [Ru]-anthracene hybrid compounds, cells were imaged after being exposed to the complexes for different lengths of time. Figure 4 shows representative images for cells treated with complexes **3**, **4**, or **5** for 0 min, 5 min, or 48 h.

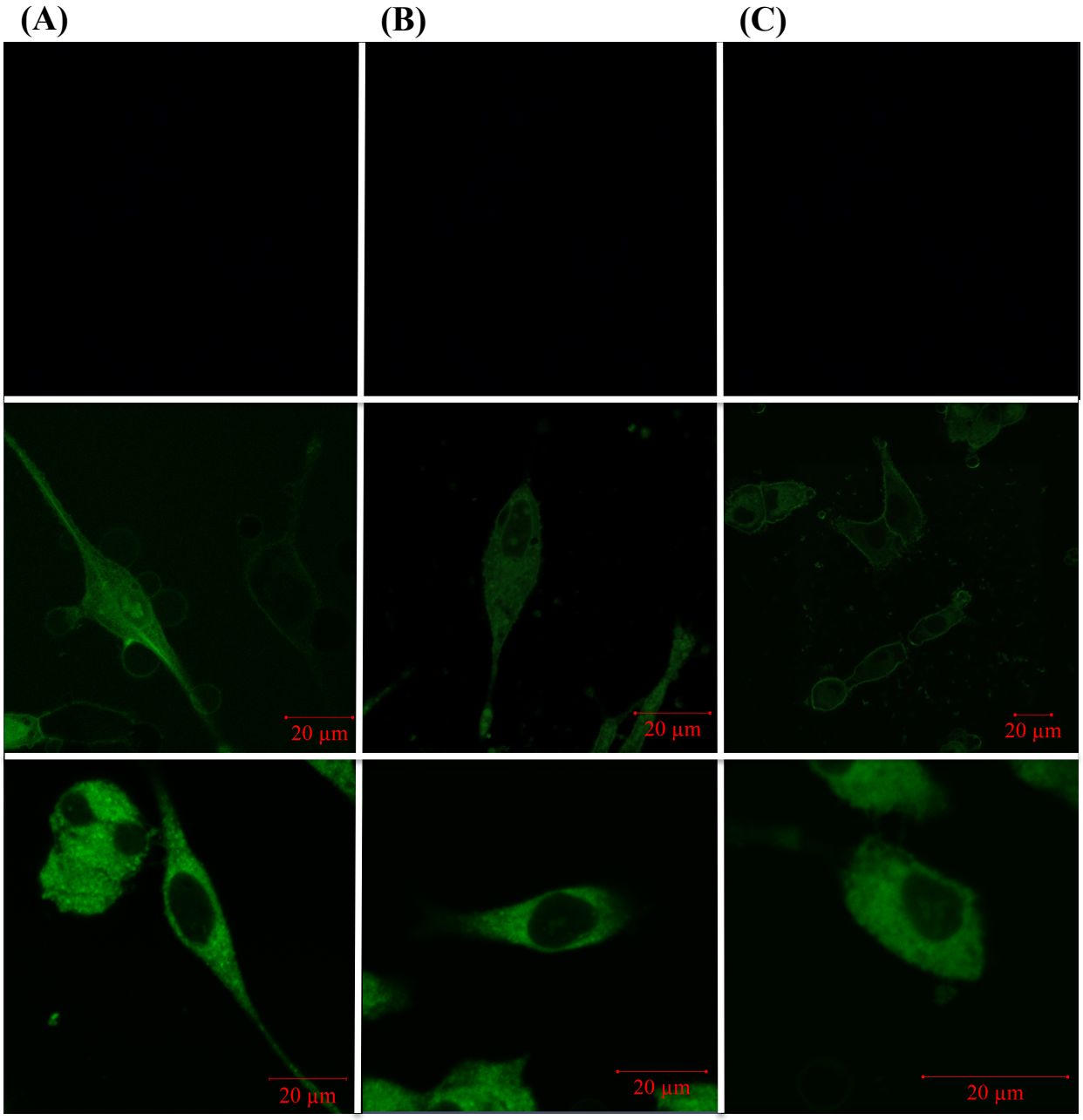

Figure 4. Changes in distribution of the [Ru]-anthracene complexes in F98 MG cells over time. Cells were incubated with [Ru]-anthracene complex for 15 min at 37 °C, washed, and then incubated in growth medium in the absence of complex for an additional 0 min (top), 5 min (center) or 48 h (bottom) prior to collecting images at 630 – 700 nm (l_{ex} = 488 nm). (A) $[(AnthbpyMe)Ru(bpy)_2]^{2+}$ (**3**), (B) $[(AnthbpyMe)(bpy)Ru(dpp)]^{2+}$(**4**), or (C) $[(AnthbpyMe)_2Ru(dpp)]^{2+}$ (**5**).

As expected, no luminescence was observed prior to addition of the complexes (0 min, top row). However, all three [Ru]-anthracene systems were detectable within 1 – 2 min [time

lapse videos can be found in the supporting information (SI)] and by 5 min were concentrated along the cell membrane and also within the cytoplasm (Figure 4, center panels). Complexes **4** and **5** also appeared to be concentrated in nucleoli within the nucleus, similar to what has been reported for $[Ru(bpy)(HP\text{-}bpy)_2]^{2+}$ (HP-bpy=4-(4-hydroxyphenyl)-2,2'-bipyridine).[62] More than two nucleoli were observed in a number of these cells, characteristic of many malignant cell lines.[63] This rapid internalization has been reported previously for other Ru polyazine systems, with the uptake attributed to passive diffusion.[64-68] A different distribution pattern was observed in samples treated for 48 h; in this case all three complexes were localized primarily in discrete dot-like vesicular structures within the cytoplasm, with little or no fluorescence emanating from nuclei or nuceoli. Subtle differences in cell morphology were also noted (Figure S2).

Previous studies have shown that the parent molecules, anthracene, $[Ru(bpy)_3]^{2+}$ (**1**), and $[(bpy)_2Ru(dpp)]^{2+}$ (**2**), have little or no cytotoxicity against F98 glioma cells in either the absence or presence of light, while the complexes with appended anthracene moieties (**3**, **4**, and **5**) display moderate toxicity in the dark, an effect that is substantially enhanced upon exposure to light.[44]

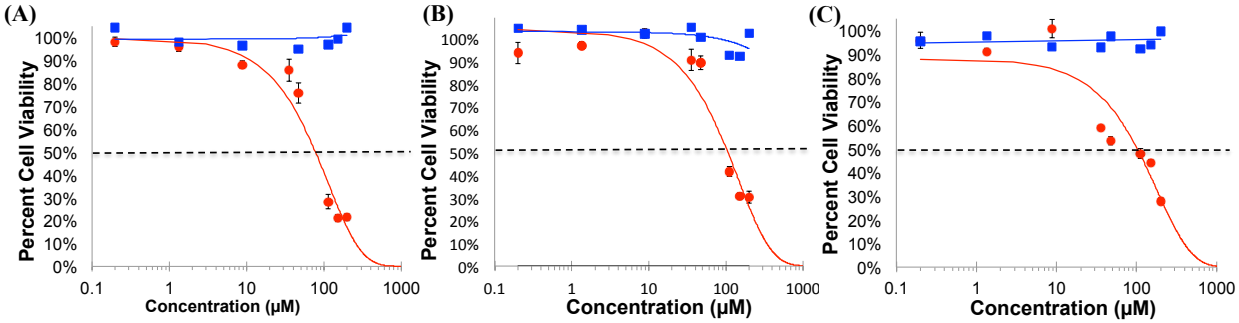

Figure 5. Dose response curves comparing cell cytotoxicity (solid blue squares) and photocytotoxicity (solid red circles) of F98 cells treated with $[(AnthbpyMe)Ru(bpy)_2]^{2+}$ (A) $[(AnthbpyMe)(bpy)Ru(dpp)]^{2+}$ (B), and $[(AnthbpyMe)_2Ru(dpp)]^{2+}$ (C). Viability counts were performed in triplicate; bars are standard error.

To extend these initial observations, IC_{50} values were determined by measuring dose-response relationships, which examined the effects of different concentrations of [Ru]-anthracene agents on cell viability with and without light activation. In each case, cells were treated for 15 min with the complex over a concentration range of 0.2 – 200 μM, washed to remove excess complex, and then incubated for 1 h in the dark or under illumination at 455 nm using a custom-designed photoarray apparatus.[69,70] Cell viability tests were conducted 48 h after PDT treatment using an AlamarBlue assay (Figure 5). Consistent with previous observations, all three complexes displayed minimal effects on cell viability in the dark.[47] However, upon photolysis at 455 nm for 1 h all three [Ru]-anthracene systems displayed substantial toxicity toward F98 cells, with comparable IC_{50} values of 72 ± 1 μM, 107 ± 1 μM, and 85 ± 1 μM for complexes **4**, **5**, and **6**, respectively. This light-enhanced toxicity is hypothesized to result from the previously-reported dynamic excited state properties and reactivity towards multiple biologic substrates as well as the rapid uptake properties of these novel complexes.

4.4 Conclusions

In this study we demonstrated that [Ru]-anthracene PDT agents $[(AnthbpyMe)Ru(bpy)_2]^{2+}$, $[(AnthbpyMe)(bpy)Ru(dpp)]^{2+}$, and $[(AnthbpyMe)_2Ru(dpp)]^{2+}$ localize primarily along the cell membrane and dot-like vesicles within the cytoplasm within 5 min of initial exposure. The rapid uptake of the Ru(II) complexes and their high lipophilicity suggests that passive diffusion is a potential mechanism of uptake. At longer times after exposure, cells treated with $[(AnthbpyMe)(bpy)Ru(dpp)]^{2+}$ and $[(AnthbpyMe)_2Ru(dpp)]^{2+}$ appear to undergo changes in morphology, including the dimensions of the nucleus, which may be related to the ability of the dpp ligand to chelate biologically-relevant cations including Na^+, K^+, Ca^{2+}, Mn^{2+}, and Fe^{2+}.[42] Dose response curves for cell toxicity of F98 cells treated with [Ru]-

anthracene complexes demonstrate that all three complexes have little or no effect on cell viability in the dark, but upon photolysis display substantial toxicity. Studies are currently under way to optimize PDT treatment and further characterize the photocytotoxicity of these [Ru]-anthracene systems and their effects on F98 cell morphology and viability. Furthermore, future work is directed to covalently coupling cisplatin-inspired DNA binding motifs to anthracene-[Ru]-dpp systems as a means to improve the cellular uptake of Ru(II)-Pt(II) systems.

4.5 Experimental

Materials. All solvents/chemicals were used as received, unless otherwise noted. Anthracene (1) was purchased from Sigma Aldrich, while compounds $[Ru(bpy)_3](PF_6)_2$ (2), $[(AnthbpyMe)Ru(bpy)_2](PF_6)_2$ (3), $[(bpy)_2Ru(dpp)](PF_6)_2$ (4), and $[(AnthbpyMe)_2Ru(dpp)](PF_6)_2$ (5) were synthesized as described previously.[44,49,71] Life Technologies supplied 0.05% Trypsin-EDTA and phosphate buffered saline (PBS). Dimethyl sulfoxide (DMSO) was obtained from Sigma Aldrich. F98 MG rat cancer cells were purchased from the American Type Culture Collection (ATCC® CRL-2397™) with an initial passage of seven. Dulbecco's Modified Eagle's Medium (DMEM), Fetal Bovine Serum (FBS), and penicillin-streptomycin antibiotic solutions were also from ATCC®.

Determination of Log$P_{o/w}$. Partition coefficients were determined for the complexes using the shake flask method of octanol/PBS phase partition.[36] The PF_6^- compounds were first converted to the Cl^- salt by dissolving a small amount solid in acetonitrile and then flash participated to the Cl^- salt from a saturated solution of acetone containing tetrabutyl ammonium chloride. The solution was centrifuged on a Fisher Scientific Centrific Centrifuge Fisher Scientific 225 Lab Benchtop Variable Speed Centrific Centrifuge at 6500 RPM for 1 min at room temperature and the solid was collected and dried. The complexes were then dissolved in 3 ml PBS, pH 7. To this

solution, 3 ml of octanol was added and stirred vigorously for 15 min. The phases were allowed to separate and the concentrations of the complexes were determined by spectrophotometry.

Cell Culturing. Cells were handled in class II, type A2 biological safety cabinet and incubated in a Nuaire auto flow CO_2 water jacketed incubator at 37 ºC with 5% CO_2. Cells were collected by centrifugation at 120g, 4°C, for 5 min and counted using a Vi-CELL cell viability analyzer (Beckman Coulter). F98 MG cells were grown in DMEM in a T75 flask (75 cm^2 Thermo Fisher Scientific tissue flask) at 37 ºC and 5% CO_2. The cells were cultured in fresh DMEM supplemented with 10% FBS and 1% penicillin-streptomycin antibiotic solution (ATCC) for 24 h prior to use in experiments. Cells were passaged when approaching a confluence of 85%–95%. All culture work and seeding processes were carried out in a class II, type A2 biological safety cabinet. Additional information on culturing cells for these experiments is provided in the SI.

Cell Imaging. After the cells were grown and allowed to adhere in 6-well glass plates for 24 h, the compounds were introduced at a 75 μM concentration followed by incubation for 1 h. The compounds remaining in solution were removed by washing the cells with PBS and replenished with 2 ml of fresh medium followed immediately by imaging. For the time course experiments, cells were incubated with complex for 15 min at 37 °C, washed, and then incubated in growth medium in the absence of complex for an additional 5 min or 48 h prior to collecting.

For DAPI staining experiments, cells were imaged immediately after washing. In brief, a 14.3 mM DAPI stock solution was freshly prepared in PBS, using sonication to dissolve the DAPI. After the cells were treated with complexes for 15 min under similar conditions as described above, 1.4 μL of DAPI stock solution was added to the wells containing the treated cells and 2 ml of fresh medium to obtain approximaly 10 μM of DAPI. The cells were then incubated for 15 min to allow uptake of DAPI. The DAPI remaining in solution was removed by

washing the cells with PBS and replenished with 2 ml of non-phenol red-containing followed immediately by imaging.

Confocal Laser Scanning Microscopy. For all imaging studies F98 cells were seeded onto 6-well uncoated glass plate with a 1.5 mm thickness and 14 mm glass diameter. The plates were imaged with a Zeiss LSM 880 confocal microscope with argon light source (l_{ex} = 408 nm and 488 nm), C-Apochromat 40 × /1.2 W Korr FCS M27 objective, and Zen Blue (v.2) data collection and analysis software.

Photocytotoxicity Studies. Photolysis treatments were conducted in 6-well plates containing ~0.4 x 10^6 cells/well in DMEM that had been incubated at 37 °C and 5% CO_2 for 24 h prior to treatment. The medium was evacuated from each well and replaced with 75 μM solutions of complex dissolved in DMEM and DMSO (≤5%v/v). Control wells contained DMEM and DMSO (≤5%v/v) only. The cells were then incubated at 37 °C and 5% CO_2 for 15 min, the solution was then evacuated, and the cells were washed with PBS several times before incubation with DMEM without phenol red for 12 h. The cells were then photolyzed with a custom-made photoarray for 1 h, while the dark controls were subjected to the same conditions except without the light (procedure found in SI).[70,72]

Cell Viability Assay. Cell viability was assessed 24 and 48 h after photolysis using the alamarBlue cell viability assay protocol provided by AbD Serotec® (procedure and calculation found in SI).

4.6 Acknowledgements

The authors are grateful to the National Science Foundation (grant CHE–1301131) for funding this work. Roberto Padilla received additional support from the National Institutes of Health (grant VT–IMSD-GM072767).

Keywords: photocytotoxicity • photodynamic therapy • metal-organic • photochemistry • singlet oxygen

4.7 Supporting information: Exploring the Intracellular Localization and Photocytotoxicity of a New Class of Ru(II) Polyazine Complexes for Photodynamic Therapy

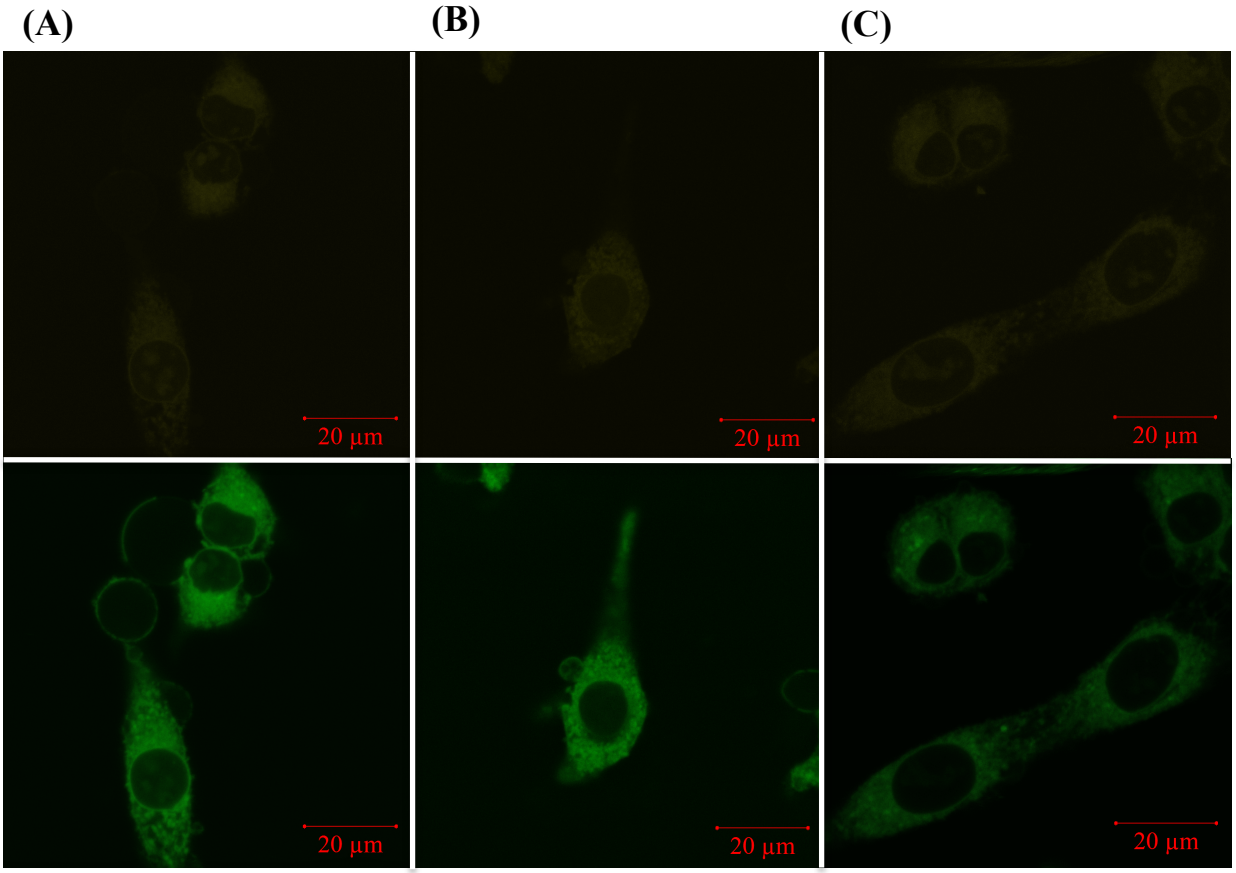

Figure 4.1. Evidence that the Ru (II) **and anthracene unit(s) can be independently excited in live F98 MG cells.** Confocal images of luminescence from anthracene (top) and Ru(II) (bottom) units in live F98 MG cells incubated for 1 h at 37°C with $[(AnthbpyMe)Ru(bpy)_2]^{2+}$ (A), $[(AnthbpyMe)(bpy)Ru(dpp)]^{2+}$ (B) and $[(AnthbpyMe)_2Ru(dpp)]^{2+}$ (C). Images were collected at 420 – 550 nm (left, l_{ex} = 408 nm) or 630 – 700 nm (right, l_{ex} = 488 nm).

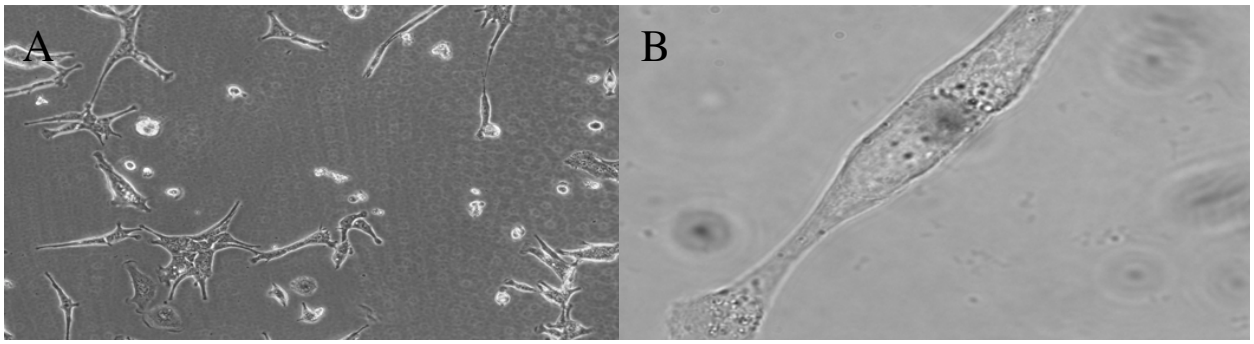

Figure 4.2. Transmitted light images (overview (A) and single cells (B)) of live F98 MG at 37°C after incubation for 24 h showing the morphology of untreated cells.

4.8 References

1. Durham, B.; Caspar, J. V.; Nagle, J. K.; Meyer, T. J., Photochemistry of [tris(2,2'-bipyridine)ruthenium]$^{2+}$ ion *Journal of the American Chemical Society.* **1982**, *104,* 4803-4810.
2. Liu, Y.; Hammitt, R.; Lutterman, D. A.; Joyce, L. E.; Thummel, R. P.; Turro, C., Ru(II) complexes of new tridentate ligands: Unexpected high yield of sensitized $^1O_2$ *Inorganic Chemistry.* **2009**, *48,* 375-385.
3. Sun, Y.; Joyce, L. E.; Dickson, N. M.; Turro, C., Efficient DNA photocleavage by [Ru(bpy)$_2$(dppn)]$^{2+}$ with visible light *Chemical Communications.* **2010**, *46,* 2426-2428.
4. Fiers, W.; Beyaert, R.; Declercq, W.; Vandenabeele, P., More than one way to die: apoptosis, necrosis and reactive oxygen damage *Oncogene.* **1999**, *18,* 7719.
5. Sharman, W. M.; Allen, C. M.; van Lier, J. E., Photodynamic therapeutics: basic principles and clinical applications *Drug Discovery Today.* **1999**, *4,* 507-517.
6. Gomer, C. J., Preclinical examination of first and second generation photosensitizers used in photodynamic therapy *Photochemistry and Photobiology.* **1991**, *54,* 1093-1107.
7. Szaciłowski, K.; Macyk, W.; Drzewiecka-Matuszek, A.; Brindell, M.; Stochel, G., Bioinorganic photochemistry: Frontiers and mechanisms *Chemical Reviews.* **2005**, *105,* 2647-2694.
8. Muller, P. J.; Wilson, B. C., Photodynamic therapy of brain tumors-A work in progress *Lasers in Surgery and Medicine.* **2006**, *38,* 384-389.
9. Josefsen, L. B.; Boyle, R. W., Photodynamic therapy: novel third-generation photosensitizers one step closer? *British Journal of Pharmacology.* **2008**, *154,* 1-3.
10. Moan, J., Properties for optimal PDT sensitizers *Journal of Photochemistry and Photobiology B.* **1990**, *5,* 521-524.
11. Heidary, D. K.; Howerton, B. S.; Glazer, E. C., Coordination of hydroxyquinolines to a ruthenium bis-dimethyl-phenanthroline scaffold radically improves potency for potential as antineoplastic agents *Journal of Medicinal Chemistry.* **2014**, *57,* 8936-8946.
12. Heidary, D. K.; Glazer, E. C., A light-activated metal complex targets both DNA and RNA in a fluorescent in vitro transcription and translation assay *ChemBioChem.* **2014**, *15,* 507-511.
13. Shi, G.; Monro, S.; Hennigar, R.; Colpitts, J.; Fong, J.; Kasimova, K.; Yin, H.; DeCoste, R.; Spencer, C.; Chamberlain, L.; Mandel, A.; Lilge, L.; McFarland, S. A., Ru(II) dyads derived from α-oligothiophenes: A new class of potent and versatile photosensitizers for PDT *Coordination Chemistry Reviews.* **2015**, *282–283,* 127-138.
14. Plaetzer, K.; Krammer, B.; Berlanda, J.; Berr, F.; Kiesslich, T., Photophysics and photochemistry of photodynamic therapy: fundamental aspects *Lasers in Medical Science.* **2009**, *24,* 259-268.
15. Glazer, E. C., Light-activated metal complexes that covalently modify DNA *Israel Journal of Chemistry.* **2013**, *53,* 391-400.
16. Basu, U.; Khan, I.; Hussain, A.; Kondaiah, P.; Chakravarty, A. R., Photodynamic effect in near-IR light by a photocytotoxic iron(III) cellular imaging agent *Angewandte Chemie International Edition.* **2012**, *51,* 2658-2661.

17. Saha, S.; Majumdar, R.; Roy, M.; Dighe, R. R.; Chakravarty, A. R., An iron complex of dipyridophenazine as a potent photocytotoxic agent in visible light *Inorganic Chemistry.* **2009**, *48,* 2652-2663.
18. Sasmal, P. K.; Saha, S.; Majumdar, R.; Dighe, R. R.; Chakravarty, A. R., Oxovanadium(IV)-based near-IR PDT agents: design to biological evaluation *Chemical Communications.* **2009**, 1703-1705.
19. Maity, B.; Roy, M.; Banik, B.; Majumdar, R.; Dighe, R. R.; Chakravarty, A. R., Ferrocene-promoted photoactivated DNA cleavage and anticancer activity of terpyridyl copper(II) phenanthroline complexes *Organometallics.* **2010**, *29,* 3632-3641.
20. Knoll, J. D.; Turro, C., Control and utilization of ruthenium and rhodium metal complex excited states for photoactivated cancer therapy *Coordination Chemistry Reviews.* **2015**, *282–283,* 110-126.
21. Joyce, L. E.; Aguirre, J. D.; Angeles-Boza, A. M.; Chouai, A.; Fu, P. K. L.; Dunbar, K. R.; Turro, C., Photophysical properties, DNA photocleavage, and photocytotoxicity of a series of dppn dirhodium(II,II) complexes *Inorganic Chemistry.* **2010**, *49,* 5371-5376.
22. Higgins, S. L. H.; White, T. A.; Winkel, B. S. J.; Brewer, K. J., Redox, spectroscopic, and photophysical properties of Ru-Pt mixed-metal complexes incorporating 4,7-diphenyl-1,10-phenanthroline as efficient DNA binding and photocleaving agents *Inorganic Chemistry.* **2011**, *50,* 463-470.
23. Higgins, S. L. H.; Tucker, A. J.; Winkel, B. S. J.; Brewer, K. J., Metal to ligand charge transfer induced DNA photobinding in a Ru(II)-Pt(II) supramolecule using red light in the therapeutic window: a new mechanism for DNA modification *Chemical Communications.* **2012**, *48,* 67-69.
24. Higgins, S. L. H.; Brewer, K. J., Designing red-light-activated multifunctional agents for the photodynamic therapy *Angewandte Chemie International Edition.* **2012**, *51,* 11420-11422.
25. Creutz, C.; Chou, M.; Netzel, T. L.; Okumura, M.; Sutin, N., Lifetimes, spectra, and quenching of the excited states of polypyridine complexes of iron(II), ruthenium(II), and osmium(II) *Journal of the American Chemical Society.* **1980**, *102,* 1309-1319.
26. Meyer, T. J., Photochemistry of metal coordination complexes: metal to ligand charge transfer excited states. In *Pure and Applied Chemistry*, 1986; Vol. 58, p 1193.
27. Damrauer, N. H.; McCusker, J. K., Ultrafast dynamics in the metal-to-ligand charge transfer excited-state evolution of $[Ru(4,4'\text{-diphenyl-}2,2'\text{-bipyridine})_3]^{2+}$ *Journal of Physical Chemistry A.* **1999**, *103,* 8440-8446.
28. McClenaghan, N. D.; Barigelletti, F.; Maubert, B.; Campagna, S., Towards ruthenium(II) polypyridine complexes with prolonged and predetermined excited state lifetimes *Chemical Communications.* **2002**, 602-603.
29. Wang, H. t.; Li, H. h.; Huang, M. q.; Huang, W. x.; Ma, C. s.; Wang, M. l.; He, C. x.; Liu, J. h.; Zhang, Q. l., Photocleavage of DNA and adenine–thymine inclined binding by a novel ruthenium(II) complex with 3,4-dibromo-imidazo[4,5-f][1,10]phenanthroline ligand *Inorganic Chemistry Communications.* **2015**, *55,* 30-35.
30. Sun, B.; Guan, J. X.; Xu, L.; Yu, B. L.; Jiang, L.; Kou, J. F.; Wang, L.; Ding, X. D.; Chao, H.; Ji, L. N., DNA condensation induced by ruthenium(II) polypyridyl complexes $[Ru(bpy)_2(PIPSH)]_{2+}$ and $[Ru(bpy)_2(PIPNH)]_{2+}$ *Inorganic Chemistry.* **2009**, *48,* 4637-4639.

31. Winkler, J. R.; Gray, H. B., Electron transfer in ruthenium-modified proteins *Chemical Reviews.* **1992**, *92,* 369-379.
32. Fleisher, M. B.; Waterman, K. C.; Turro, N. J.; Barton, J. K., Light-induced cleavage of DNA by metal complexes [1] *Inorganic Chemistry.* **1986**, *25,* 3549-3551.
33. Dobrucki, J. W., Interaction of oxygen-sensitive luminescent probes $[Ru(phen)_3]^{2+}$ and $[Ru(bipy)]_3^{2+}$ with animal and plant cells in vitro: Mechanism of phototoxicity and conditions for non-invasive oxygen measurements *Journal of Photochemistry and Photobiology B.* **2001**, *65,* 136-144.
34. Edwards, M. P.; Price, D. A., Chapter 23 - Role of physicochemical properties and ligand lipophilicity efficiency in addressing drug safety risks. In *Annual Reports in Medicinal Chemistry*, John, E. M., Ed. Academic Press: 2010; Vol. Volume 45, pp 380-391.
35. Leeson, P. D.; Springthorpe, B., The influence of drug-like concepts on decision-making in medicinal chemistry *Nat Rev Drug Discov.* **2007**, *6,* 881-890.
36. Mariappan, M.; Maiya, B. G., Effects of Anthracene and Pyrene Units on the Interactions of Novel Polypyridylruthenium(II) Mixed-Ligand Complexes with DNA *European Journal of Inorganic Chemistry.* **2005**, *2005,* 2164-2173.
37. Liu, J.; Chen, Y.; Li, G.; Zhang, P.; Jin, C.; Zeng, L.; Ji, L.; Chao, H., Ruthenium(II) polypyridyl complexes as mitochondria-targeted two-photon photodynamic anticancer agents *Biomaterials.* **2015**, *56,* 140-153.
38. Mari, C.; Pierroz, V.; Ferrari, S.; Gasser, G., Combination of Ru(II) complexes and light: new frontiers in cancer therapy *Chemical Science.* **2015**, *6,* 2660-2686.
39. Stephenson, M.; Reichardt, C.; Pinto, M.; Wächtler, M.; Sainuddin, T.; Shi, G.; Yin, H.; Monro, S.; Sampson, E.; Dietzek, B.; McFarland, S. A., Ru(II) Dyads Derived from 2-(1-Pyrenyl)-1H-imidazo[4,5-f][1,10]phenanthroline: Versatile Photosensitizers for Photodynamic Applications *The Journal of Physical Chemistry A.* **2014**, *118,* 10507-10521.
40. Monro, S.; Scott, J.; Chouai, A.; Lincoln, R.; Zong, R.; Thummel, R. P.; McFarland, S. A., Photobiological activity of Ru(II) dyads based on (pyren-1-yl)ethynyl derivatives of 1,10-phenanthroline *Inorganic Chemistry.* **2010**, *49,* 2889-2900.
41. Lincoln, R.; Kohler, L.; Monro, S.; Yin, H.; Stephenson, M.; Zong, R.; Chouai, A.; Dorsey, C.; Hennigar, R.; Thummel, R. P.; McFarland, S. A., Exploitation of long-lived ^{3}IL excited states for metal–organic photodynamic therapy: verification in a metastatic melanoma model *Journal of the American Chemical Society.* **2013**, *135,* 17161-17175.
42. Castano, A. P.; Demidova, T. N.; Hamblin, M. R., Mechanisms in photodynamic therapy: part one—photosensitizers, photochemistry and cellular localization *Photodiagnosis and Photodynamic Therapy.* **2004**, *1,* 279-293.
43. Padilla, R.; Corrales, J. A. R.; Donohoe, L. E.; Winkel, B. S. J.; Brewer, K. J., A new class of Ru(II) polyazine agents with potential for photodynamic therapy *Just accepted Chemical Communicaion.* **2015**, *Under Review*.
44. Padilla, R.; Maza, W. A.; Dominijanni, A. J.; Winkel, B. S. J.; Morris, A. J.; J., B. K., Pushing the limits of structurally-diverse light-harvesting Ru(II) metal-organic chromophores for photodynamic therapy *Journal of photochemistry and photobiology A.* **2015**.
45. Maher, E. A.; Furnari, F. B.; Bachoo, R. M.; Rowitch, D. H.; Louis, D. N.; Cavenee, W. K.; DePinho, R. A., Malignant glioma: genetics and biology of a grave matter *Genes and Development.* **2001**, *15,* 1311-1333.

46. Castro, M. G.; Cowen, R.; Williamson, I. K.; David, A.; Jimenez-Dalmaroni, M. J.; Yuan, X.; Bigliari, A.; Williams, J. C.; Hu, J.; Lowenstein, P. R., Current and future strategies for the treatment of malignant brain tumors *Pharmacology and Therapeutics.* **2003**, *98,* 71-108.
47. Reardon, D. A.; Rich, J. N.; Friedman, H. S.; Bigner, D. D., Recent advances in the treatment of malignant astrocytoma *Journal of Clinical Oncology.* **2006**, *24,* 1253-1265.
48. Mongelli, M. T.; Heinecke, J.; Mayfield, S.; Okyere, B.; Winkel, B. S. J.; Brewer, K. J., Variation of DNA photocleavage efficiency for [(TL)2Ru(dpp)]Cl2 complexes where TL = 2,2′-bipyridine, 1,10-phenanthroline, or 4,7-diphenyl-1,10-phenanthroline *Journal of Inorganic Biochemistry.* **2006**, *100,* 1983-1987.
49. de Carvalho, I. M. M.; de Sousa Moreira, Í.; Gehlen, M. H., Synthesis, characterization, and photophysical studies of new bichromophoric ruthenium(II) complexes *Inorganic Chemistry.* **2003**, *42,* 1525-1531.
50. Padilla, R.; Maza, W. A.; Dominijanni, A. J.; Winkel, B. S. J.; Morris, A. J.; Brewer, K. J., Pushing the Limits of Structurally-Diverse Light-Harvesting Ru(II) Metal-Organic Chromophores for PDT *Journal of Photochemistry and Photobiology A.* **2015**, *Under Review*.
51. Padilla, R.; Corrales, J. A. R.; Donohoe, L. E.; Winkel, B. S. J.; Brewer, K. J., A new class of Ru(II) polyazine agents with potential for photodynamic therapy *Chemical Communicaion.* **2015**, *Under Review*.
52. Lipinski, C. A.; Lombardo, F.; Dominy, B. W.; Feeney, P. J., Experimental and computational approaches to estimate solubility and permeability in drug discovery and development settings1 *Advanced Drug Delivery Reviews.* **2001**, *46,* 3-26.
53. Haynes, W. M.; Bruno, T. J.; Lide, D. R., *CRC handbook of chemistry and physics*. CRC Press: 2014; Vol. 95thition, Internet version 2015.
54. Buß, I.; Garmann, D.; Galanski, M.; Weber, G.; Kalayda, G. V.; Keppler, B. K.; Jaehde, U., Enhancing lipophilicity as a strategy to overcome resistance against platinum complexes? *Journal of Inorganic Biochemistry.* **2011**, *105,* 709-717.
55. Pajouhesh, H.; Lenz, G. R., Medicinal chemical properties of successful central nervous system drugs *NeuroRx.* **2005**, *2,* 541-553.
56. Screnci, D.; McKeage, M. J.; Galettis, P.; Hambley, T. W.; Palmer, B. D.; Baguley, B. C., Relationships between hydrophobicity, reactivity, accumulation and peripheral nerve toxicity of a series of platinum drugs *British Journal of Cancer.* **2000**, *82,* 966-972.
57. Zhou, Q.; Gallo, J. M., Differential effect of sunitinib on the distribution of temozolomide in an orthotopic glioma model *Neuro-Oncology.* **2009**, *11,* 301-310.
58. Mongelli, M. T.; Brewer, K. J., Synthesis and study of the light absorbing, redox and photophysical properties of Ru(II) and Os(II) complexes of 4,7-diphenyl-1,10-phenanthroline containing the polyazine bridging ligand 2,3-bis(2-pyridyl)pyrazine *Inorganic Chemistry Communications.* **2006**, *9,* 877-881.
59. Barth, R. F.; Kaur, B., Rat brain tumor models in experimental neuro-oncology: the C6, 9L, T9, RG2, F98, BT4C, RT-2 and CNS-1 gliomas *Journal of Neuro-Oncology.* **2009**, *94,* 299-312.
60. Ghosh, K.; Sarkar, A. R.; Ghorai, A.; Ghosh, U., Design and synthesis of anthracene-based bispyridinium amides: anion binding, cell staining and DNA interaction studies *New Journal of Chemistry.* **2012**, *36,* 1231-1245.

61. Nazarov, A. A.; Risse, J.; Ang, W. H.; Schmitt, F.; Zava, O.; Ruggi, A.; Groessl, M.; Scopelitti, R.; Juillerat-Jeanneret, L.; Hartinger, C. G.; Dyson, P. J., Anthracene-tethered ruthenium(II) arene complexes as tools to visualize the cellular localization of putative organometallic anticancer compounds *Inorganic Chemistry.* **2012**, *51,* 3633-3639.
62. Zhang, R.; Ye, Z.; Yin, Y.; Wang, G.; Jin, D.; Yuan, J.; Piper, J. A., Developing red-emissive ruthenium(II) complex-based luminescent Probes for cellular imaging *Bioconjugate Chemistry.* **2012**, *23,* 725-733.
63. Towner, R. A.; Gillespie, D. L.; Schwager, A.; Saunders, D. G.; Smith, N.; Njoku, C. E.; Krysiak, R. S.; Larabee, C.; Iqbal, H.; Floyd, R. A.; Bourne, D. W. A.; Abdullah, O.; Hsu, E. W.; Jensen, R. L., Regression of glioma tumor growth in F98 and U87 rat glioma models by the Nitrone OKN-007 *Neuro-Oncology.* **2013**, *15,* 330-340.
64. Neugebauer, U.; Pellegrin, Y.; Devocelle, M.; Forster, R. J.; Signac, W.; Moran, N.; Keyes, T. E., Ruthenium polypyridyl peptide conjugates: membrane permeable probes for cellular imaging *Chemical Communications.* **2008**, 5307-5309.
65. Dickerson, M.; Sun, Y.; Howerton, B.; Glazer, E. C., Modifying charge and hydrophilicity of simple Ru(II) polypyridyl complexes radically alters biological activities: Old complexes, surprising new tricks *Inorganic Chemistry.* **2014**, *53,* 10370-10377.
66. Puckett, C. A.; Barton, J. K., Methods to explore cellular uptake of ruthenium complexes *Journal of the American Chemical Society.* **2007**, *129,* 46-47.
67. Puckett, C. A.; Barton, J. K., Mechanism of cellular uptake of a ruthenium polypyridyl complex *Biochemistry.* **2008**, *47,* 11711-11716.
68. Puckett, C. A.; Barton, J. K., Fluorescein redirects a ruthenium-octaarginine conjugate to the nucleus *Journal of the American Chemical Society.* **2009**, *131,* 8738-8739.
69. Garner, R. N.; Joyce, L. E.; Turro, C., Effect of electronic structure on the photoinducedligand exchange of Ru(II) polypyridine complexes *Inorganic Chemistry.* **2011**, *50,* 4384-4391.
70. Zhu, J.; Prussin, R.; Dominijanni, A.; Brewer, K. J.; Robertson, J. L., Exploring cellular activity of a polyazine bridged Ru(II)–Pt(II) supramolecule in rat malignant glioma F98 *Manuscript in progress.* **2015**.
71. Kawanishi, Y.; Kitamura, N.; Tazuke, S., Dependence of spectroscopic, electrochemical, and excited-state properties of tris chelate ruthenium(II) complexes on ligand structure *Inorganic Chemistry.* **1989**, *28,* 2968-2975.
72. Prussin Ii, A. J.; Zigler, D. F.; Jain, A.; Brown, J. R.; Winkel, B. S. J.; Brewer, K. J., Photochemical methods to assay DNA photocleavage using supercoiled pUC18 DNA and LED or xenon arc lamp excitation *Journal of Inorganic Biochemistry.* **2008**, *102,* 731-739.
73. Padilla, R.; Maza, W. A.; Dominijanni, A. J.; Winkel, B. S. J.; Morris, A. J.; J., B. K., Pushing the limits of structurally-diverse light-harvesting Ru(II) metal-organic chromophores for photodynamic therapy *Journal of photochemistry and photobiology A.* **2015**, *Under Review*.

Chapter 5: Overall Conclusions and Future Directions

The research presented in this dissertation has demonstrated the potential of the Ru(II) complexes $[(AnthbpyMe)(bpy)Ru(dpp)]^{2+}$ and $[(AnthbpyMe)_2Ru(dpp)]^{2+}$ as PDT agents and as synthetic intermediates for fluorescent Ru(II)-Pt(II) assemblies. As described in Chapter 1, Ru(II)-Pt(II) systems of the form $[(bpy)_2Ru(dpp)PtCl_2]^{2+}$ have shown excellent potential as multifunctional PDT agents, even though there is limited information about their *in vitro* uptake distribution and chemical reactivity within mammalian cells. In response to this knowledge gap, one of the long-term research goals in Prof. Karen Brewer's group has been to develop a fluorescent-tagged Ru(II)-Pt(II) complex of the type shown in Figure 5.1 and explore its photophysical properties, its interaction with DNA and proteins, and its localization within mammalian cells.

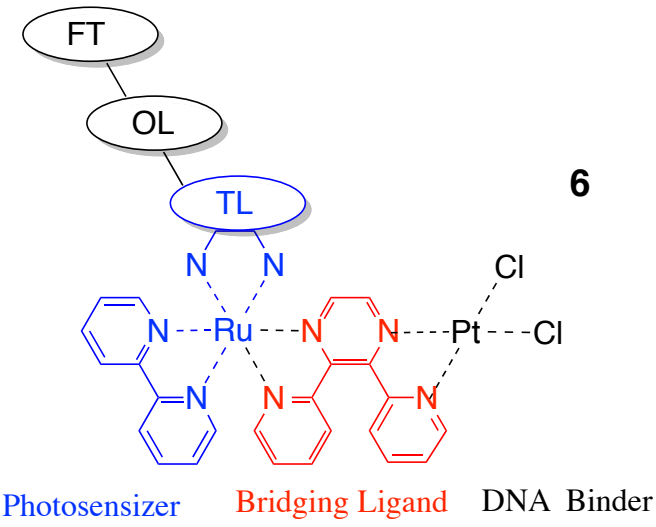

Figure 5.1 Illustration that describes fluorescent Ru(II)-Pt(II) complexes of the form $[(FT)(TL)Ru(BL)PtCl_2]^{2+}$.

The stepwise strategy used to develop novel multimetallic systems dictated that we first examine the properties of tagged Ru(II) photosensitizers lacking Pt(II) so that we could ultimately determine the specific additional functionality contributed by the second metal unit. Two novel anthracene-Ru-dpp complexes exhibiting variations in the number and

regiochemical attachment of the anthracene groups, together with a control complex lacking a tag, were synthesized and examined using photochemical and electrochemical methods. These complexes demonstrated bichromatic behavior: the fluorescent properties of the anthracene tag and the MLCT-based photochemistry of the Ru(II) photosensitizer, both potentially useful for cell imaging, were found to be largely independent (Chapter 2). These anthracene-Ru-dpp systems exhibited dynamic photoreactivity towards DNA in the presence and absence of oxygen, while newly-established protein assays demonstrated photodegradation of proteins via an $^3O_2$-mediated mechanism (Chapter 3). The anthracene-Ru-dpp systems were observed to localize primarily along the cell membrane and to associate with dot-like vesicles within the cytoplasm and nucleoli within 5 min of initial exposure (Chapter 4), while photocytoxicity assays revealed enhanced PDT potency of these complexes against mammalian cancer cells (Chapters 2 and 4).

This dissertation also raised important new questions regarding the mechanisms of cell uptake and cell death including the and intracellular targets of these Ru(II) systems in mammalian cells. The next series of studies should be directed at understanding the mechanism of cell death initiated by photoactivation of the anthracene-[Ru]-dpp systems. Fluorescent stain experiments can be used to detect and distinguish between apoptosis and necrosis based on cell membrane integrity and changes in cell morphology.[1-3] An ethidium bromide (EB)/acridine orange (AO) dual staining technique can be used to monitor cell death based on membrane integrity; AO traverse plasma membrane to stain the DNA of live cells, while EB is excluded from the viable cells but can traverse the compromised plasma membrane to stain the DNA of dead cells. Propidium iodide stains can also be used to distinguish between necrotic, apoptotic, and healthy cells.[4] These techniques can be used to

examine the change in cell morphology upon treating with the complexes with and without irradiation. Caspase and protease assays are the standard for defining apoptosis and can be employed to further investigate the mechanism of cell death mediated by these complexes.

Detailed studies regarding the mechanism of cell uptake for these systems are also necessary to understand the relationship between cellular uptake and PDT potency. Preliminary studies suggest that the strong association with the cell membrane and rapid permeation into the cytoplasm of $[(AnthbpyMe)(bpy)Ru(dpp)]^{2+}$ and $[(AnthbpyMe)_2Ru(dpp)]^{2+}$, consistent with a passive diffusion mechanism of uptake. Change in the membrane fluidity monitored through temperature-controlled confocal microscopy or cholesterol depletion can be used to further investigate whether passive diffusion is the actual and/or only mechanism of uptake.[5-7]

A related area of interest is the primary intracellular targets of anthracene-Ru-dpp complexes. Anthracene-Ru-dpp systems appear to be excluded from the nucleus of the cell at prolonged time intervals (48 h), which suggests that nuclear DNA may not be the primary target. Nevertheless, extranuclear substrates such as RNA, enzymes, and structural proteins could potentially serve as the binding target for anthracene-Ru-dpp and its analogues at these later time points.

An important feature of these anthracene-Ru-dpp systems is that they offer the potential for appending additional metals such as Pt(II) that could enhance the interaction with DNA and other biological macromolecules, analogous to cisplatin, carboplatin, and other widely-used (non-PDT) anti-cancer agents. Although covalently coupling a Pt(II) metal to anthracene-Ru-dpp PSs is predicted to diminish the excited state properties of the Ru(II) units that were ideal for cell imaging, the anthracene could provide an alternative fluorescent

tag for monitoring the Ru(II)-P(II) complex within cells. In fact, we have recently isolated a novel fluorescent Ru(II)-Pt(II) system by adapting a general literature procedure reported by Brewer et al.[8] A preliminary effort to couple Pt(II) to the (anthracene)$_2$-[Ru]-dpp photosensitizer produced the desired bimetallic complex, albeit at low yield. Further optimization of the reaction and purification protocol would undoubtedly improve the efficiency of this synthesis. The presence of the $[(AnthbpyMe)_2Ru(dpp)PtCl_2]^{2+}$ cation in the sample was confirmed using ESI-MS (Figure 5.2). Steady state emission showed that excitation of $[(AnthbpyMe)_2Ru(dpp)PtCl_2]^{2+}$ with λ_{ex} = 340 nm gives rise to emissive high energy transitions with maxima located at 440 nm a(Figure 5.3)nd excitation with λ_{ex} = 520 nm gives rise to emission from the Ru(II) ^{3}MLCT state centered at ~740 nm (Figure 5.4). Although emission from the Ru(II) was, as anticipated, outside the range of detection for current optical techniques, this preliminary result indicates that the anthracene motif can provide a very useful alternative probe for tracking the localization and biological targeting of Ru(II)-Pt(II) systems within cells, in addition to substantially enhancing the cellular uptake of these systems.

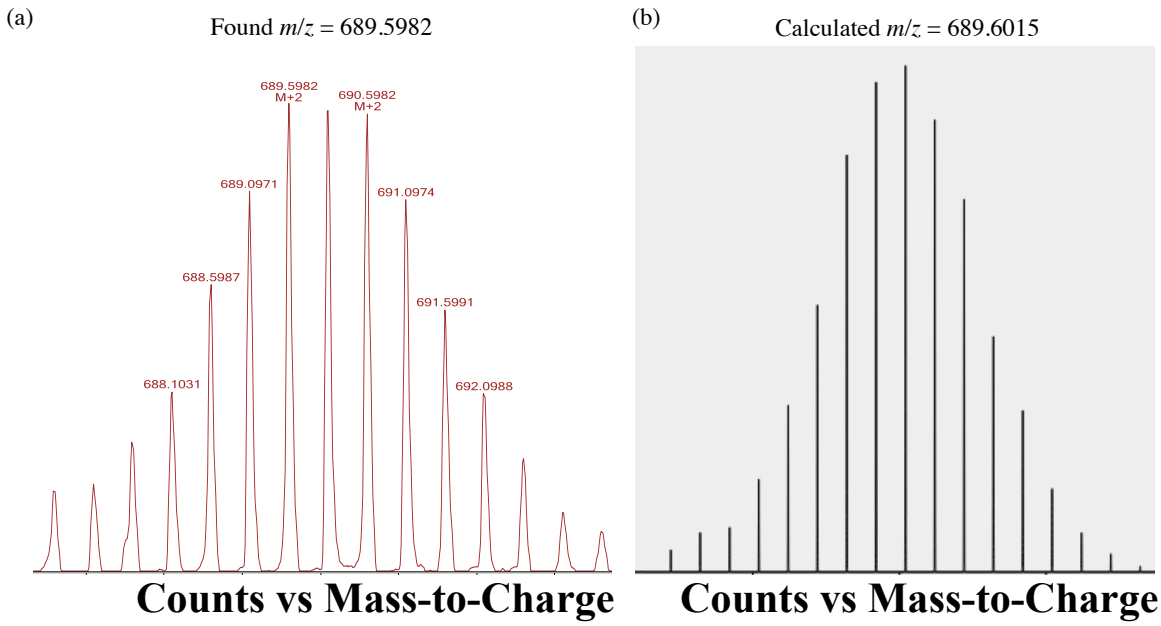

Figure 5.2. ESI-MS spectrum of $[(AnthbpyMe)_2Ru(dpp)PtCl_2]^{2+}$ (a) and calculated isotopic distribution pattern with the ChemCalc (b).

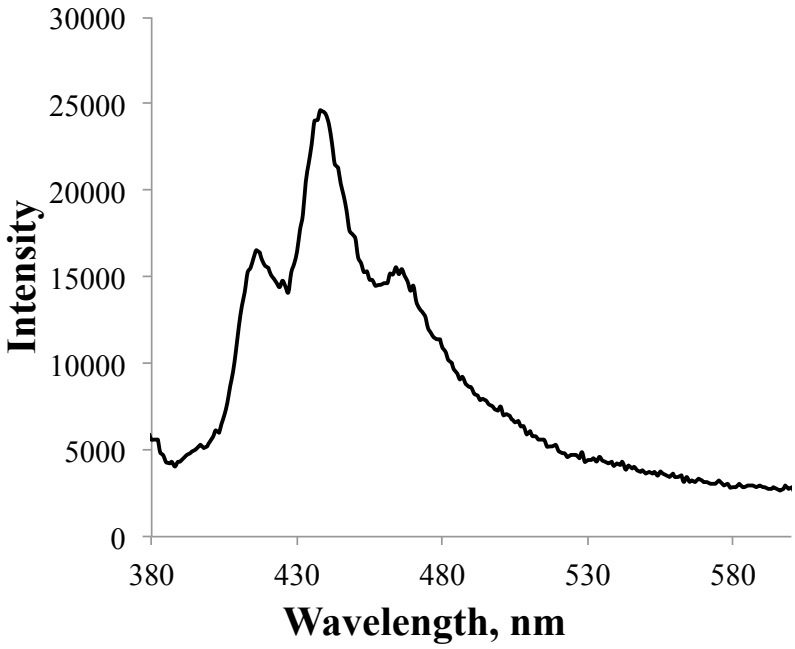

Figure 5.3. Steady state emission profile of $[(AnthbpyMe)_2Ru(dpp)PtCl_2]^{2+}$ excite at 304 nm in acetonitrile.

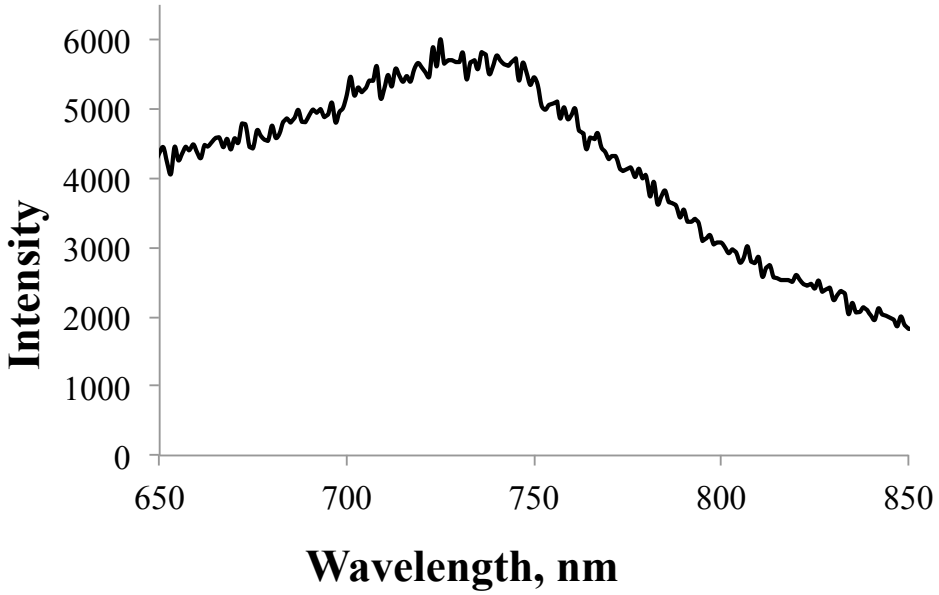

Figure 5.4. Steady state emission profile of $[(AnthbpyMe)_2Ru(dpp)PtCl_2]^{2+}$ excite at 304 nm in acetonitrile.

It must be emphasized that coupling Pt(II) units to fluorescent $[(bpy)_2Ru(dpp)]^{2+}$ photosensitizers *can potentially influence their intracellular localization* compared to anthracene-Ru-dpp systems. Other Ru(II) complexes have recently been shown to localize within nuclei. Thus a future and clear direction of this project is to explore the internalization of these fluorescent Ru(II)-Pt(II) systems and their potential as highly-potent PDT agents for use in the treatment of a variety of diseases, including cancer.[9,10]

5.1 References

1. Liu, K.; Liu, P.-c.; Liu, R.; Wu, X., Dual AO/EB staining to detect apoptosis in osteosarcoma cells compared with flow cytometry *Medical Science Monitor Basic Research.* **2015**, *21,* 15-20.
2. Baskic, D.; Popovic, S.; Ristic, P.; Arsenijevic, N. N., Analysis of cycloheximide-induced apoptosis in human leukocytes: Fluorescence microscopy using annexin V/propidium iodide versus acridin orange/ethidium bromide *Cell Biology International.* **2006**, *30,* 924-932.
3. Basu, U.; Khan, I.; Hussain, A.; Gole, B.; Kondaiah, P.; Chakravarty, A. R., Carbohydrate-appended tumor targeting iron(III) complexes showing photocytotoxicity in red light *Inorganic Chemistry.* **2014**, *53,* 2152-2162.
4. Lecoeur, H., Nuclear apoptosis detection by flow cytometry: Influence of endogenous endonucleases *Experimental Cell Research.* **2002**, *277,* 1-14.

5. Ohtani, Y.; Irie, T.; Uekama, K.; Fukunaga, K.; Pitha, J., Differential effects of α-, β- and γ-cyclodextrins on human erythrocytes *European Journal of Biochemistry.* **1989**, *186,* 17-22.
6. Kilsdonk, E. P. C.; Yancey, P. G.; Stoudt, G. W.; Bangerter, F. W.; Johnson, W. J.; Phillips, M. C.; Rothblat, G. H., Cellular cholesterol efflux mediated by cyclodextrins *Journal of Biological Chemistry.* **1995**, *270,* 17250-17256.
7. Puckett, C. A.; Ernst, R. J.; Barton, J. K., Exploring the cellular accumulation of metal complexes *Dalton Transactions.* **2010**, *39,* 1159-1170.
8. Higgins, S. L. H.; White, T. A.; Winkel, B. S. J.; Brewer, K. J., Redox, spectroscopic, and photophysical properties of Ru-Pt mixed-metal complexes incorporating 4,7-diphenyl-1,10-phenanthroline as efficient DNA binding and photocleaving agents *Inorganic Chemistry.* **2011**, *50,* 463-470.
9. Siddik, Z. H., Cisplatin: mode of cytotoxic action and molecular basis of resistance *Oncogene.* **0000**, *22,* 7265-7279.
10. Zhang, R.; Ye, Z.; Yin, Y.; Wang, G.; Jin, D.; Yuan, J.; Piper, J. A., Developing red-emissive ruthenium(II) complex-based luminescent Probes for cellular imaging *Bioconjugate Chemistry.* **2012**, *23,* 725-733.